Democratic and Popular Republic of Algeria
Ministry of higher education and scientific research
University—Ferhat Abbas Sétif 1
Faculty of Sciences
Department of Physics

Domain : Materials Science
Field : Materials Physics

Dissertation submitted for the completion of the Master's degree in Materials Physics

THEME

HIGH-PERFORMANCE LIQUID SENSING USING PHONONIC CRYSTALS : EXPERIMENTS AND NUMERICAL ANALYSIS

Presented by : Mr BOURAS Ilyas

Publicly defended : 22 june 2025

In front of the jury :

Dr	GUITOUME Djamal eddine	(Senior Researcher, Class A)	President
Dr	LAIDOUDI Farouk	(Senior Researcher, Class A)	Examiner
Dr	KANOUNI Fares	(Senior Researcher, Class A)	Supervisor

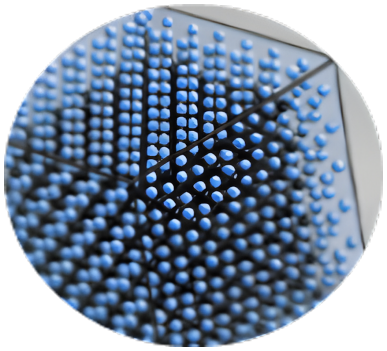

Physics Department-Faculty of Sciences

University of Farhat Abbas
Setif

HIGH-PERFORMANCE LIQUID SENSING USING PHONONIC CRYSTALS : EXPERMENTS AND NUMERICAL ANALYSIS

BOURAS Ilyas

Setif 1 University - Ferhat ABBAS

CDTA

Supervisor: Dr. KANOUNI Fares
Senior Researcher, Class A
Photonic Crystals Team, Research Unit in Optics and Photonics

Research Unit in Optics and Photonics UROP
Center for Development of Advanced Technologies (UROP-CDTA)
19000, Setif, El-Bez, Algeria

ABSTRACT

This work describes the complete development of a two-dimensional phononic crystal (2D PnC) sensor for liquid mixture characterization. This research is divided into three distinct sections. The first part of this work involves creating a COMSOL Multiphysics model of the phononic-fluidic sensor to study acoustic wave propagation and sensor response through detailed simulations. The second section describ the optimization process followed by fabrication of the 2D phononic crystal, which features a square lattice of air holes inside a stainless steel matrix. The developed structure served for identifying different unknown liquid mixtures, including acetone–water, nickel chloride–water, and sodium chloride–water solutions. In addition, the experimental measurement of the acoustic transmission spectra led to the development of calibration curves for each mixture, which enables concentration identification. Moreover, this study evaluates the sensor performance through measurements of sensitivity and quality factor (Q-factor). The third section of this research involves creating a graphical user interface (GUI) to support real-time data acquisition and analysis. The interface underwent testing, which confirmed its reliable operational performance.

RÉSUMÉ

Ce travail décrit le développement complet d'un capteur à cristaux phononiques bidimensionnels (2D PnC) pour la caractérisation des mélanges liquides complexes. Cette recherche se divise en trois sections principales. La première partie inclut la création d'un modèle en utilisant COMSOL Multiphysics pour ce capteur acoustique afin d'étudier la propagation des ondes sonores et la réponse du capteur à travers une simulation détaillée. La deuxième section décrit le processus d'optimisation qui a suivi la fabrication de la structure phononique bidimensionnelle, caractérisée par un réseau carré de trous à l'intérieur d'une matrice en acier inoxydable. Ce capteur a été utilisé pour identifier des concentration des mélanges liquides inconnus, y compris le mélange acétone-eau, le mélange chlorure de nickel-eau et le mélange chlorure de sodium-eau. De plus, les mesures expérimentales du spectre de transmission acoustique ont conduit au développement de courbes d'étalon- nage pour chaque mélange, permettant ainsi de déterminer la concentration. Cette étude a également montré les performances du capteur à travers des mesures de sensibilité et du facteur de qualité (Q-factor). La troisième section a inclus la création d'une interface utilisateur graphique (GUI) pour soutenir la collecter et analyser les données en temps réel. L'interface a été testée, confirmant ainsi ses performances opérationnelles fiables.

الملخص

يصف هذا العمل التطوير الشامل لجهاز استشعار بلورة صوتية ثنائية الأبعاد لتوصيف الخلطات السائلة. ينقسم هذا البحث إلى ثلاثة أقسام رئيسية. الجزء الأول تضمن إنشاء نموذج باستخدام COMSOL Multiphysics لهذا الجهاز الاستشعار الصوتي لدراسة انتشار الموجات الصوتية واستجابة المستشعر من خلال محاكاة مفصلة. القسم الثاني يصف عملية التحسين التي تلتها تصنيع البلورة الصوتية ثنائية الأبعاد، والتي تتميز بشبكة مربعة من الثقوب الهوائية داخل مصفوفة من الفولاذ المقاوم للصدأ. استخدم هذا المستشعر لتحديد مختلف الخلطات السائلة غير المعروفة، بما في ذلك خليط الأسيتون والماء، وخليط كلوريد النيكل والماء، وخليط كلوريد الصوديوم والماء. بالإضافة إلى ذلك، أدت القياسات التجريبية لطيف الانتقال الصوتي إلى تطوير منحنيات المعايرة لكل مزيج، مما مكن من تحديد التركيز. كما بينت هذه الدراسة أداء المستشعر من خلال قياسات الحساسية وعامل الجودة (Q-factor). القسم الثالث تضمن إنشاء واجهة مستخدم رسومية (GUI) لدعم جمع البيانات وتحليلها في الوقت الفعلي. خضعت الواجهة للاختبار الذي أكد أدائها التشغيلي الموثوق .

PREFACE

This master's thesis was conducted in the context of the master's program in Physics of Materials, taught by the physics department of the Setif University. The research was carried out within the Research Unit in Optics and Photonics (UROP) at the CDTA (Centre de Développement des Technologies Avancées). The research presented in this thesis was carried out between February 2, 2025, and May 25, 2025, at the Photonic Crystal Lab, affiliated with UROP-CDTA. This project was conducted under the supervisor Dr. KANOUNI Fares, a Senior Researcher Class A and team leader at UROP.

ACKNOWLEDGEMENTS

First and foremost, I would like to thank my master's thesis supervisor, **Dr. KANOUNI Fares**, Senior Researcher (Class A) at the Research Unit in Optics and Photonics, affiliated with the Centre for Advanced Technology Development (CDTA), for his unwavering support.I am deeply grateful for his patience, motivation, and valuable guidance throughout the entire process.

I also extend my sincere gratitude to **Dr. ARAB Fahima** for her expert guidance and support, which greatly assisted me during the research and writing of this thesis.

My heartfelt thanks go to **CHETTOUH A. Nidhal and Dr. Youcef Bougherira**, director of UROP who provided an exceptional research environment and continuous support during my studies. Special thanks are due to all **CDTA** members, especially **Dr. GUITOUME Djamel, Dr. RAHMANI Mahdi, and MOSBAH Daamouche,** for their excellence in the fields of chemistry and mechanics. Their unconditional help and expertise contributed significantly to the smooth progress of this project.

It must also be acknowledged that the foundation of this research lies in the longstanding tradition of excellence at CDTA. I am grateful to the faculty and staff of the **Physics Department** at the **University of Ferhat Abbas Sétif** for providing a stimulating academic environment and access to essential resources. Special thanks go to the **Chemistry Department** for providing key materials used in chemical applications during the development of this thesis.

Finally, I owe my deepest personal gratitude to my parents and siblings for their steadfast belief in me throughout the challenges of this journey. Their encouragement was a constant source of motivation. This thesis is the result of collective efforts, and I am sincerely appreciative of everyone who contributed to its completion.

Thank you.

CONTENTS

INTRODUCTION

Phononic crystals (PnCs) represent a class of artificially structured materials, designed to control, manipulate, and direct the propagation of acoustic waves through periodic arrangements of elastic materials with different acoustic properties [1-3]. The distinct feature of phononic crystals is their ability to exhibit phononic bandgap, a frequency ranges within which wave propagation is prohibited [4].

Phononic crystals can be classified based on their dimensionality into one-dimensional (1D), two-dimensional (2D), and three-dimensional (3D) structures [5-8]. 1D phononic crystals have periodicity along a single axis, are typically formed by alternating layers of materials, and are used in simple acoustic filters and reflectors. 2D phononic crystals feature periodic patterns in a plane—such as arrays of holes or rods—and are widely applied in sensors, waveguides, and sound isolation devices. 3D phononic crystals exhibit periodicity in all three spatial directions, offering complete control over acoustic wave propagation and enabling full band gaps, making them ideal for advanced sensing and vibration control applications. These specific properties make them highly suitable for applications in sound insulation, frequency filtering, and sensing technologies[9-11].

One of the challenging applications is their exploitation for sensing purposes, for example, for monitoring, controlling and measuring volumetric properties of complex liquids. For this purpose, Lucklum and Li proposed a phononic-fluidic cavity sensor [12]. In contrast with classical resonant sensors [13-16], e.g. quartz crystal microbalance (QCM), surface acoustic wave (SAW), and flexural wave plate (FWP), the phononic-fluidic is able to measure bulk properties of liquids, not surface ones.

Moreover, accurately determining volumetric properties such as density and sound velocity is crucial for the precise characterization of complex mixtures. In this context, we conduct a research project on measuring in real-time the bulk properties of complex liquids such as acetone–water, nickel chloride–water and sodium chloride–water.

This dissertation is structured into four main chapters. Chapter I introduces the fundamental concepts of acoustic waves and phononic crystals, their classifications, and their technological applications, with a particular focus on liquid sensing using phononic-fluidic structures. Chapter II presents a detailed numerical study of a phononic-fluidic sensor using COMSOL Multiphysics, including geometry design, simulation of wave propagation, and analysis of transmission spectra for various liquid mixtures. Chapter III focuses on the experimental design, fabrication, and testing of 2D phononic crystal sensors, with validation through acoustic transmission measurements and performance evaluation for different liquid mixtures. Finally, Chapter IV describes the development of a custom graphical user interface (GUI) to facilitate real-time control, data acquisition, and analysis of the phononic sensor, enhancing its usability for practical sensing applications.

CHAPTER I: Phononic Crystals for Liquid Sensing Applications

CHAPTER 1

PHONONIC CRYSTALS FOR LIQUID SENSING APPLICATIONS

I.1. INTRODUCTION

In this chapter, we provide a comprehensive introduction to phononic crystals (PnCs)engineered materials that exhibit unique wave manipulation properties due to their periodic structural design.Contribute a comprehensive exploration of the principles, classifications, and technological applications of phononic crystals, with a particular emphasis on their role in advanced liquid sensing technologies.We begin by laying the groundwork with a discussion on the fundamentals of acoustic waves, including their propagation mechanisms in different media. This includes an examination of longitudinal, transverse, and surface waves.

Following this foundational overview, we delve into the principles and classifications of phononic crystals, explaining how their bandgap properties arise from periodic variations in elastic constants and mass density. We explore different types of PnCs, including one-dimensional (1D), two-dimensional (2D), and three-dimensional (3D) structures, and discuss their respective wave control capabilities. Additionally, we examine the role of symmetry, lattice geometry, and material composition in determining their acoustic properties.

Finally, we highlight the diverse industrial and technological applications of phononic crystals, emphasizing their growing importance in modern engineering. A special focus is placed on phononic-fluidic sensors, which leverage acoustic wave interactions with fluids for high-precision detection in biomedical, chemical, and environmental monitoring. We also touch upon other emerging applications, such as vibration isolation, noise control.

Through this chapter, the reader will gain an in-depth understanding of the interplay between acoustic wave physics and material engineering in phononic structures, and how this interplay gives rise to novel sensing modalities for liquid analysis.

I.2. ACOUSTIC WAVES

The acoustic waves are among the mechanical waves that propagate through different media, such as solids, liquids, and even gases [17]. These kinds of waves carry only energy without any transportation of matter, depending directly on the elasticity and inertia of the medium.

I.2.1. Fundamentals of Acoustic Waves

To understand the behavior of phononic crystals, it is essential to first establish the principles of acoustic wave propagation. Acoustic waves represent mechanical disturbances that propagate through an elastic medium, involving the oscillatory motion of particles about their equilibrium positions. In a simple fluid (liquid or gas), only longitudinal pressure waves exist, because fluids have no shear resistance; the particle motion is parallel to the direction of propagation. In contrast, an elastic solid can support both longitudinal (compressional) and transverse (shear) waves due to its shear stiffness [18]. The propagation of acoustic waves in a homogeneous, isotropic, and elastic medium is governed by the elastodynamic wave equation, which can be expressed as [19]:

$$\rho \frac{\partial^2 \mathbf{u}}{\partial t^2} = (\lambda + 2\mu)\nabla(\nabla \cdot \mathbf{u}) - \mu \nabla \times (\nabla \times \mathbf{u}) \tag{1}$$

where $\mathbf{u}$ is the displacement vector, ρ is the mass density, t is time, and λ and μ are Lamé's elastic constants characterizing the medium's stiffness. This equation gives rise to two distinct wave types with different propagation velocities:

Longitudinal (compressional) waves:

$$c_L = \sqrt{\frac{\lambda + 2\mu}{\rho}} \tag{2}$$

Transverse (shear) waves:

$$c_T = \sqrt{\frac{\mu}{\rho}} \tag{3}$$

For fluids, which typically do not support shear stress ($\mu \approx 0$), the equation simplifies to describe pressure waves by [19]:

$$\nabla^2 p = \frac{1}{c^2} \frac{\partial^2 p}{\partial t^2} \tag{4}$$

where p is the acoustic pressure, and c is the speed of sound in the medium, given by:

$$c = \sqrt{\frac{B}{\rho}} \tag{5}$$

where B represents the bulk modulus and ρ is the mass density of the medium [8].

The key parameters describing acoustic waves include frequency f, wavelength λ, angular frequency ω, and phase velocity c, which are related by $\omega = 2\pi f = c/\lambda$. The acoustic impedance Z of a medium, defined as $Z = \rho c$ for plane waves in fluids, plays a crucial role in determining the reflection and transmission of waves at an interface between two different media [20]. The classification of acoustic waves based on the frequency range and their application is shown in Figure I.1.

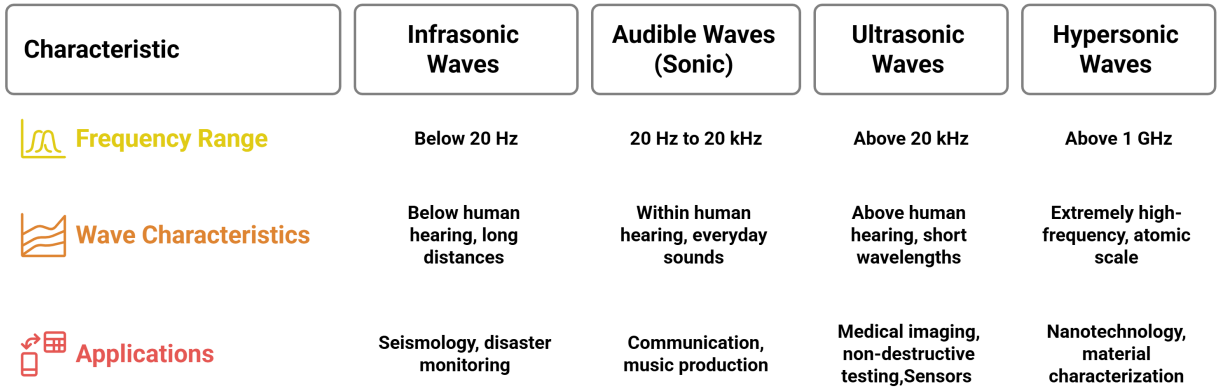

Figure I.1: Categorization of acoustic waves based on frequency range [21]

I.2.2. Types of Waves Based on Propagation Mode

I.2.2.1. Guided acoustic waves

A guided acoustic wave is a sound wave that propagates along a defined path or structure, such as a solid surface, rod, or thin film, due to the boundaries confining the wave energy. These waves are used in sensors, non-destructive testing, and telecommunications, with common types including Surface Acoustic Waves (SAWs) and Lamb waves. Their properties depend on the material and geometry of the guiding medium.. SAWs were first described by Lord Rayleigh in 1885, and they are sometimes referred to as Rayleigh waves [22].

SAWs are typically generated and detected using interdigital transducers (IDTs) on piezoelectric materials. When an alternating voltage is applied to the IDT, it creates a mechanical deformation due to the piezoelectric effect, launching a SAW along the surface of the substrate, as shown in Figure I.2

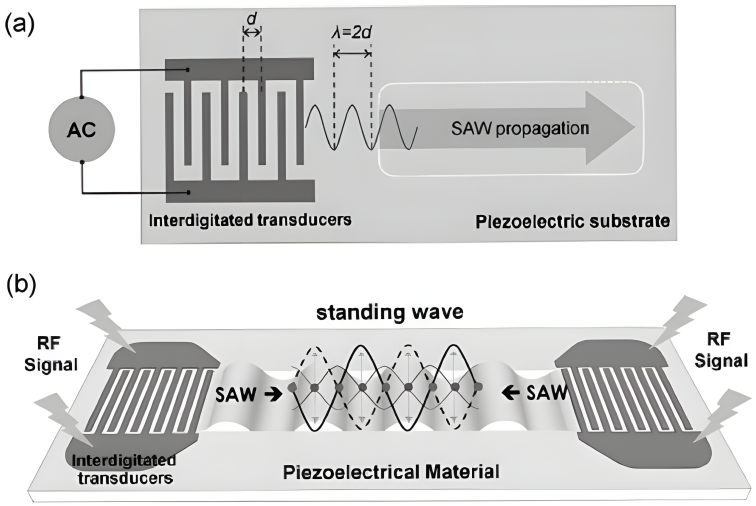

Figure I.2: Surface acoustic wave along the surface of the substrate

Table I.1 shows the different types of surface acoustic waves, their applications, and generation conditions [23-28].

Table I.1: Types of guided Waves and Their Properties

Type of Surface Wave	**Motion/Description**	**Medium**	**Speed**	**Applications/Uses**
Rayleigh Waves	Elliptical motion (like ocean waves), vertical & horizontal (e.g., Earth's crust)	Solid surfaces	Slower than body waves	Earthquake analysis, seismic studies
Love Waves	Horizontal shear motion (side-to-side)	Solids only	Faster than Rayleigh waves	Seismology, causes strong surface damage
Lamb Waves	Vibrations in thin plates, symmetric & antisymmetric	Thin solid plates	Depends on mode/frequency	Non-destructive testing, material inspection
Scholte Waves	Interface wave at solid-liquid boundary	Solid-liquid interface	Slower than Rayleigh waves	Underwater acoustics, ocean-bottom studies
Stoneley Waves	Interface wave at solid-solid boundary	Solid-solid interface	Similar to Rayleigh	Borehole acoustics, geophysical exploration
SH Wave	Shear horizontal wave, motion is perpendicular to propagation and confined to the surface	Solids	Varies with medium and frequency	Surface acoustic wave devices, sensing
Sezawa Wave	Higher-order mode in layered structures, coupled surface and guided wave	Thin film on a substrate	Faster than Rayleigh in layered media	SAW devices, thin-film characterization
Bleustein-Gulyaev Wave	Shear-horizontal surface wave in piezoelectric materials	Piezoelectric solids	Slower than SH in some materials	Acousto-electronic devices, sensors

I.2.2.2. Bulk acoustic wave (BAW)

Bulk Acoustic Waves (BAWs) are mechanical waves that propagate through the entire volume (bulk) of a material, unlike surface acoustic waves (SAWs), which are confined near the surface. BAWs are commonly used in high-frequency devices and sensors due to their efficiency and precision [29]. There are two different categories of BAW, as shown in Figure I.3:

- **Longitudinal Waves**: These waves feature particle oscillations parallel to the wave's direction of travel. They are prevalent in fluids (both gases and liquids) and can also propagate through solids. Longitudinal waves are characterized by alternating compressions and rarefactions of the medium.

- **Transverse Waves**: In these waves, particle motion is perpendicular to the wave's direction of propagation. This type of wave can propagate only in solids and not in liquids or gases since fluids cannot sustain a shear stress and only allow longitudinal waves to pass through. They play a crucial role in advancing our understanding of Earth's solid media, particularly in characterizing the mechanical properties of materials within its interior.

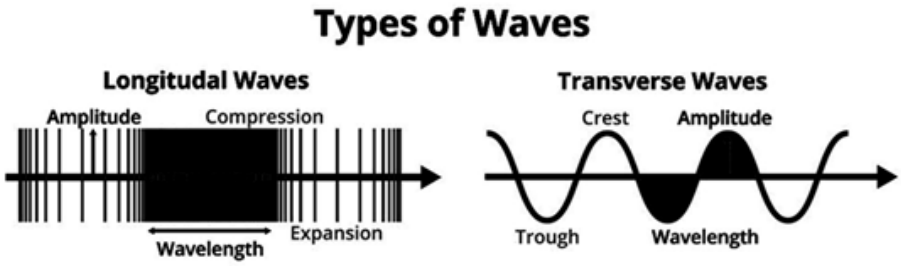

Figure I.3: Bulk Acoustic Waves (BAWs). Longitudinal and Transverse Waves

I.3: Phononic Crystals: Principles and Classifications

I.3.1. Fundamental Concepts

Phononic crystals are engineered by arranging two or more constituent materials in a periodic spatial pattern. In these composites, the local speed of sound and density vary periodically [30,31]. Figure I.4 illustrates a phononic crystal composed of a spatial periodicity of cylindrical forms of stainless steel.

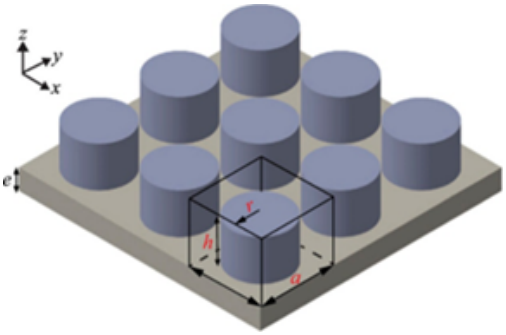

Figure I.4: Phononic crystal composed of the spatial periodicity of stainless steel

The key feature of a phononic crystal (PnC) is the phononic band gap (PnBG): a frequency interval over which no propagation of acoustic waves occurs [32]. When the acoustic wavelength becomes comparable to the lattice constant (the Bragg condition), scattered waves interfere destructively, opening a gap. In addition to Bragg gaps, local resonant mechanisms can create band gaps even for wavelengths much larger than the lattice constant [29].

I.3.1.1. Bragg Scattering Mechanism

Bragg scattering is the primary mechanism behind bandgap formation in most phononic crystals. When the wavelength of an incident wave is comparable to the lattice constant of the crystal, constructive and destructive interference leads to the formation of stop bands or bandgaps, as shown in Figure I.5. Mathematically, Bragg's condition is given by:

$$2d \sin\theta = n\lambda \tag{6}$$

where d is the spacing between scatterers, θ is the angle of incidence, and λ is the wavelength of the wave [18].

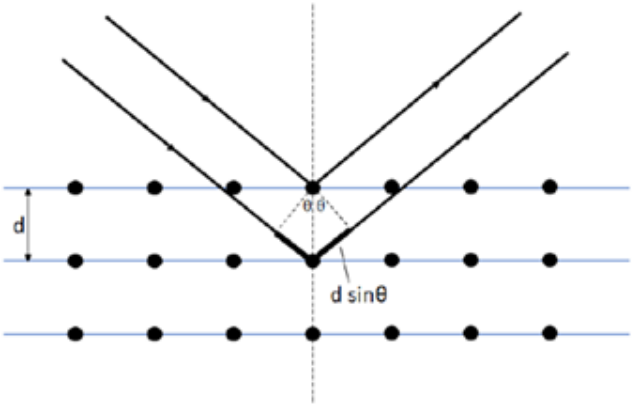

Figure I.5: Bragg Scattering Mechanism

I.3.1.2. Local Resonance Mechanism

In locally resonant PnCs, bandgaps can form at wavelengths much larger than the lattice spacing. These subwavelength bandgaps arise from the resonance of individual inclusions or scatterers embedded in a host matrix. The resonators absorb wave energy at specific frequencies, creating sharp and deep bandgaps that are tunable via the resonator's material and geometry [33].

I.3.2. Different Types of Phononic Crystals

Phononic crystals can be classified in several ways based on their configuration and characteristics, as shown in Figure I.6:

- **Based on Dimensionality**
  - **1D Phononic Crystals**: Periodic structure in one dimension only. Useful for acoustic wave filtering and vibration isolation in a specific direction.
  - **2D Phononic Crystals**: Periodic structure in two dimensions. Capable of controlling wave propagation in a plane. Useful in surface acoustic wave manipulation and waveguides.
  - **3D Phononic Crystals**: Periodicity in all three dimensions. More complex but can offer full bandgaps, blocking waves from propagating in any direction. Applied in high-performance vibration insulation and noise suppression.
- **Based on Material Composition**
  - **Solid–Solid Phononic Crystals**: Made from two or more solids with different elastic properties.
  - **Solid–Fluid Phononic Crystals**: A solid matrix with fluid inclusions, or vice versa. Suitable for underwater acoustics and bio-sensing applications.
  - **Fluid–Fluid Phononic Crystals**: Rare and challenging to fabricate. Useful in specialized fluid dynamics or waveguide systems.
- **Based on Wave Type and Control Mechanism**
  - **Bragg Scattering Phononic Crystals**: Rely on periodic interference (Bragg scattering) to create bandgap. Effective when the wavelength is comparable to the periodicity.
  - **Locally Resonant Phononic Crystals**: Contain resonant units that create bandgaps at wavelengths much larger than the unit cell. Useful for low-frequency vibration and noise control.

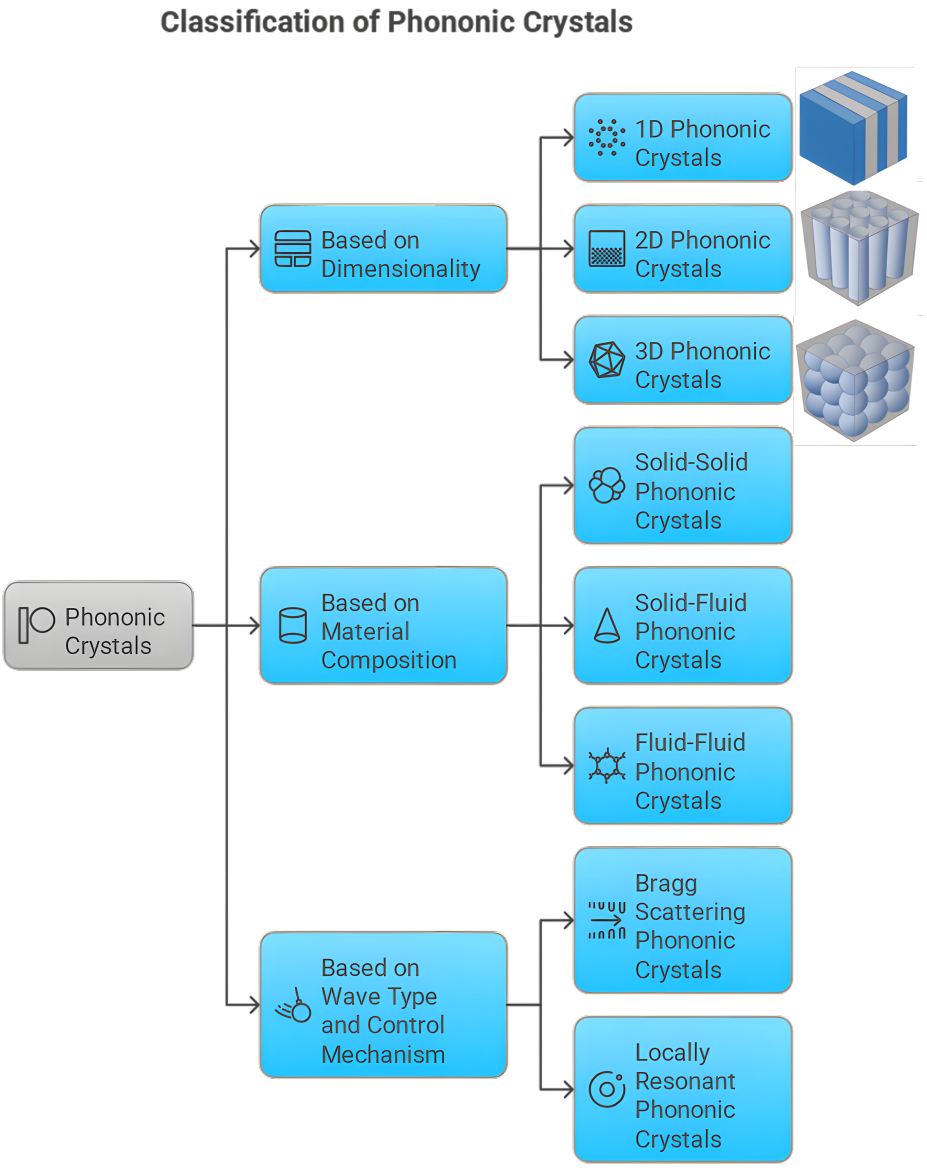

Figure I.6: Different types of phononic crystals

I.4. TECHNOLOGICAL APPLICATIONS OF PHONONIC CRYSTALS

Phononic crystals (PnCs) have unique abilities to control and manipulate the propagation of mechanical (acoustic or elastic) waves due to their periodic structure and the resulting phononic bandgaps. These characteristics enable a wide range of technological applications across various fields, from electronics and sensing to energy and healthcare [34-38]. Table I.2 summarizes the most common applications based on phononic crystals. In the following, we focus only on three applications: Acoustic Filtering and Waveguiding, Acoustic Absorber Devices, and Sensing Applications.

Application Area	Description	Example Use Cases
Waveguides	Directing acoustic waves along specific paths with minimal loss	On-chip acoustic circuits, signal routing
Vibration Isolation	Blocking mechanical vibrations within specific frequency ranges (band gaps)	Precision instruments, aerospace structures, seismic protection
Acoustic Insulation	Preventing transmission of unwanted sound through a material	Soundproofing panels, industrial noise barriers
Filters and Frequency Selectors	Allowing only specific acoustic frequencies to pass	Surface acoustic wave (SAW) filters in communication devices
Sonic Crystals / Noise Barriers	Large-scale phononic structures for environmental noise control	Roadside or railway noise barriers, airport noise shielding
Sensors	Using defect modes or resonance shifts to detect physical changes	Pressure sensors, biosensors, chemical detection
Topological Insulators	Robust wave transport immune to defects or disorder	Advanced phononic circuits, robust waveguides
Thermal Conductivity Control	Manipulating phonons to control heat flow (especially in nanoscale materials)	Thermoelectric materials, heat management in electronics
Signal Processing	Using bandgaps and localized modes for filtering, delay lines, and logic control	Acoustic signal processors, wave-based logic components, acoustic memory

Table I.2: Application Areas of Phononic Structures

I.4.1. Acoustic Filtering and Wave-guiding

Phononic crystals (PnCs) are engineered materials with a periodic structure designed to control the propagation of sound or elastic waves through precise filtering and guiding. Their unique properties arise from the formation of bandgaps—frequency ranges where wave propagation is prohibited due to destructive interference within the crystal's lattice. By strategically introducing defects, such as cavities, or channels into the periodic structure, it is possible to manipulate wave behavior, allowing waves within the bandgap frequencies to be selectively guided along predefined paths. This ability to confine and direct waves with high precision makes PnCs valuable in advanced sensing technologies applications. Furthermore, the design flexibility of PnCs, achieved through variations in material composition, geometry, and defect engineering, enables customizable solutions for controlling wave propagation in diverse engineering and scientific contexts., as

shown in Figure I.7 [39].

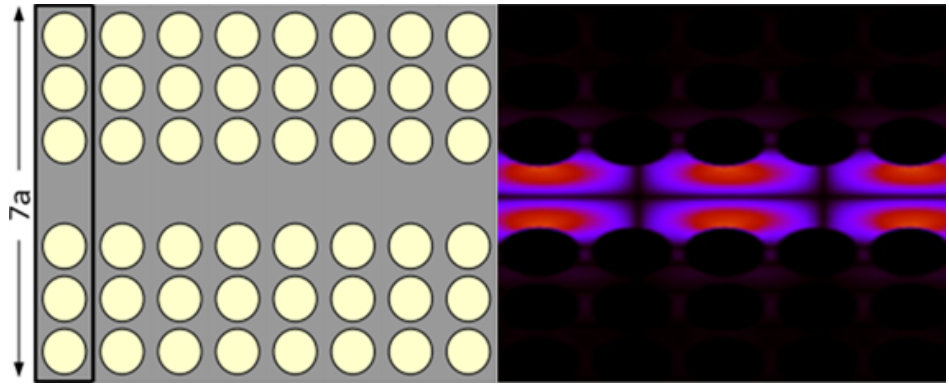

Figure I.7: Phononic crystal for acoustic filtering and waveguiding applications

I.4.2. Acoustic Absorber Devices

Phononic crystals (PnCs) are not only effective at filtering and guiding acoustic waves, but they can also be engineered to function as acoustic absorbers, especially in applications where unwanted noise or vibrations need to be suppressed [40]. These devices exploit wave scattering, local resonance, and energy dissipation mechanisms to attenuate sound energy over targeted frequency ranges, as shown in Figure I.8.

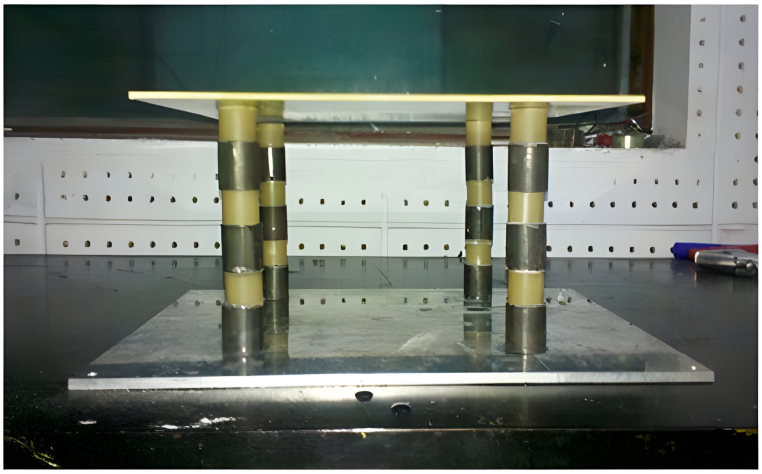

Figure I.8: Acoustic absorber devices based on phononic crystal

I.4.3. Sensing Applications

Phononic crystals (PnCs) have emerged as powerful platforms for developing highly sensitive, compact, and selective acoustic sensors [41-44]. Their periodic structures enable precise con-

trol of mechanical wave propagation, making them ideal for detecting small changes in physical, chemical, or biological environments.Figure I.9 shows the different types of phononic crystals in the sensing field. The sensing is based on small changes in the physical parameters, which correspond to changes in one parameter of the phononic crystal sensor, or so-called working modes of sensing. Table I.3 shows the different sensing modes used in phononic crystals.

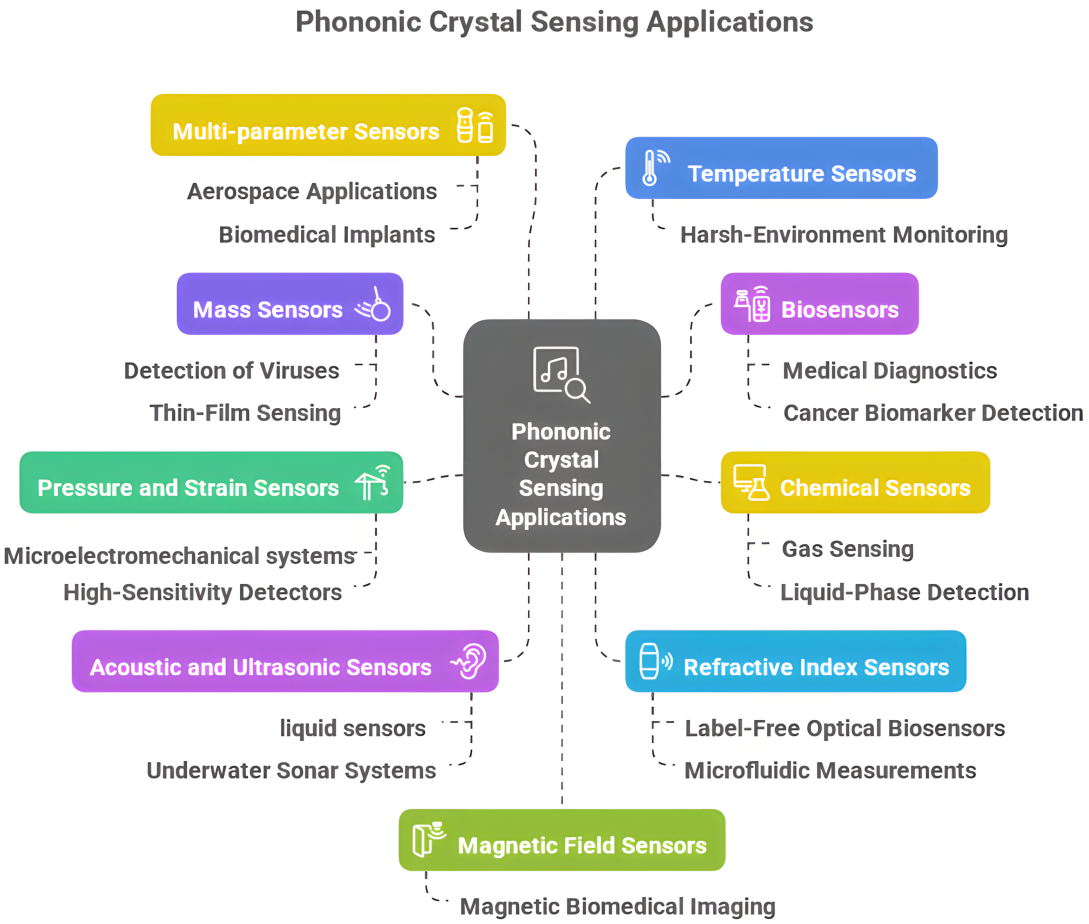

Figure I.9: Phononic crystal for sensing applications

Table I.3: Application Areas of Acoustic Wave Sensors

Mode	Sensing Target	Mechanism
Resonant Mode	*Mass loading, biomolecules*	Analyte changes local mass/stiffness, shifting resonance frequency
Bandgap Shift	*Temperature, pressure, stress*	Environmental changes alter elastic constants, shifting bandgap
Defect Mode Sensing	*Chemical/biological agents*	Analyte interaction modifies defect state, changing localized mode frequency
Wave Attenuation Mode	*Viscosity, material defects, liquids*	Presence of analyte increases wave energy loss, causing signal attenuation

I.5: PHONONIC-FLUIDIC SENSORS

Phononic-fluidic sensors are advanced sensing devices that integrate phononic crystals (PnCs) with microfluidic systems to enable precise, real-time detection of changes in fluid properties. These hybrid devices leverage the ability of phononic crystals to manipulate and control acoustic waves, making them highly sensitive to variations in a fluid's physical or chemical characteristics. The phononic crystals in 1D, 2D, and 3D are used for fluidic characterization.

I.5.1: Working Principle of Phononic-Fluidic Sensors

Phononic-fluidic sensors operate by monitoring how acoustic wave propagation is affected when a fluid interacts with a phononic structure. The presence, flow, or property change of the fluid causes measurable shifts in:

- Wave velocity
- Resonant frequency
- Bandgap structure
- Transmission or reflection spectra

These changes can be accurately correlated with specific parameters such as density, viscosity, concentration, or chemical composition.

I.5.2: Literature Review

The first phononic-fluidic cavity sensor was introduced by Lucklum and Li [12]. This study experimentally demonstrated the use of the phononic-fluidic cavity sensor to measure the volumetric properties of liquids.

Classical techniques, such as traditional ultrasonic or resonant sensors, present serious limitations in characterizing and measuring the volumetric properties of a liquid in small volumes. These limitations are primarily due to low sensitivity and the ability to probe only the surface layers of the analyte. To overcome these limitations, phononic crystals can be used as sensors for the determination of volumetric properties such as the sound speed and density of small amounts of liquid. At the core of the sensor is a cavity resonator, whose resonance frequency depends on the speed of sound in the target liquid and the physical dimensions of the cavity. This enables direct determination of the speed of sound based on the measured resonance frequency. However, using a single cavity resonator has limitations, particularly due to the typically low acoustic impedance contrast between liquids and solids, which results in broad resonance peaks and low Q-factors. To enhance the quality factor (Q-factor), the cavity is enclosed by layers of phononic crystals (PnCs). A defining characteristic of PnCs is the presence of band gaps in frequency ranges in which acoustic or elastic wave propagation is inhibited.

The concept of the phononic-fluidic system was first implemented using a 1D phononic crystal in 2009 [45]. To determine the isopropanol concentration in water, the design of a 1D phononic-fluidic sensor was developed in two configurations: a three-layer structure comprising two aluminum plates with a water-filled cavity in between, and a seven-layer PnC with alternating aluminum and water layers.

After 2009, many theoretical and experimental studies investigated the frequency response of 1D phononic-fluidic sensors. They found serious problems in this kind of sensor, including very weak sensitivity and low limit of detection (LOD) in the small concentration range.

To overcome these issues, phononic crystals with 2D architecture were used [16]. It was proved that the use of a sensor made of a steel-based 2D PnC and a slit cavity resonator improved the LOD [16]. More recently, the slit cavity was replaced by a central cylindrical defect within a 2D steel PnC, which introduced an axisymmetric mode. This mode is characterized by the absence of shear displacement at the liquid interface, making it significantly less sensitive to shear viscosity [46].

To further improve the sensitivity and the quality factor, researchers developed a new type of phononic-fluidic sensor based on 3D architectures. Many complex geometries of 3D phononic crystals have been proposed to characterize liquids [47]. Thanks to the recent development of additive manufacturing techniques, these 3D phononic crystals are rapidly fabricated [48]. 3D PnCs are very attractive because they provide a larger width of band gaps with stronger suppression and cover all propagation directions of elastic waves [49].

I.5.3:Phononic Crystal for Liquid Characterization

In the following sections, we discuss the use of phononic-fluidic systems in all three dimensions of space (1D, 2D, and 3D) for liquid characterization.

I.5.3.1. One Dimensional Phononic Crystal for Liquid Detection

One-dimensional phononic crystals have attracted great attention due to their various applications, such as sensing [50], waveguiding [51], acoustic focusing [52], and topological phononics [53]. The most interesting application of 1D phononic crystals is liquid sensing for a wide range of applications, including environmental monitoring, the medical sector, and manufacturing control [54].

This type of liquid sensor relies on both the acoustic band gap properties of the material and the characteristics of the defect mode. The defect mode emerges within the phononic band gap (PnBG) and exhibits high transmission intensity. Its formation results from the intentional disruption of the periodic structure in the phononic crystal (PnC).

The properties of this defect mode, particularly its frequency position and transmission amplitude, are highly sensitive to changes in the acoustic properties of the liquid, such as density and speed of sound. As a result, 1D PnC-based sensors enable accurate monitoring of liquid composition and concentration by tracking shifts in the resonant peak. Their straightforward configuration and high performance make them well-suited for compact and cost-effective sensing platforms. The principal steps explaining the working of a one-dimensional phononic crystal as a liquid sensor are shown in Figure I.10 .

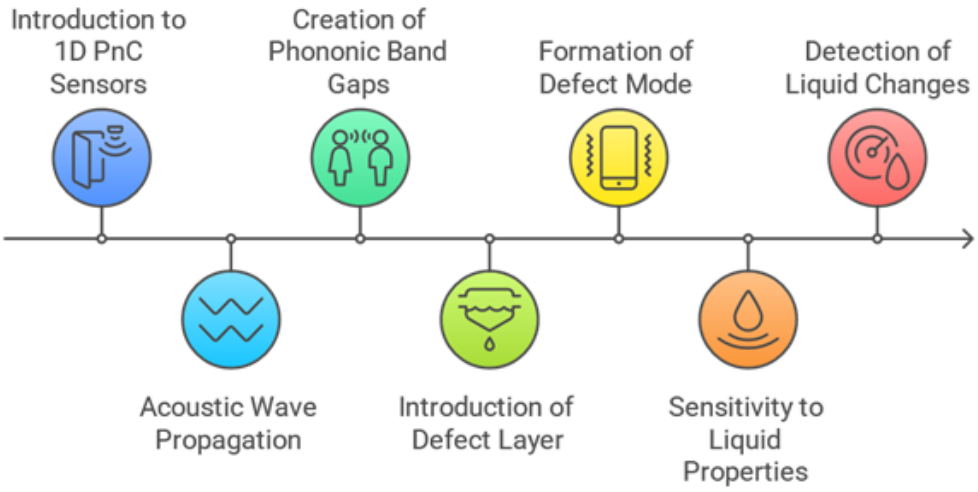

Figure I.10: Principal working of one-dimensional phononic crystal for liquid detection

Many theoretical and experimental works have explored the use of one-dimensional phononic crystals for liquid characterization. An experimental work by S. Villa-Arango and his team proposed a new form of 1D phononic crystal composed of multilayered glass and water [55]. The defect mode was introduced by changing the central layer thickness, resulting in the appearance of a defect frequency in the phononic band gap, as shown in Figure I.11.

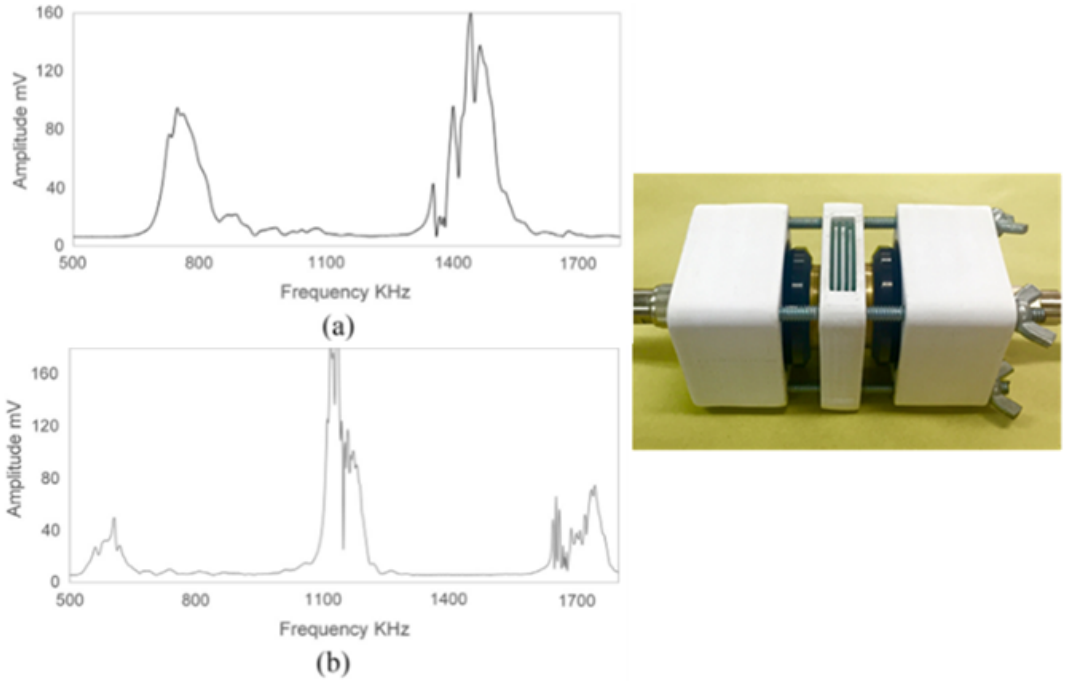

Figure I.11: experimental results of 1D phononic crystal composed of multilayered glass and water using water (a) and ethanol (b) as analytes.

The experimental results utilizing defect modes to generate a well-defined transmission peak inside the bandgap of the regular 1D Phononic crystal for measuring variations in the concentration of analytes in small liquid samples was developed,showing a bandgap between 0.8 MHz and 1.4 MHz, with a clear transmission peak close to 1.1 MHz. The peak stands out nicely within the bandgap—it's much higher than the noise and doesn't overlap with any other signals, making it easy to identify.

Gaurav Sharma and his team proposed a new design of a Si–SiO_2 phoxonic crystal with a defect layer for simultaneous sensing of biodiesel in a binary mixture of diesel through optical and acoustic waves, as shown in Figure I.12 [56]. The proposed model shows the feasibility of the phoxonic crystal sensor concept through acoustic and optical properties of an unknown liquid filled in a cavity. These structures can be useful for tailoring photon–phonon interaction with the simultaneous confinement of acoustic and optical waves in the GHz- and THz-range, respectively.

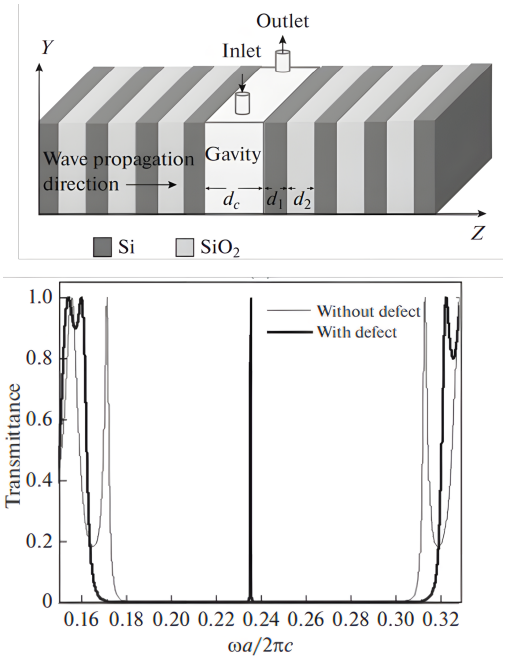

Figure I.12: Phoxonic crystal sensor concept through acoustic and optical properties of unknown liquid filled in cavity

Another attractive experimental work on one-dimensional phononic crystals was proposed by Hyeonu Heo et al. [57].

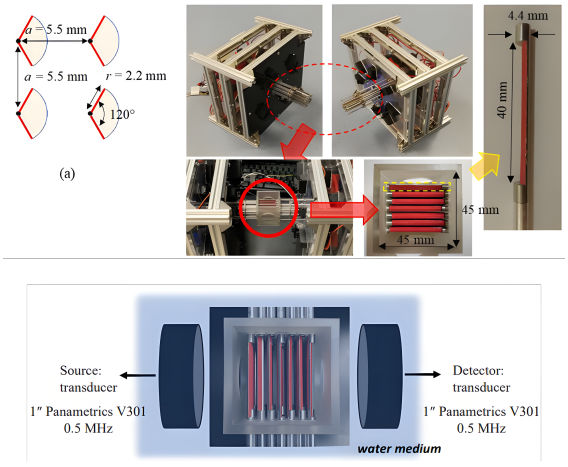

Figure I.13: Multifunctional acoustic device based on phononic crystal with independently controlled asymmetric rotating rods

They proposed a multifunctional acoustic device based on a phononic crystal with independently controlled asymmetric rotating rods, as shown in Figure I.13. In the proposed model, the elastic properties can be modulated by the rotation of asymmetric solid scatterers immersed in water.

I.5.3.2. 2D Phononic Crystal for Liquid Characterization

Two-dimensional phononic crystals are very attractive devices in several fields of application. For liquid characterization, a defect is intentionally introduced into the 2D PnC structure, such as a central cavity or a missing inclusion, which acts as a resonant cavity. This defect mode localizes acoustic energy and creates a sharp resonance peak within the band gap. The resonance frequency is strongly influenced by the acoustic properties of the liquid filling the defect, including density, viscosity, and speed of sound. By monitoring the shifts in resonance frequency or transmission amplitude, small changes in the liquid's physical or chemical composition can be detected. The axisymmetric modes supported in certain 2D configurations are particularly useful, as they minimize shear interactions at the liquid interface, enhancing sensitivity to bulk properties and reducing effects from shear viscosity. 2D PnC-based sensors offer high Q-factors, enhanced sensitivity, and compact designs, making them ideal for high-precision liquid characterization in applications such as chemical analysis, biosensing, and environmental monitoring.

A. Oseev and his team proposed a 2D phononic crystal made of stainless steel for the octane number (RON) determination of gasoline [58]. as shown in Figure I.14.

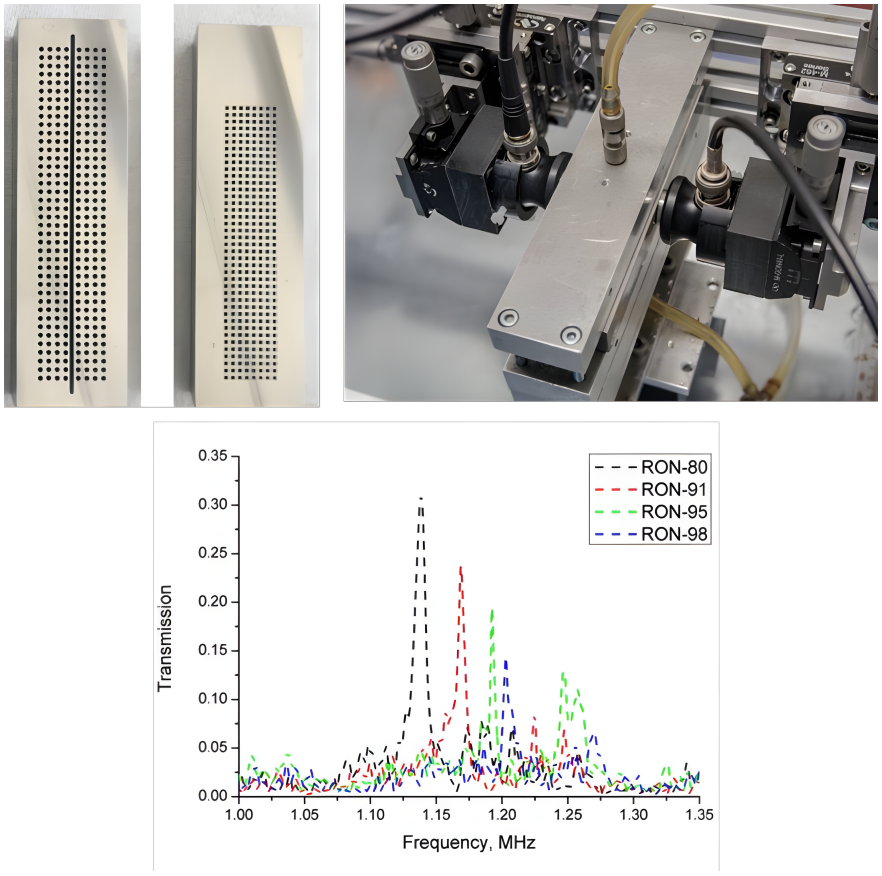

Figure I.14: 2D phononic crystal made of stainless steel for the octane number determination of gasoline

This study used a 2D phononic crystal as a sensing platform for a measuring system for real-time gasoline octane number determination. The method is based on the analysis of the transmission spectrum of a phononic crystal sensor filled with the liquid gasoline blend,The team showed that phononic crystal sensors can be considered prospective, competitive, and inexpensive devices for octane number determination.

Nikolay Mukhin and his team studied solid-liquid composite arrangements as alternative solutions for phononic crystal-based liquid sensors [59]. The authors proposed a novel concept of a narrow band solid-liquid composite arrangement. They demonstrated two different concepts to design narrow band structures and showed the results of theoretical studies and experimental investigations that confirm the theoretical predictions, as shown in Figure I.15.

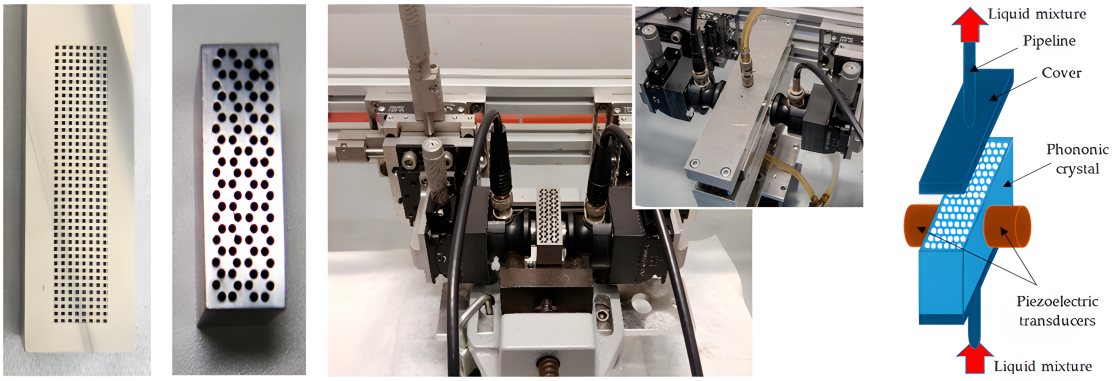

Figure I.15: 2D phononic crystal sensor with normal incidence of sound for liquid characterization

R. Lucklum and his colleagues investigated a 2D phononic crystal sensor with normal incidence of sound for liquid characterization [60]. This study demonstrates the sensing capabilities of resonance-induced extraordinary acoustic transmission through a phononic crystal composed of a metal plate perforated with a periodic square lattice of holes, under normal incidence of sound waves, as shown in Figure I.16.

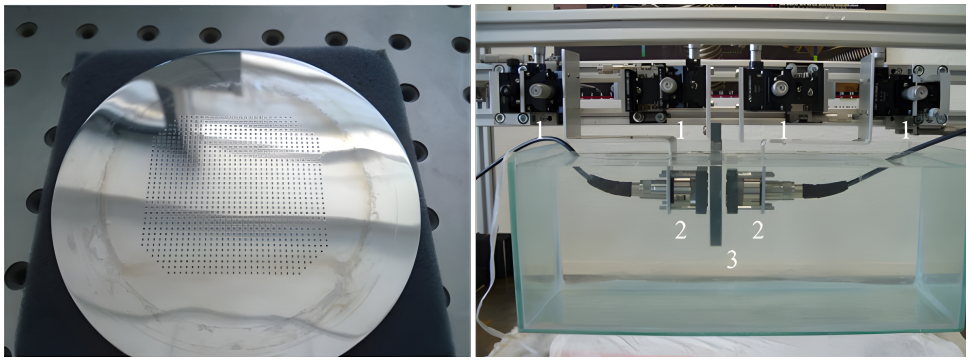

Figure I.16: 2D phononic crystal sensor with normal incidence of sound for liquid characterization

The characteristic transmission peak is highly sensitive to the speed of sound in the liquid. As a result, the frequency at which this peak occurs can be used as a reliable indicator for liquid analysis.

Ezekiel Walker and his team proposed a tunable 2D ultrasonic phononic crystal controlled by infrared radiation [61]. The proposed phononic crystal-based ultrasonic filter was designed by modulating the phase of a polymeric material embedded within a periodic structure through infrared (IR) radiation stimulation. This phononic crystal was engineered with a periodic structure to enable transmission in the ultrasonic frequency range. The same phononic crystal was filled with PNIPAm hydrogel at room temperature. Transmission spectra of the structure without PNIPAm were measured at 21°C and 38°C. The observed blueshift in the transmission bands is attributed to the increased speed of sound in water at elevated temperatures, as shown in Figure I.17.

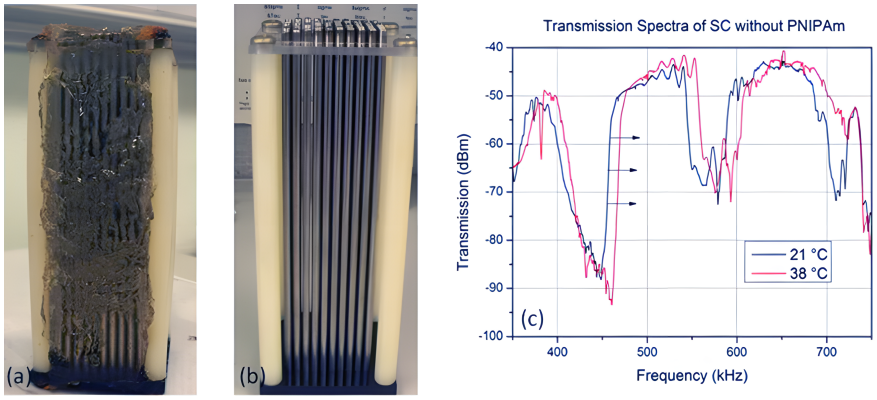

Figure I.17: 2D ultrasonic phononic crystal controlled by infrared radiation

I.5.3.3. 3D Printed Phononic Crystal for Liquid Characterization

Additive manufacturing techniques, such as 3D printing, have enabled the fabrication of complex three-dimensional phononic crystals (3D PnCs) with precise control over geometry and material composition. These structures exhibit full band gaps in all spatial directions, making them highly effective for manipulating acoustic wave propagation. When integrated with defect cavities, 3D PnCs can localize acoustic energy and exhibit resonance modes that are highly sensitive to the acoustic properties of liquids, such as speed of sound, density, and viscosity. By embedding liquid analytes into the defect regions, the resulting shift in resonance frequency can be used for accurate liquid characterization.

The use of 3D printing not only allows for rapid prototyping and customization of sensor architectures but also supports the integration of lightweight, compact, and cost-effective sensing devices. These printed 3D PnC-based sensors hold great potential for applications in chemical analysis, biomedical diagnostics, and environmental monitoring.

Several experimental works validated by COMSOL simulation were proposed for 3D-printed phononic crystals designed for liquid characterization. Frieder Lucklum and Michael J. Vellekoop proposed a 3D-printed phononic-fluidic cavity sensor to measure the volumetric physical properties of a liquid [62]. Their proposed geometry offers an ultra-sensitive determination of sodium chloride and glucose concentrations in aqueous solutions, as shown in Figure I.18.

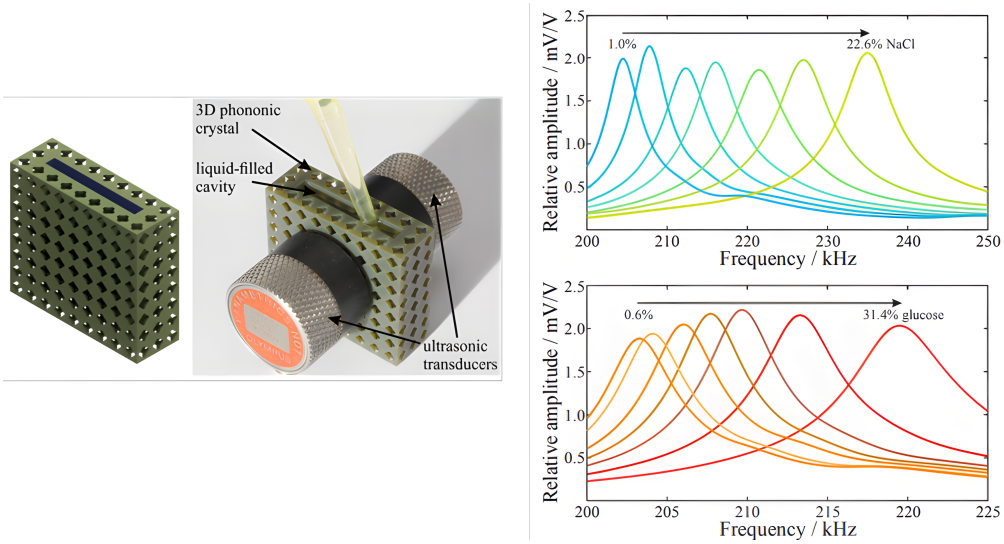

Figure I.18: 3D printed phononic crystal designed for liquid characterization

The same author, Frieder Lucklum, studied experimentally and numerically the complete acoustic band gaps in three-dimensional phononic crystals [63].Figure I.19 shows the 3D unit cell geometries considered in this study. This complete characterization illustrates their suitability as building blocks with well-defined, wide band gaps for use in phononic-fluidic sensor systems.

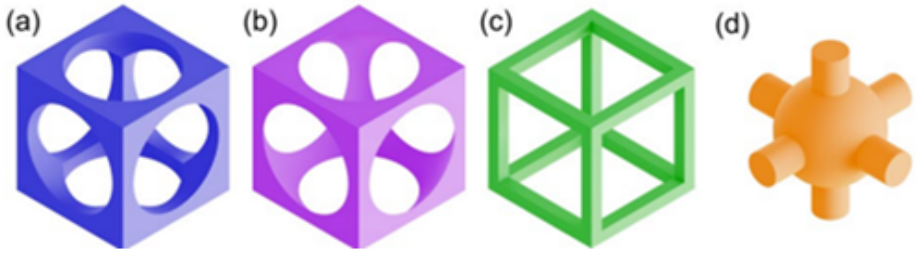

Figure I.19: Different 3D unit cell geometries considered for phononic band gap calculation: (a) Three cylindrical holes, (b) spherical cavity, (c) quadratic scaffold, and (d) ball suspended by three cylindrical beams

Yauheni Belahurau and Frieder Lucklum designed a 3D ultrasonic phononic-fluidic sensor using a cubic cell with a spherical void [64]. The focus of this study is a phononic-fluidic cavity sensor designed to measure the volumetric properties of liquids, as shown in Figure I.20. Based on the simulation results, they fabricated the most promising sensor designs using microstereolithographic 3D printing and conducted transmission measurements for different concentrations of 2-propanol in water.

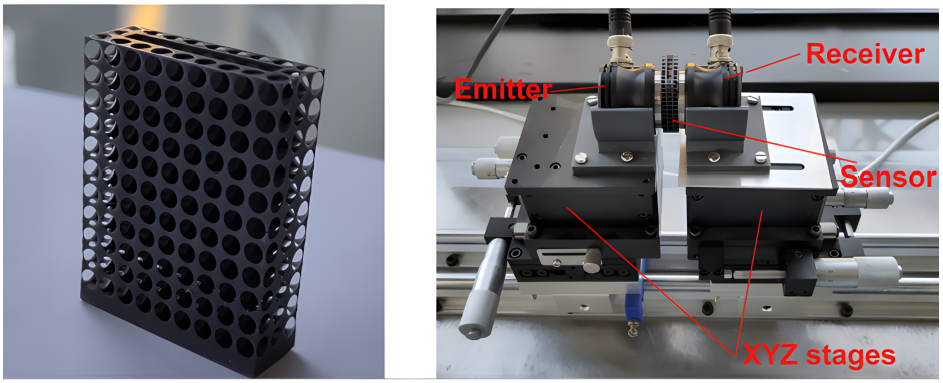

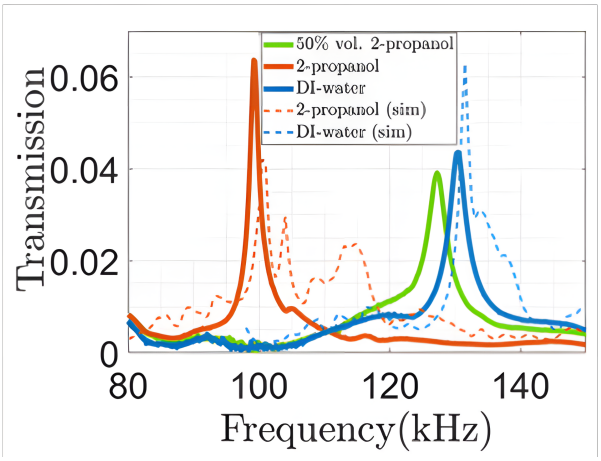

Figure I.20: 3D ultrasonic phononic-fluidic sensor using a cubic cell with spherical void and its acoustic transmission

I.6. CONCLUSION

In this chapter, we discussed the fundamental concepts of acoustic waves and phononic crystals, their classifications, and their technological applications, with a particular focus on liquid sensing using phononic structures. In addition, we described the recent developments in phononic-fluidic sensors for liquid characterization. Moreover, we discussed 3D-printed phononic crystals and their applications in determining the bulk properties of fluids, such as density, acoustic velocity, and viscosity.

CHAPTER II: COMSOL-Based Numerical Analysis of a Phononic-Fluidic Sensor

CHAPTER 2

COMSOL-BASED NUMERICAL ANALYSIS OF A PHONONIC-FLUIDIC SENSOR

II.1. INTRODUCTION

In this chapter, we discuss the theoretical and the experimental parts of the phononic crystal based liquid sensor. The theoretical analysis of the transmission spectrum and band diagrams of the fabricated 2D phononic was performed on the basis of numerical simulations with COMSOL Multiphysics software.

- Firstly, we describe the COMSOL Multiphysics implementation, including all computational steps from initial design to final optimization and simulation of the 2D phononic crystal liquid sensor.

- Secondly, we discuss the optimization and the fabrication of the phononic crystal used for complex liquid characterization.

- Thirdly, we experimentally test the frequency response of the phononic sensor with and without water as reference liquid. Moreover, we describe the preparation methodology for Acetone,Nikel Chloride and Sodium Chloride water-mixtures. The steps used for the acoustic transmission measurement is also presented in this section.

II.2. NUMERICAL ANALYSIS OF PHONONIC CRYSTAL

Analyses of transmission spectrum and band diagrams of the proposed phononic crystals were performed on the basis of numerical simulation with **COMSOLT Multiphysics** software. The band diagram was obtained by calculating discrete eigenfrequencies for wave vectors within the irreducible Brillouin zone. **Bloch-Floquet boundary** conditions were applied to the unit cell to account for periodicity. Next, we will discuss each step taken to determine the phononic band structure and the acoustic transmission.

II.2.1. Geometry construction

In order to compare numerical and experimental results, we have to consider a finite structural model, which represents the actual sensor element. Since the full 3D multiphysical finite element model with a long frequency sweep is computationally demanding, we decided to take only 2D modeling for the phononic crystal.

For our numerical experiments, we analyzed the model of phononic crystal made of a stainless steel matrix with a 2D periodic arrangement of air holes. **The periodic lattice parameter is set to a=4.5mm, and the hole diameter is d=4 mm**. The height of the phononic crystal is set to **h=25 mm**. The Figure II.1 show the different configurations of the phononic crystal geometry used in this study

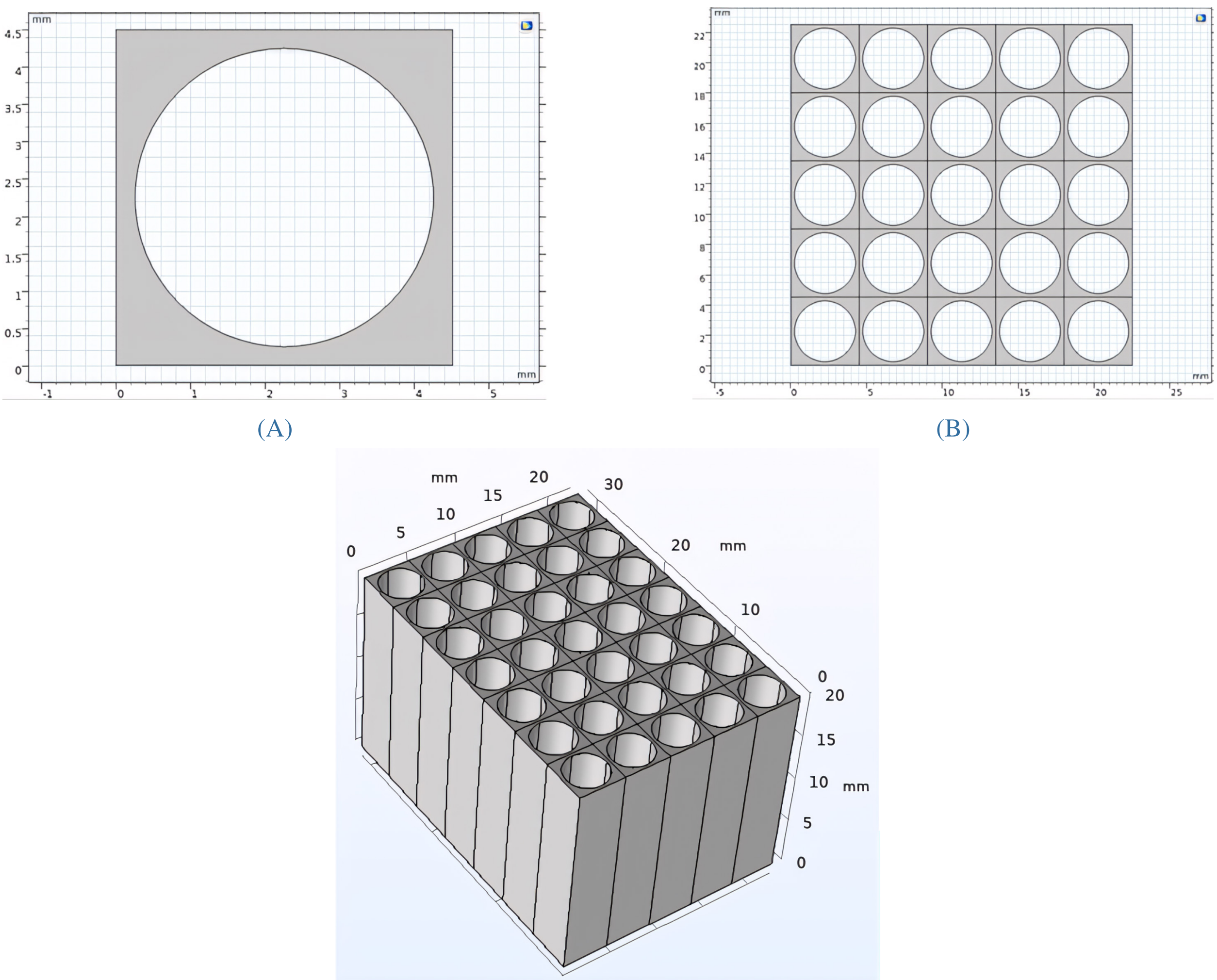

(A) (B) (C)

Figure II.1: Different configurations of the phononic crystal geometry. (a) Unit cell, (b) 5*5 cell 2D phononic crystal, and (c) 3D real structure

II.2.2. Solid-mechanic and Bloch's theorem

The numerical calculation and analysis of the frequency characteristics of phononic crystal was performed on the basis of the equation for the propagation of mechanical waves in an elastic medium [65].

$$\rho \frac{\partial^2 u_i}{\partial t^2} = \frac{\partial T_{ij}}{\partial x_j} i, j = 1, 2, 3 \tag{1}$$

where u_i are elastic displacement field components; T_{ij} are stress tensor components; ρ is the solid matrix density; x_j is vector coordinates; t is time.Figure II.2 show the mechanical stress of our proposed phononic crystal at the frequency of 0.879MHz

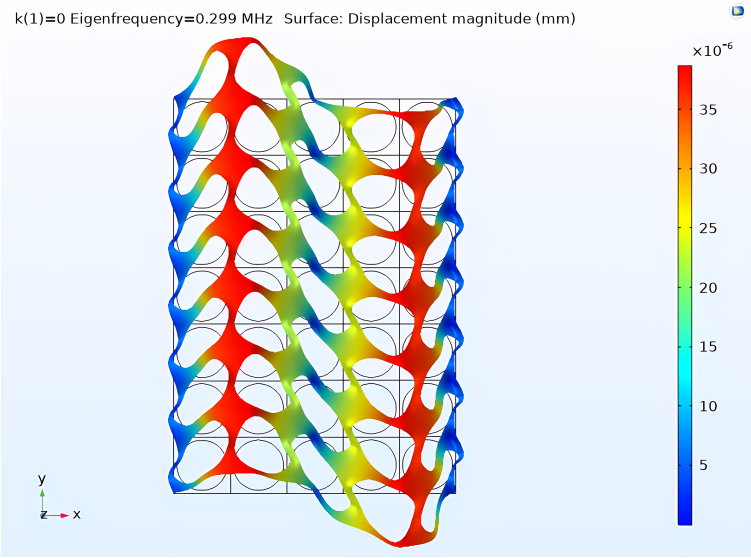

Figure II.2: Mechanical stress of our real (5*7 cell) phononic crystal at specific frequency

Considering that the structure is a periodic arrangement, we apply Bloch's theorem to obtain the eigenfrequencies solutions as a product of propagating wave and periodic function of phononic structure. The periodic conditions used in this work are shown in Figure II.3. The displacement vector can be represented in a following way:

$$u(\mathbf{r}, t) = e^{i(\mathbf{k}\cdot\mathbf{r} - \omega t)} u_{\mathbf{k}}(\mathbf{r}) \tag{2}$$

where $u_{\mathbf{k}}(\mathbf{r})$ is a periodic function of $\mathbf{r}$ with the same periodicity as the structure; $\mathbf{k}$ is a wave vector; $\mathbf{r}$ is lattice parameter.

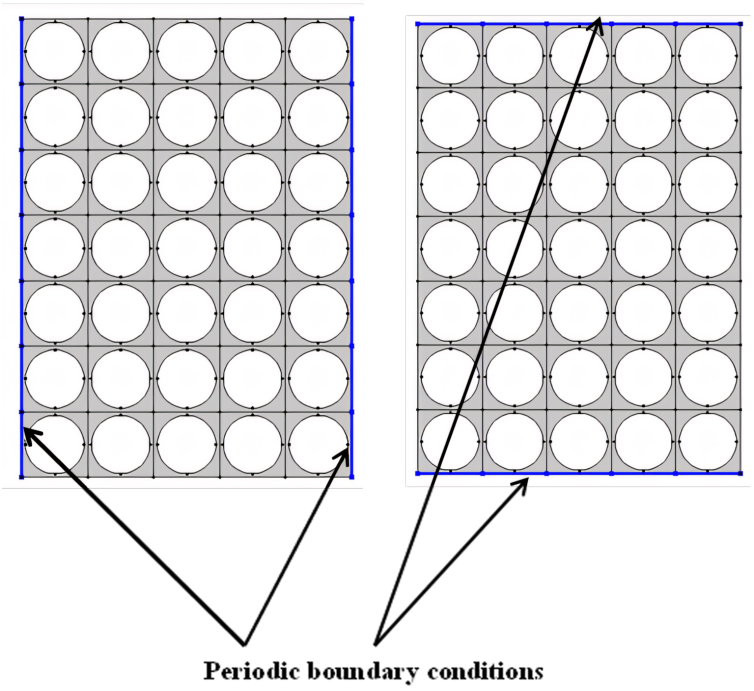

Figure II.3: Periodic conditions used in this work

II.2.3. Pressure acoustic module for phononic-fluidic structure

The objective of this study is to investigate the frequency characteristics of a phononic crystal containing a liquid-filled central cavity. The presence of the liquid induces pressure resonances within the cylindrical structure, see the Figure II.4. The resonant modes are determined by solving the eigenvalue problem for acoustic waves in a cylindrical cavity. The governing equation for harmonic pressure wave propagation is the Helmholtz equation, expressed as [65]

$$\nabla^2 p + \frac{\omega^2}{c^2} p = 0 \tag{3}$$

where p is pressure; ω is circular frequency; c is the speed of sound in a liquid. **The conditions at the solid–liquid interfaces are:**

$$-\mathbf{n} \cdot \nabla p = \rho \mathbf{n} \cdot \frac{\partial^2 \mathbf{u}}{\partial t^2} \tag{4}$$

where $\mathbf{n}$ is the normal vector directed from the solid-state body; $\mathbf{u}$ is the vector of mechanical displacement in a solid. The solid–liquid interfaces defined in this work are show in Figure II.5.

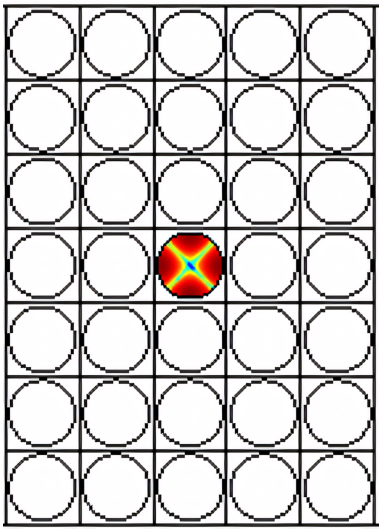

Figure II.4: Symmetrical Resonant mode of the liquid induces pressure resonances within the cylindrical structure

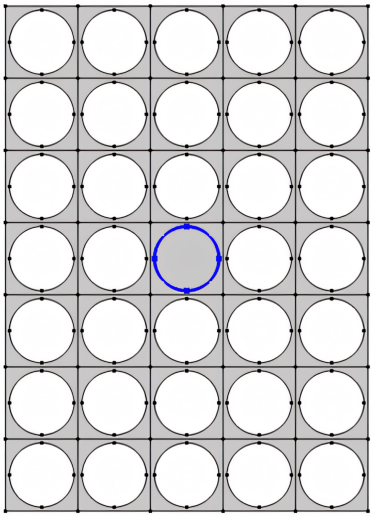

Figure II.5: The solid–liquid interfaces defined in this work

To calculate viscosity losses, **the Navier–Stokes equation** should be used instead of the Helmholtz equation [66]:

$$\rho\left(\frac{\partial \mathbf{v}}{\partial t}+(\mathbf{v}\cdot\nabla)\mathbf{v}\right)=-\nabla p+\mu\nabla^2\mathbf{v}+\left(\zeta+\frac{\mu}{3}\right)\nabla(\nabla\cdot\mathbf{v}) \tag{5}$$

where $\mathbf{v}$ is the velocity vector of the liquid; μ is the shear viscosity; ζ is the bulk viscosity; c is the speed of sound.

The described Equations (1), (3), (4), (5) and (6) together with the boundary conditions (2) are sufficient for calculating the propagation of acoustic waves in solid and liquid media

II.2.4. Mesh condition

The model is meshed finely enough to capture the minimum wavelength encountered in this study, as show in the Figure II.6. As a rule of thumb, this required eight elements per lattice constant. Thus, the maximum element size is set as

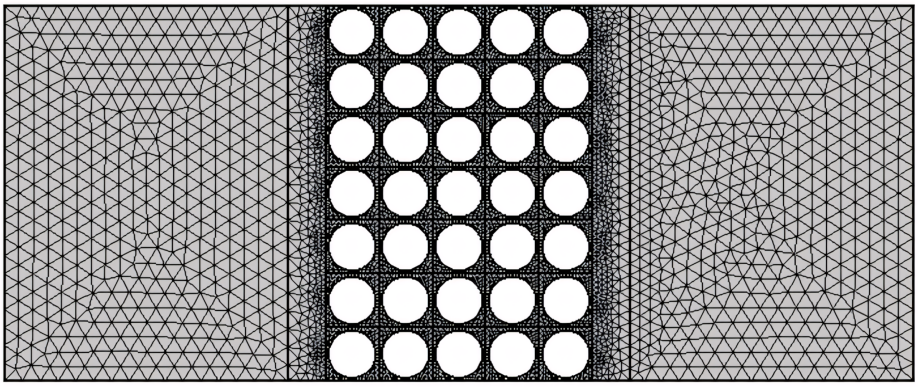

Figure II.6: The mesh of the our real model of phononic-fluidic structure used in this work

II.3. STUDY OF TRANSMISSION SPECTRUM AND BAND DIAGRAMS

II.3.1. Phononic crystal without liquid defect

In this part, the modeling results of the band diagram of an empty phononic crystal (PnC) as well as the acoustic transmission of a finite structure of the PnC without point defect are investigated. Figure II.7 shows the band diagram of a two-dimensional phononic crystal made of steel with a periodic arrangement of cylindrical empty holes.in this work, we have studied four different geometrics: Unite cell, translational supercell with **3*a** side, translational supercell with **5*a** side and the real structure **(5a*9a)**. The phononic band structures are determined according to the coordinates of direction points of special symmetry in the first Brillouin zone as follows:
Γ-X-M-Γ.

For all different configurations, the phononic band structure of an empty PnC show an area of forbidden propagation of acoustic waves, so-called a bandgap, **from 315 to 460 kHz**. This area is highlighted in grey

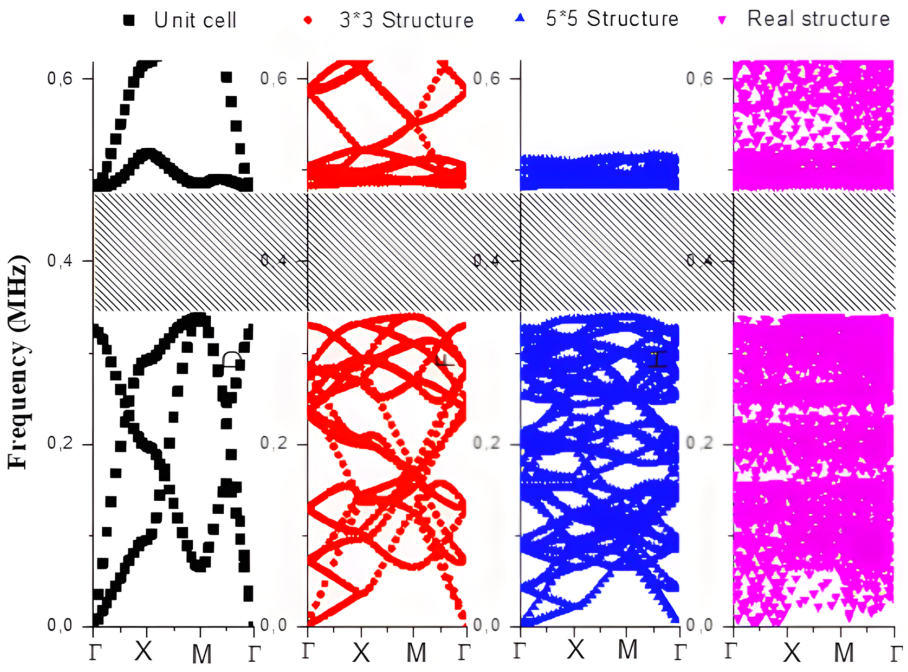

Figure II.7: band diagram of a two-dimensional phononic for four different configurations: Unite cell, translational supercell with 3*a side, translational supercell with 5*a side and the real structure (5a*9a)

To validate these findings, we conducted a complementary numerical transmission analysis. The finite element model was extended from a unit cell to a semi-infinite lattice configuration, employing periodic boundary conditions in directions perpendicular to wave propagation. A normal displacement of 1 mm (time-harmonic, constant amplitude) was applied to the excitation face, while a low-reflecting boundary condition was implemented on the opposite termination face, see Figure II.8 and Figure II.9

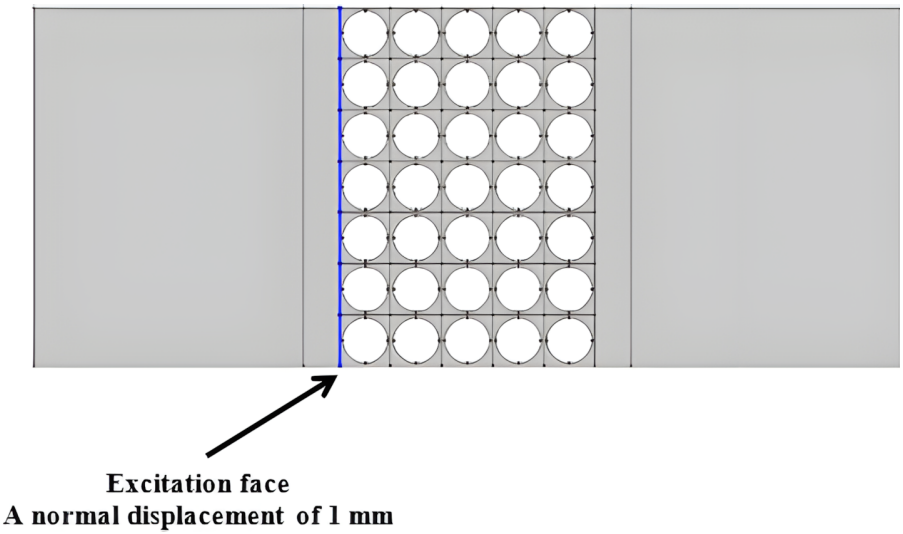

Figure II.8: Longitudinal waves acoustic wave excitation using a normal displacement at excitation.

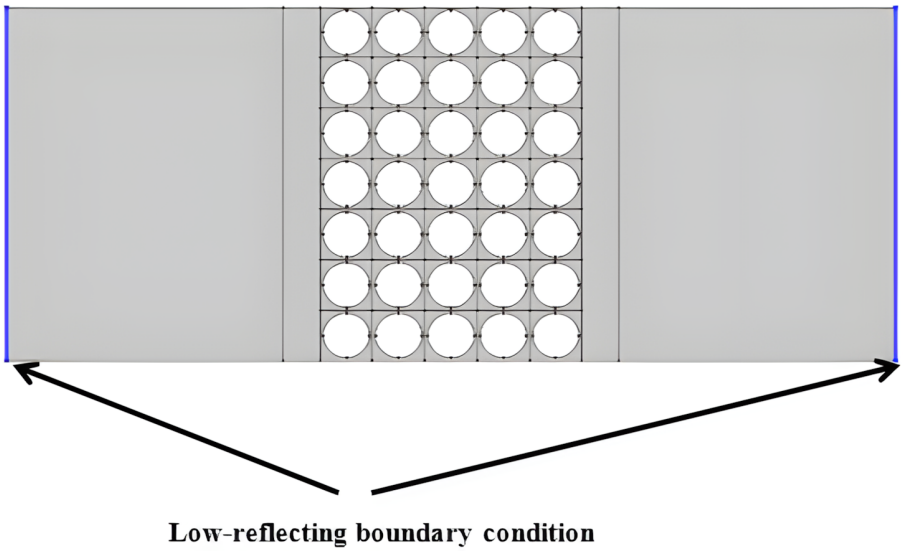

Figure II.9: Low-reflecting boundary condition implemented on the opposite terminations faces

The transmission coefficient was computed as the ratio of transmitted to incident energy flux. The resulting transmission spectrum, presented as disable amplitude versus frequency, is shown alongside the band structure in Figure II.10, demonstrating good agreement between the phononic band gaps highlighted in gray.

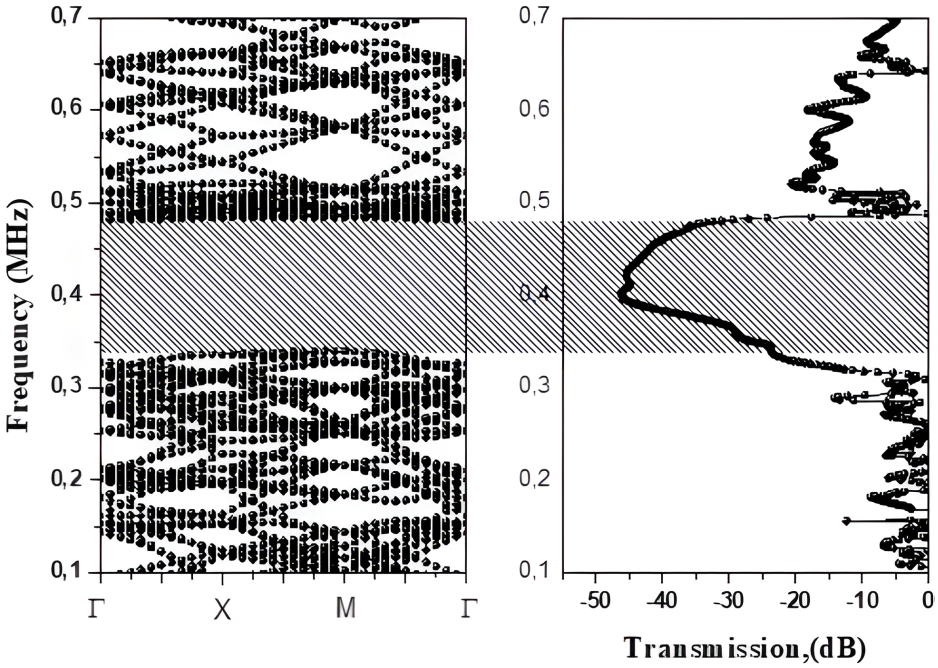

Figure II.10: Transmission spectrum versus frequency, is shown alongside the band structure of an empty phononic crystal

II.3.2. Phononic crystal with distilled water defect Mode

In this work, the distilled water is used as reference liquid for all mixtures. As the first step and in order to test the sensitivity of our phononic sensor to known liquid (water), we added the distilled water in the phononic sensor based on two different configurations:

- **Point defect modes**: the liquid is added in the central hole of the phononic crystal
- **Line defect modes**: the liquid cover the whole line perpendicular to the propagation direction of the acoustic wave

II.3.2.1. Point defect modes

The principal configuration used in this work is the **point defect model**. In this structure, the pure water is putted in the central hole of the phononic crystal, as it's shown in the Figure II.11. In this figure, we show the total acoustic pressure of the symmetric mode of the distilled water induced in the central hole of the phononic crystal at a specific frequency

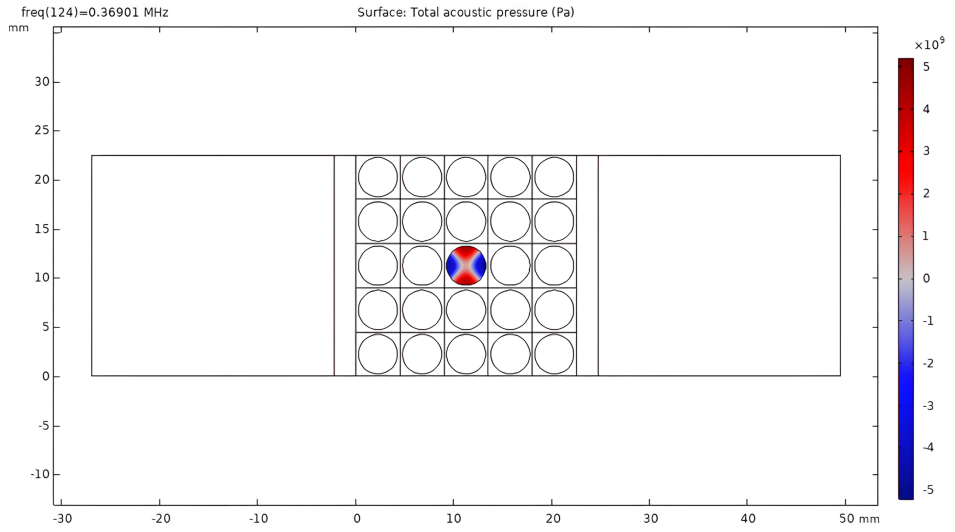

Figure II.11: Total acoustic pressure of the symmetric mode of the distilled water induced in the central hole of the phononic crystal at a specific frequency

Figure II.12 show the acoustic transmission spectrum versus frequency, alongside with the band structure of a phononic crystal with distilled water in the center point defect. The phononic band structures are determinates according to the coordinates of points of special symmetry in the first Brillouin zone are determined as follows: Γ-X-M-Γ. From this figure, two defects vibrations modes correspond to the distilled water appear in the phononic band gaps, one at 0.367MHz and another one at 0.441MHz. This result is validating by the two forms, the acoustic transmission

and the phononic band structure. The physical origin for the apparition of these two modes is the breakdown the periodicity of the phononic crystal by the liquid.

In order to identify these modes, we used the acoustic pressure model in the COMSOL multiphysics. The first one is symmetric mode as shown in the Figure II.11 and another one is non-symmetric mode.

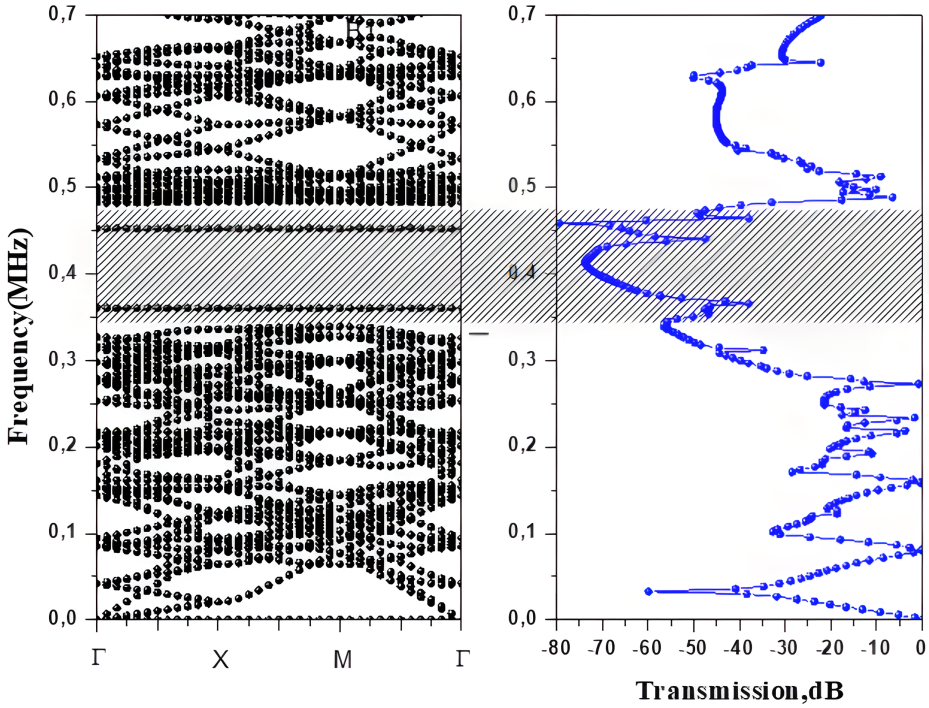

Figure II.12: Transmission spectrum versus frequency, is shown alongside the band structure of an phononic crystal with distilled water in the center point defect

Key Difference

- **MHz** measures **frequency** (how fast a wave oscillates).
- **dB** measures **intensity or power** (how strong the signal or sound is).

Where:

- **MHz (Megahertz)**
  - **Definition:** A unit of frequency equal to **one million hertz** (10^6 Hz).
  - **Usage:** Measures the number of cycles per second in periodic signals, such as sound waves, radio waves, or processor clock speeds.

- **dB (Decibel)**
  - **Definition:** A **logarithmic unit** used to express the **intensity (amplitude) of sound, power, or signal strength** relative to a reference level.
  - **Usage:**
    * **Sound Pressure Level (dB SPL):** Measures loudness (e.g., 60 dB is normal conversation, 120 dB is a jet engine).
    * **Signal Gain/Loss (dB):** Quantifies amplification or attenuation in electronics or acoustics.

II.3.2.2. Line defect modes

In this configuration featuring line defect modes, water is introduced uniformly along the entire channel perpendicular to the acoustic wave propagation direction . The figure displays the total acoustic pressure field of the symmetric mode in distilled water within the phononic crystal's line defect at a specified resonant frequency.which is visualized in (Figure II.13) as a localized acoustic pressure field along the defect channel.

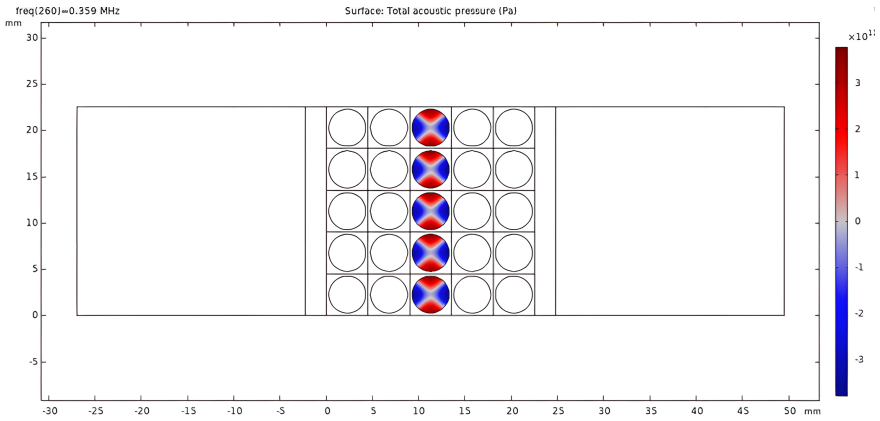

Figure II.13: Total acoustic pressure of the symmetric mode of the distilled water induced in the line defect of the phononic crystal at a specific frequency

Figure II.14 show the acoustic transmission spectrum versus frequency with the band structure of phononic crystal with distilled water introduced uniformly along the entire channel perpendicular to the acoustic wave propagation direction. The phononic band structures are determinates according to the coordinates of points of special symmetry in the first Brillouin zone are determined as follows:Γ-X-M-Γ.A superposition of fives defect modes is localized in phononic band gap and observed on the acoustic transmission as well as the phononic band gap.

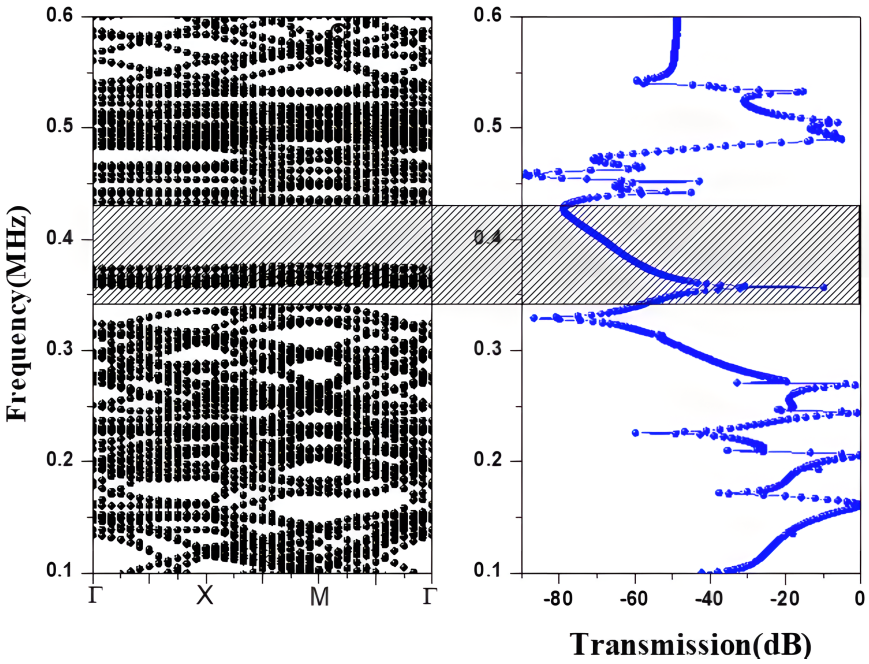

Figure II.14: Transmission spectrum versus frequency, is shown alongside the band structure of an phononic crystal with distilled water introduced uniformly along the entire channel perpendicular to the acoustic wave propagation direction

II.4. PHONONIC CRYSTAL SENSOR FOR LIQUID MIXTURE ANALYSIS

This study investigated three distinct liquid mixtures based on point defect to assess the phononic crystal's sensing performance: Water-acetone (organic-aqueous system), Nickel chloride-water (transition metal salt solution), Sodium chloride-water (alkali metal electrolyte)

The selected mixtures represent fundamentally different chemical systems, enabling comprehensive evaluation of the sensor's response to various solute types, including polar organics, transition metal ions, and simple electrolytes

II.4.1 Acetone–Water Mixture Characterization

II.4.1.1. Acoustic transmission

In this part, we discussed the acoustic transmission of our proposed phononic crystal used as sensor for complexes mixtures characterization .in the first case; we study the Acetone–Water Mixture for different acetone concentrations ranging from 0 to 100%.

Figure II.15 show the magnitude of the acoustic transmission for longitudinal wave propagation for acetone-Water Mixture for different acetone concentration. The transmissions for each acetone

concentrations are obtained using our proposed real model of phononic crystal. The COMSOL model of phononic crystal deal with unknown liquid by two parameters: **the acoustic velocity and the density.** Based on this, we identified each acetone concentration by its corresponding longitudinal acoustic velocity and mass density [67]. As shown in the figure, we found the formation of phononic band gap localized between 0.315MHz and 0.46MHz. In addition, the transmission peaks appear within the band gap, with each peak position being acetone concentration-correspondence. Based on the resonant frequency of each acetone concentration, the acoustic velocity could be determinate.

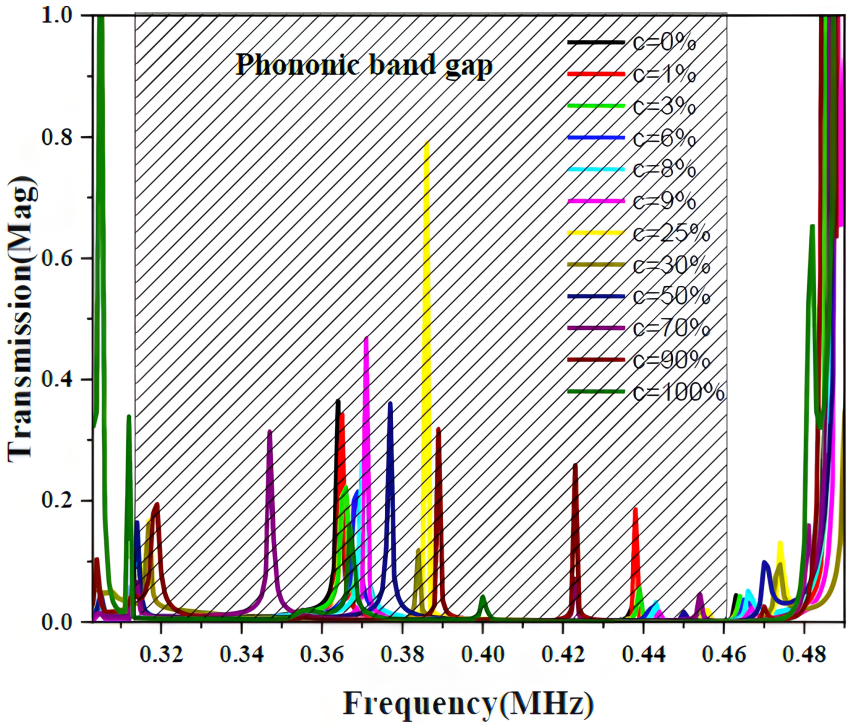

Figure II.15: the magnitude of the acoustic transmission acetone-Water Mixture for different acetone concentration

II.4.1.2. Calibration curve

In analytical chemistry, a calibration curve (or standard curve) serves as a fundamental quantitative tool for determining analyte concentrations in unknown samples. This method involves:

- Measuring responses from standard solutions of known concentrations
- Establishing a mathematical relationship between signal response and concentration
- Interpolating unknown sample concentrations from this reference curve”

In our work, the calibration curve is represented by the variation of the resonant frequencies of each concentration as function of acetone concentrations, see the Figure II.16. In the low acetone concentrations, we found only one vibrating mode, increases as acetone concentration increases and the frequency reach it maximum at acetone concentration equal to 22% and started to decreases. **The analysis reveals a concentration-dependent emergence of acoustic modes within the phononic band gap. For high acetone concentrations (up to 70%), we observe the appearance of additional acoustic modes. Specifically:**

- **70% concentration** exhibits two distinct vibrational modes (consistent with the 80% sample).
- **90-100% concentrations** demonstrate three acoustic modes

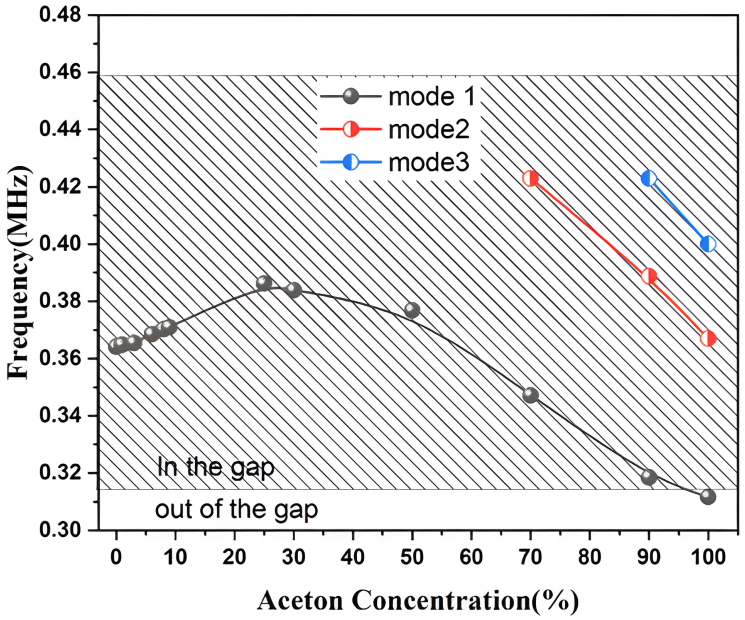

Figure II.16: The dependence of the resonant frequency on the acetone concentration of the acetone-Water Mixture

In order to explain the behavior of the acoustic transmission caused by the acetone concentration, the resonant frequencies of the first mode and its corresponding mass densities are plotted as function of the acetone concentration, as shown in Figure II.17. The results reflect the acoustic transmission response of the phononic crystal to a change of density and speed of sound (depend on the resonant frequency) of the liquid confined in central hole.

With the increase of acetone concentration (0—25%), the resonant frequency (speed of sound) gradually increases and reaches a maximum at the concentration of 25%. When the acetone concentration is further increased, the resonant frequency decreased with the increasing of acetone

concentration. When the concentration is more than 25%, the solubility of acetone in water started to change. Therefore, the relationship between the resonant frequency (speed of sound) and acetone concentration showed an opposite change.

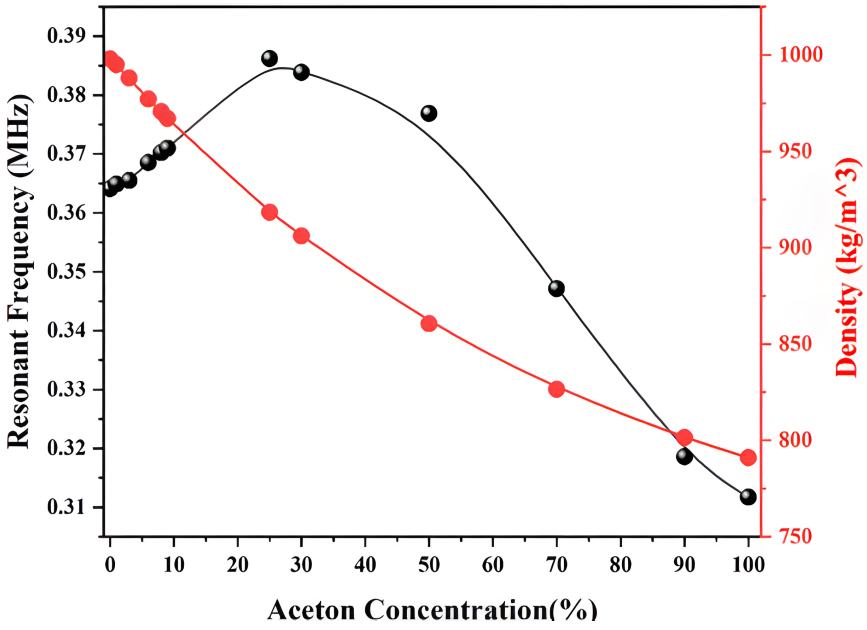

Figure II.17: Calibration curve of the Acetone–Water Mixture plotted with masse density

With the concentration of 25% or more, acetone is completely dissolved in water, and water is saturated with acetone. Therefore, using pure water as a reference, we divide the calibration curve into two parts (low concentration (1–9%) and high concentration (25–100%) to calculate the sensor performance parameters

II.4.1.3. Quality factor (Q-factor), Sensitivity, and Figure of Merit (FoM)

To investigate the performance quality of the liquid phononic sensor for Acetone–Water Mixture Characterization, we obtained the **Quality factor (Q-factor), Sensitivity, and Figure of Merit (FoM)**, tabulating the results inTable II.1. To achieve this, we used the obtained acoustic transmission along with the following equations:[68,69]

1. **The quality factor (Q-factor)** of a phononic crystal is a key parameter that quantifies the resonance sharpness and energy dissipation in the system. It is defined as:

$$Q = \frac{f_r}{f_{HBW}} \tag{6}$$

where:

- f_r: **Resonant frequency** (peak frequency of transmission)
- f_{HBW}: **Full width at half maximum** (FWHM, of the resonance peak)

2. **The sensitivity** of a phononic sensor quantifies its ability to detect small changes in the target parameter (concentration). For concentration sensor, sensitivity can be defined as:

$$S = \frac{\Delta f}{\Delta C} \tag{7}$$

where:

- Δf = Shift in resonant frequency (Hz)
- ΔC = Change in concentration (mol/kg or %)

3. **Figure of Merit (FoM)** of the phononic sensor is a dimensionless parameter that quantifies its **overall performance** by combining **sensitivity (S)** and **quality factor (Q)**, it is defined as:

$$FoM = \frac{Q}{f_{HBW}} \tag{8}$$

where:

- **S** = Sensitivity (frequency shift per concentration change)
- **Q** = Quality factor (dimensionless, from resonance sharpness)

As seen from Table II.1, we get very acceptable Quality factor and sensitivity of about 298.47541 and 0.0076 Hz for just a concentration change of 1% by our PnC sensor. Besides the high sensitivity, the sensor showed very high values for other parameters. Also, all parameters are reversely proportional to concentration increases.

Table II.1: Performance parameters for Acetone–Water Mixture Characterization

Concentration %	Frequency MHz	Density Kg/m^3	FWHM MHz	Quality Factor	Sensitivity kHz	FOM
0	0.36414	998	0.00122	298.47	–	–
1	0.3649	995.05	0.00106	344.24	0.76	0.71
3	0.3655	987.96	0.00165	221.51	0.68	0.41
6	0.36853	977.09	4.38E-4	841.39	1.46	3.33
8	0.37025	970.58	0.00136	272.24	3.055	2.24
9	0.37098	967	8.36E-4	443.75	6.84	8.18
25	0.38622	918.30	7.11E-4	543.20	1.38	1.94
30	0.38387	906.08	0.00101	380.06	3.94	3.90
50	0.37688	860.45	0.00109	345.76	0.63	0.58
70	0.34715	826.41	0.00117	296.70	0.84	0.72
90	0.31856	801.4	0.00177	179.97	2.27	1.28
100	0.31169	791	4.39E-4	710	5.24	11.94

II.4.2 Nickel chloride ($NiCl_2$)–Water Mixture Characterization

II.4.2.1. Acoustic transmission

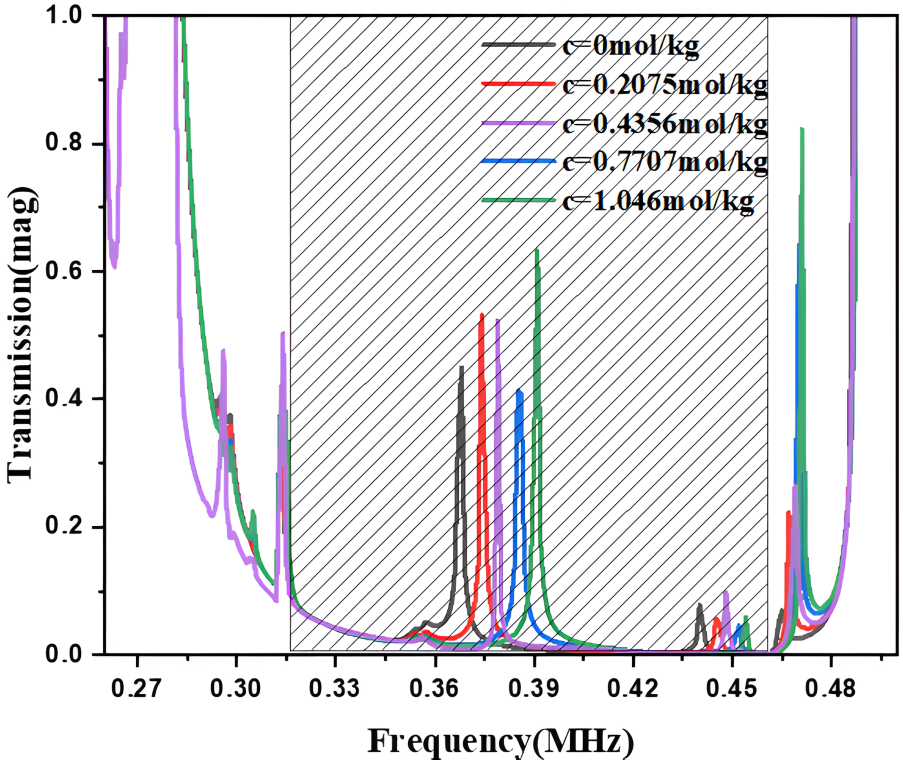

Figure II.18: The magnitude of the acoustic transmission Nickel (II) chloride–Water Mixture for different NiCl2 concentration

Following the proposed procedure of simulation, we have used the same phononic sensor to charctrize Nickel (II) chloride–Water Mixture. When the central defect hole in the phononic crystal (PnC) is filled with a nickel (II) chloride-water mixture, each concentration (0 mol/Kg to 1.046 mol/Kg) produces a distinct resonant peak at a characteristic frequency within the band gap, as shown in Figure II.18. From this figure, we can see that resonant frequency shift up to the higher frequencies when the NiCl2 concentration increases. For $NiCl_2$ concentration equal to 0% (pure water) the resonant frequency equal to 0.367MHz and when the $NiCl_2$ concentration equal to 1.046mol/Kg, the resonant frequency equal to 0.3908MHz.

II.4.2.2. Calibration curve

Figure II.19 shows the dependency of the resonant frequency and the mass density on the NiCl2 concentration. Both of The resonant frequency and the density of the mixture increase linearly as the concentration of NiCl2 increases.The main factors contributing for this behavior are density and stiffness. Higher ion concentration strengthens intermolecular forces, effectively raising the solution's bulk modulus **while both density and stiffness increase with salt content; the bulk modulus dominates over density in the acoustic velocity and resonant frequency equation.**

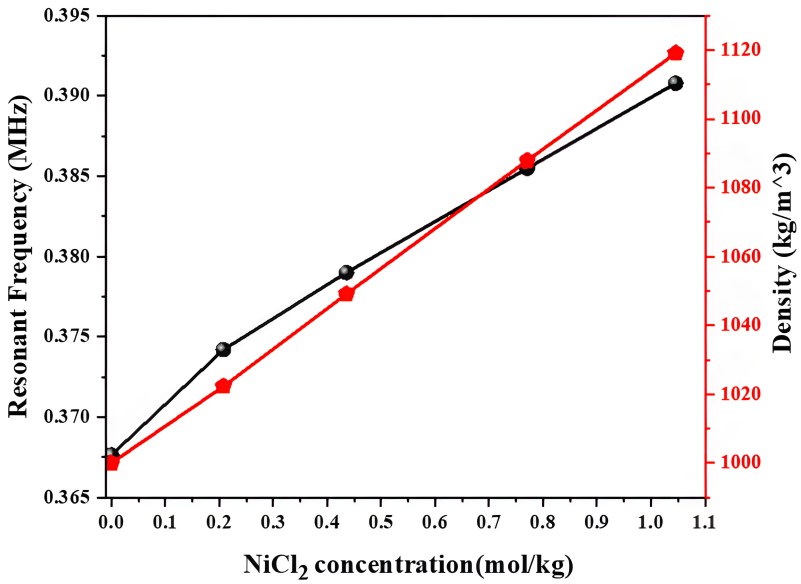

Figure II.19: Calibration curve of the Nickel (II) chloride–Water Mixture plotted with masse density

II.4.2.3. Quality factor (Q-factor), Sensitivity and Figure of Merit (FoM)

Figure II.20 show the variation of calculated quality factor (Q-factor), sensitivity, and Figure of Merit (FoM) as function of $NiCl_2$ concentration. We can see that the phononic sensor performance is highly affected by the $NiCl_2$ concentration. From this figure we observe that of the sensitivity and

Figure of Merit (FoM) are both increases with the raising of the $NiCl_2$ concentration.In addition, we observe a pronounced minimum in the quality factor plot at a concentration of 0.43 mol/kg. This reduction in the quality factor arises due to large transmission peak and high full width at half maximum (FWHM) at this concentration, indicating a potential resonance damping effect or energy dissipation mechanism under these conditions."

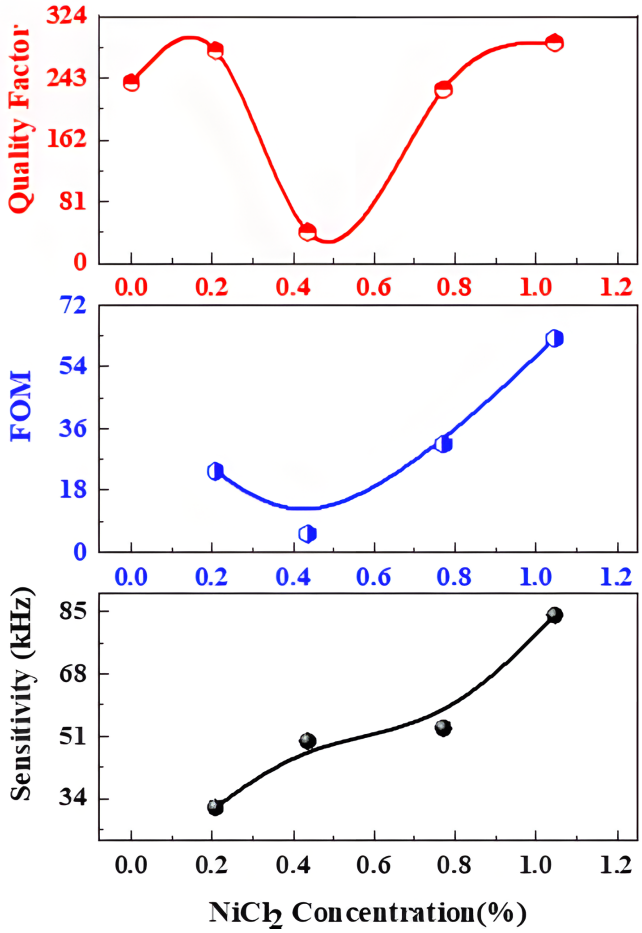

Figure II.20: Quality factor (Q-factor), Sensitivity and Figure of Merit (FoM) of phononic crystal sensor for Nickel chloride–Water Mixture characterization

II.4.3 Sodium chloride (NaCl)–Water Mixture Characterization

II.4.3.1. Acoustic transmission

We have done the same work on the charctrize the mixture Sodium chloride (NaCl)–Water with different concentration of NaCl, ranging from 0% to 22.6%. The Figure II.21 show the magnitude of acoustic transmission for the mixture and each concentration has its corresponding transmission peak with well-defined resonant frequency. As the same as Nickel chloride (NiCl2)–Water Mixture, the resonant frequency shift-up to the higher frequency as the NaCl concentration increase.

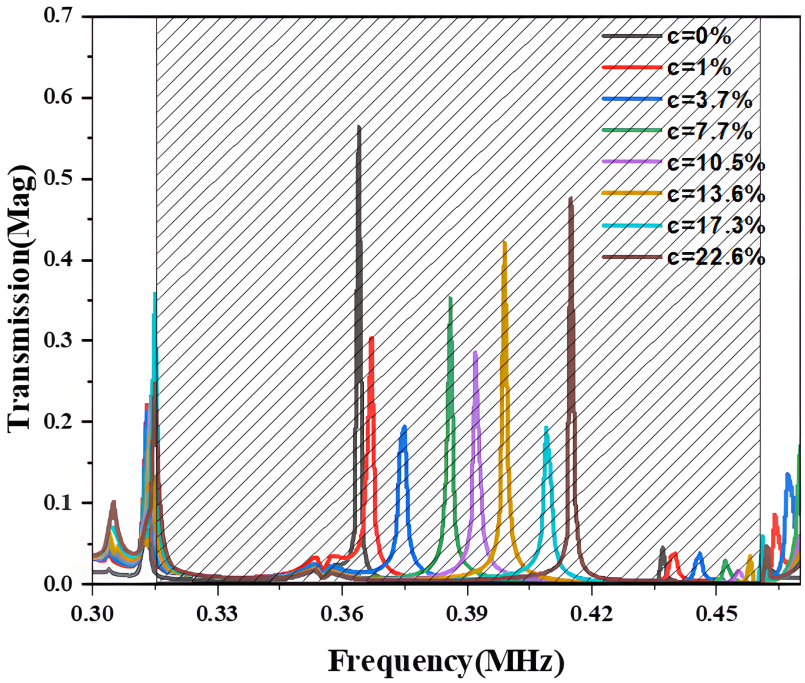

Figure II.21: The magnitude of the acoustic transmission Sodium chloride (NaCl)–Water Mixture for different NaCl concentration

II.4.3.2. Calibration curve

Figure III.22 presents the calibration curve for the phononic crystal sensor used in sodium chloride (NaCl)-water mixture characterization, plotting resonant frequency and the mass density versus NaCl concentration.

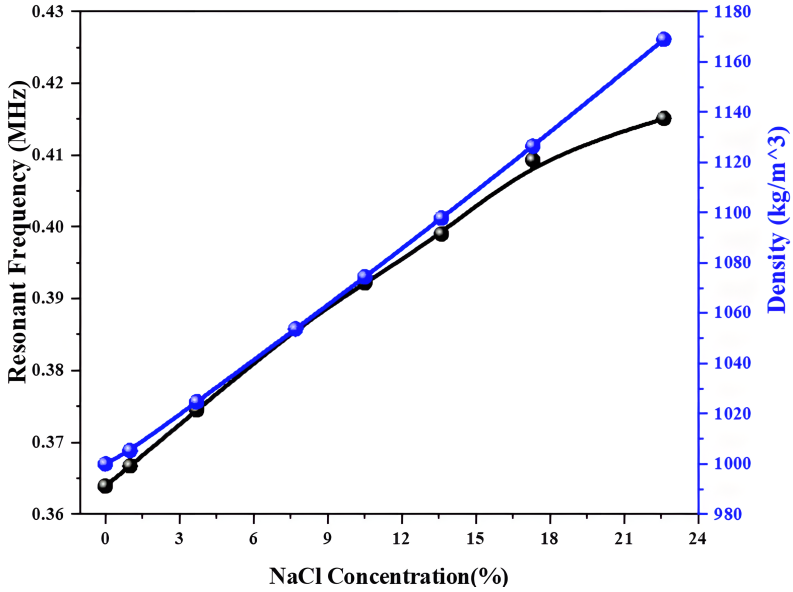

Figure II.22: Calibration curve of the Sodium chloride (NaCl)–Water Mixture plotted with masse density

These results demonstrate a clear increase in resonant frequency with concentration. In addition, a linear relationship between NaCl concentration and solution density is observed.

II.4.3.3. Quality factor (Q-factor), Sensitivity and Figure of Merit (FoM)

Table II.2: Performance parameters for Sodium chloride (NaCl)–Water Mixture Characterization

Concentration %	**Q-Factor**	**Sensitivity** KHz	**FOM**
0	443.78	–	–
1	308.15	2.8	2352.94
3.7	234.06	3.92	2450
7.7	324.20	5.475	4600.84
10.5	304.03	10.1	7829.45
13.6	369.44	11.32	10481.48
17.3	265.77	12.27	7967.53
22.6	461.22	9.66	10733.33

II.5. CONCLUSION

In this chapter, we present a detailed numerical study of a phononic-fluidic sensor using COMSOL Multiphysics, including geometry design, simulation of wave propagation, and analysis of transmission spectra for various liquid mixtures. In addition, we numerically determine the effect of concentration on the acoustic transmission and the sensor performances of three different complex mixtures: acetone-water, NiCl-water and NaCl-water.

CHAPTER III: Experimental Investigation of Phononic Crystals for Liquid Sensing Applications

CHAPTER 3

EXPERIMENTAL INVESTIGATION OF PHONONIC CRYSTALS FOR LIQUID SENSING APPLICATIONS

III.I. INTRODUCTION

In this chapter, we presents the results of the frequency response of our fabricated phononic crystal. Additionally, we explore its potential as a sensor for liquid mixture characterization and the identification of unknown concentrations. Three different liquid mixtures were tested: water-acetone, nickel chloride ($NiCl_2$)-water, and Sodium chloride (NaCl)-water. These mixtures were chosen to evaluate the phononic crystal's performance across different types of substances, including organic and inorganic. To characterize these liquids, we have experimentally measured the acoustic transmission and the phononic band gap of the phononic crystal with a point defect filled with the liquid mixture. Furthermore, we have determine the calibration curve, which represents the variation of the resonant frequency as a function of concentration. In addition, key performance parameters such as quality factor, sensitivity, and figure of merit were also investigated experimentally.

III.2 PHONONIC CRYSTAL DESIGN AND FABRICATION

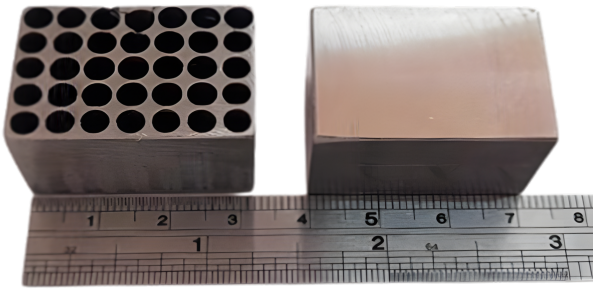

Figure III.1: Two-dimensional phononic crystal composed of a stainless-steel matrix with a 2D periodic arrangement of air holes.

In this work, we have fabricated a two-dimensional phononic crystal composed of a stainless steel matrix with a 2D periodic arrangement of air holes (see Figure III.1). **The periodic lattice parameter is set to a=4.5mm, and the hole diameter is d=4 mm**. The height of the phononic crystal is set to**h=25 mm**. This is for two reasons: first, it depends on the active surface of the ultrasonic transducer, and second, it is significantly larger than the lattice parameters to reduce boundary effects and make the properties of the three-dimensional structure closer to those of a two-dimensional phononic crystal.

Stainless steel was chosen as the material for the phononic crystal for several reasons:

1. The fabrication technology for phononic crystals based on stainless steel allows for highly precise periodic structures.
2. Stainless steel has a high acoustic impedance (due to its high sound velocity and density) compared to liquids, providing strong acoustic contrast.
3. It is well known that stainless steel exhibits very low mechanical losses, which is highly beneficial for high-performance phononic crystal-based sensors.

In this work, COMSOL Multiphysics is used to carry out the design and analysis of band diagrams and transmission spectra of the phononic crystal as a liquid sensor. The numerical machining at CDTA (Center for development of advanced technologies) was used for the mechanical fabrication of the phononic crystal with high precision.

III.3 EXPERIMENTAL ANALYSIS OF THE PHONONIC BAND GAP

III.3.1 Phononic Band Gap without Liquid

In this section, we explore the experimental methodologies employed to investigate the phononic band gap in the absence of liquid, as detailed in the following analysis.Figure III.2 presents the experimental setup for three different cases:

1. **Direct transducer-to-transducer contact:** This step was performed for calibration purposes, allowing us to eliminate the intrinsic frequency response of the ultrasonic transducers from the analysis of the phononic band gap. Additionally, it helped ensure proper alignment of the transducers to achieve maximum acoustic transmission.
2. **Solid stainless steel block:** We tested an unstructured stainless steel block to assess the impact of the air-hole engraving found in the phononic crystal structure by comparing it with a non-patterned block.

3. **Stainless steel phononic crystal (empty):** In this case, we evaluated the transmission through an empty phononic crystal (i.e., with no liquid in the air holes) to observe the emergence of the phononic band gap caused by the periodic structure.

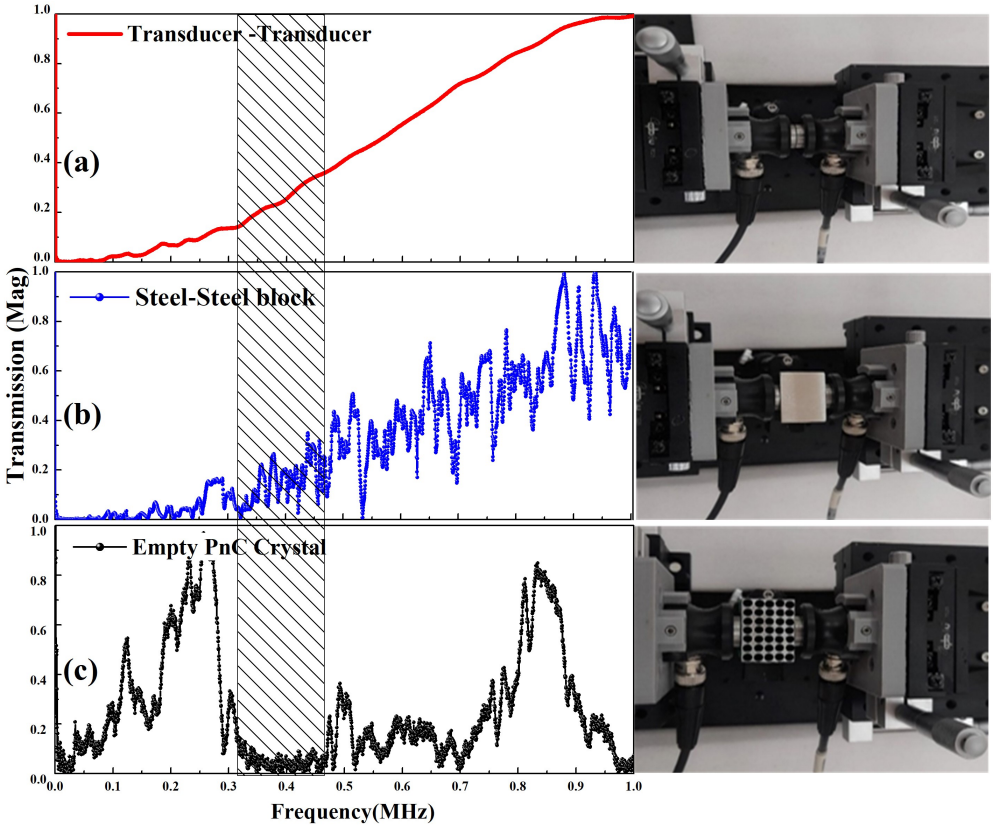

Figure III.2: The experimental setup for three different cases. a. Direct transducer-to-transducer contact, b. Solid stainless steel block, c. Stainless steel phononic crystal (empty)

III.3.2 Phononic Crystal Sensor Filled with Distilled Water

In this configuration, the phononic crystal sensor is filled with distilled water in the central air hole, corresponding to the defect point, to investigate the effect of the liquid medium on acoustic transmission and the phononic band gap; see Figure see Figure III.3. In order to observe the impact of distilled water on the phononic band gap, we plotted the acoustic transmission with and without the water-filled defect mode, as shown in Figure Figure III.4. From Figure Figure III.4a, **we can see the formation of a phononic band gap localized between 0.315 MHz and 0.46 MHz**, which is caused by destructive interference due to the periodic arrangement of air holes in the stainless steel matrix. In Figure Figure III.4b, a new peak appears, indicating a localized mode within the phononic crystal.

This peak corresponds directly to a defect mode introduced by filling the central hole with water. **The acoustic velocity of the distilled water can be calculated as the product of the resonance frequency and the hole diameter d, which is given:**

$$v = f \cdot d = 0.367 \times 4 \times 10^3 \approx 1468\,\text{m/s}$$

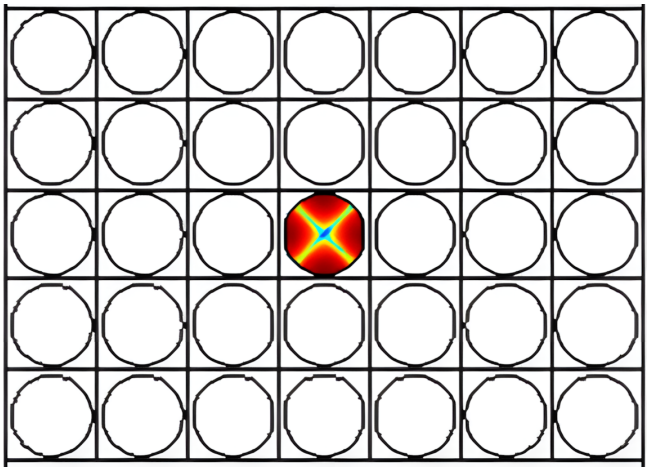

Figure III.3: Phononic crystal sensor is filled with distilled water in the central air hole

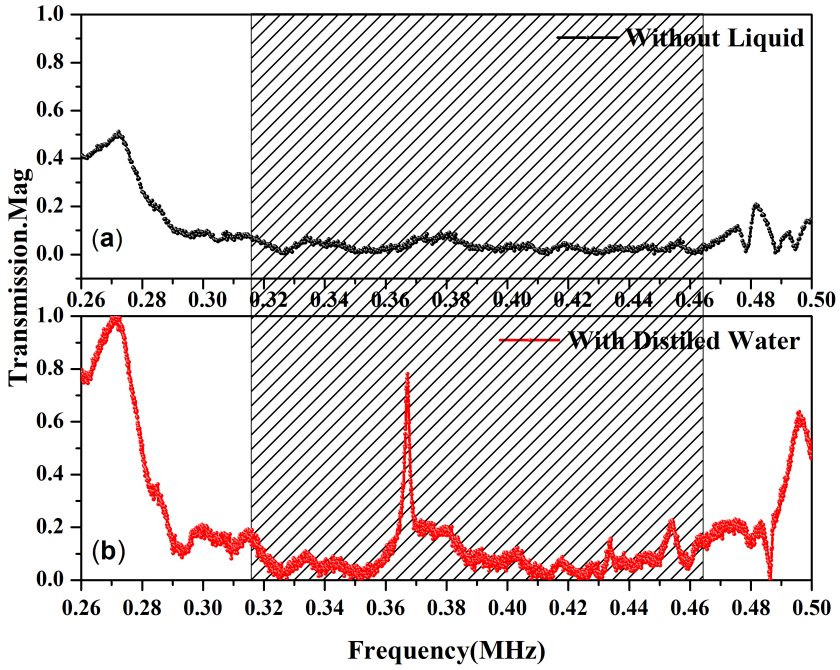

Figure III.4: Measured transmission of the phononic crystal sensor with point defect: (a) without liquid. (b) with distilled water.

III.4 SAMPLES PREPARATION AND MEASUREMENT STEPS

III.4.1 Samples Preparation

In order to test the quality and performance of our phononic crystal sensor for liquid characterization and concentration identification, we tested three different liquid mixtures: **acetone–water, nickel chloride ($NiCl_2$)–water, and sodium chloride (NaCl)–water**. The procedure followed is outlined below:

1. **Cleaning and Drying:** In our work, we followed a strict cleaning protocol, justified by the fact that even small concentrations of dust or residual water can significantly influence the measurements. All containers and equipment were cleaned using an ultrasonic bath for 10 minutes. After cleaning, the 20 mL beakers were dried using a drying oven (étuve) to ensure they were completely moisture-free before use; Figure III.5.

(a) (b)

Figure III.5: (a) Ultrasonic bath, (b) Drying oven

This rigorous cleaning and drying protocol is critical in minimizing contamination and ensuring the reliability of the acoustic response in the phononic crystal sensor. Any trace amounts of dust, oils, or moisture could affect wave propagation characteristics, leading to false interpretations of concentration levels or fluid type, Ensuring sample purity through ultrasonic cleaning and drying not only enhances measurement accuracy but also promotes repeatability and consistency across experiments.

2. **Preparation of the Mixtures:** Each liquid mixture was prepared with precise control over concentration. For acetone–water mixtures, we used a high-precision pipette. For nickel chloride ($NiCl_2$) and sodium chloride (NaCl) solutions, we measured the appropriate mass using a high-precision laboratory balance. See Figure Figure III.6.

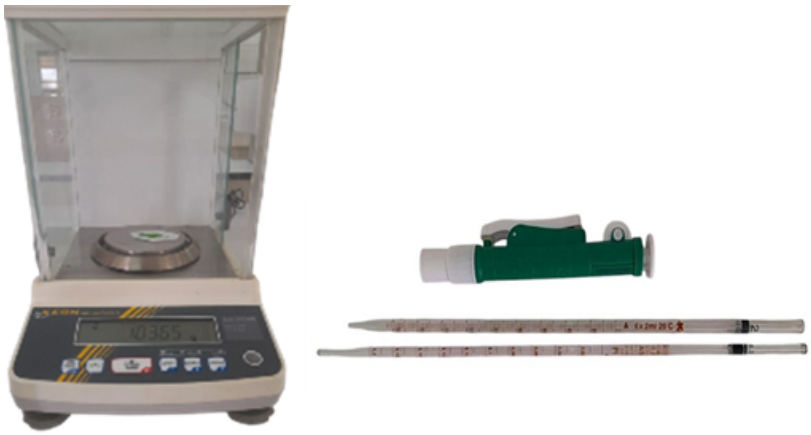

Figure III.6: Laboratory balance and high-precision pipette used in the experiment

3. **Magnetic Agitation:** To ensure homogeneous mixtures, we employed magnetic agitation at a fixed temperature, as shown in Figure III.7. Finally, we obtained homogeneous mixtures with different concentrations, as illustrated in Figure III.8.

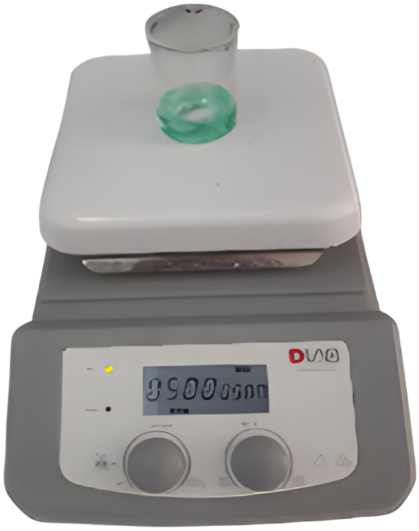

Figure III.7: Magnetic agitation at fixed temperature.

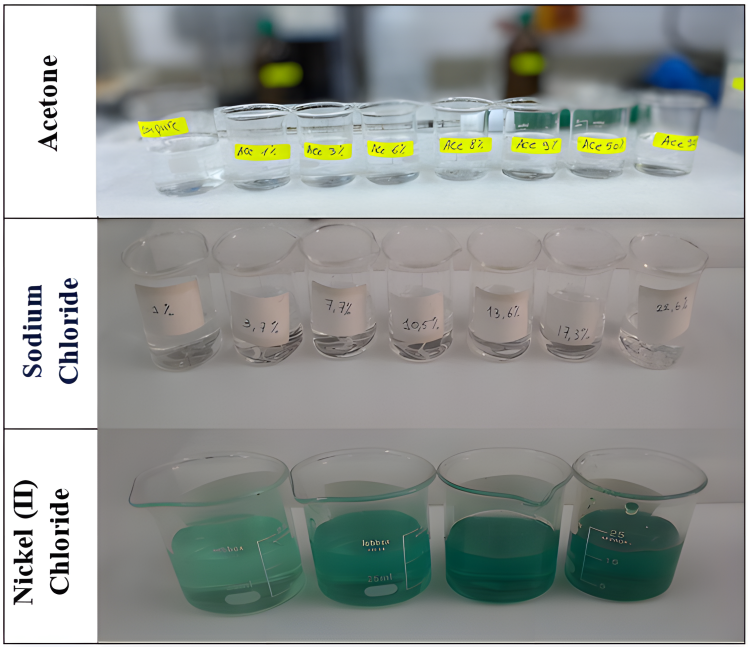

Figure III.8: Homogeneous mixtures tested experimentally. Acetone, sodium chloride (NaCl), and nickel (II) chloride ($NiCl_2$)

III.4.2 Measurement steps

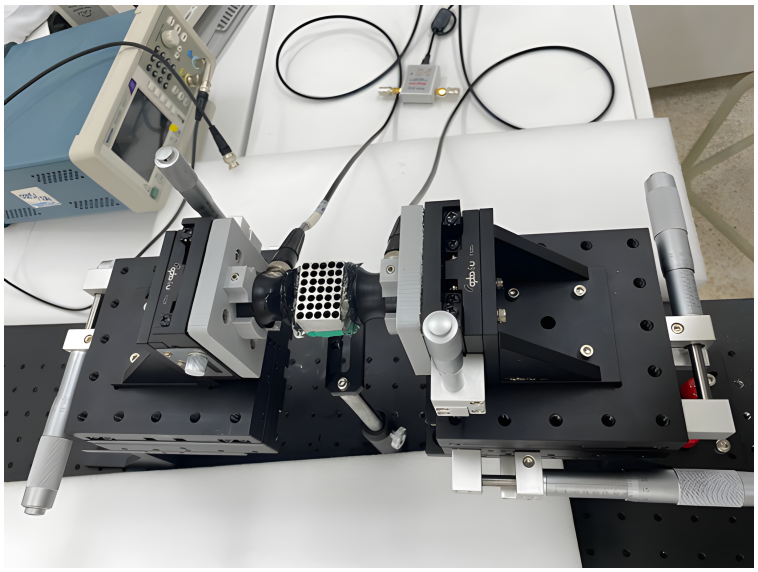

Figure III.9: Measurement bench for phononic crystal sensor

The phononic crystal sensor, without any liquid, is placed between two ultrasonic transducers, one functioning as the emitter and the other as the receiver (see Figure III.9). The emitting transducer is excited by a sinusoidal signal generated by a Vector Network Analyzer (VNA), which converts the

electrical signal into a mechanical longitudinal wave. This longitudinal wave propagates through the phononic crystal and is scattered by the periodic array of air holes. The wave is then received by the opposite ultrasonic transducer, which converts it back into an electrical signal. The VNA processes this signal to analyze the transmission characteristics.

The acoustic transmission of the phononic crystal is experimentally obtained by measuring the S_{21} parameter, which represents the ratio of the output signal to the input signal. The phononic band gap is identified as the frequency range where the transmission reaches a minimum, indicating strong attenuation due to the structure's periodicity; see Figure III.2. It is important to note that a special ultrasonic gel was used to ensure optimal acoustic transmission between the phononic crystal and the ultrasonic transducers; see Figure III.10.

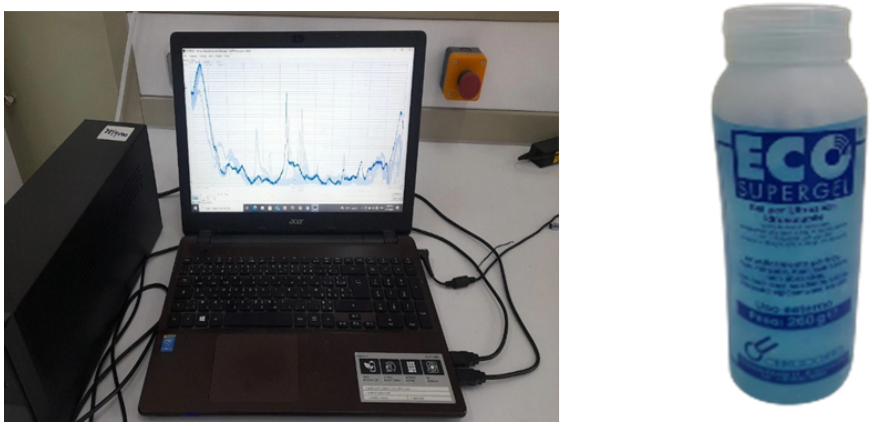

Figure III.10: Acoustic transmission of the phononic crystal, experimentally obtained by measuring the S21 parameter /Special ultrasonic gel was used in the experiment

III.5 PHONONIC CRYSTAL SENSOR FOR LIQUID CHARACTERIZATION

III.5.1 Acetone–Water Mixture Characterization

III.5.1.1 Transmission measurement

Figure III.11 shows the measured transmission of the phononic crystal sensor used to detect acetone in water at two different concentration ranges: low concentrations from 1% to 9% (a) and high concentrations from 25% to 100% (b). From this figure, we can observe that each acetone concentration corresponds to a specific transmission peak localized within the phononic band gap. That transmitted peak refers to the amount of acoustic energy transmitted through the band gap, and that shows an essential characteristic property for PnCs appeared when the defect layer filled with fluids, as that resonance frequency related to the acoustic properties of the fluid material. At

a concentration of 0% (water), there would be a sharp resonant or transmitted peak generated at the normalized frequency of 0.3671 MHz, and the resonance frequency value will change for other acetone concentrations.

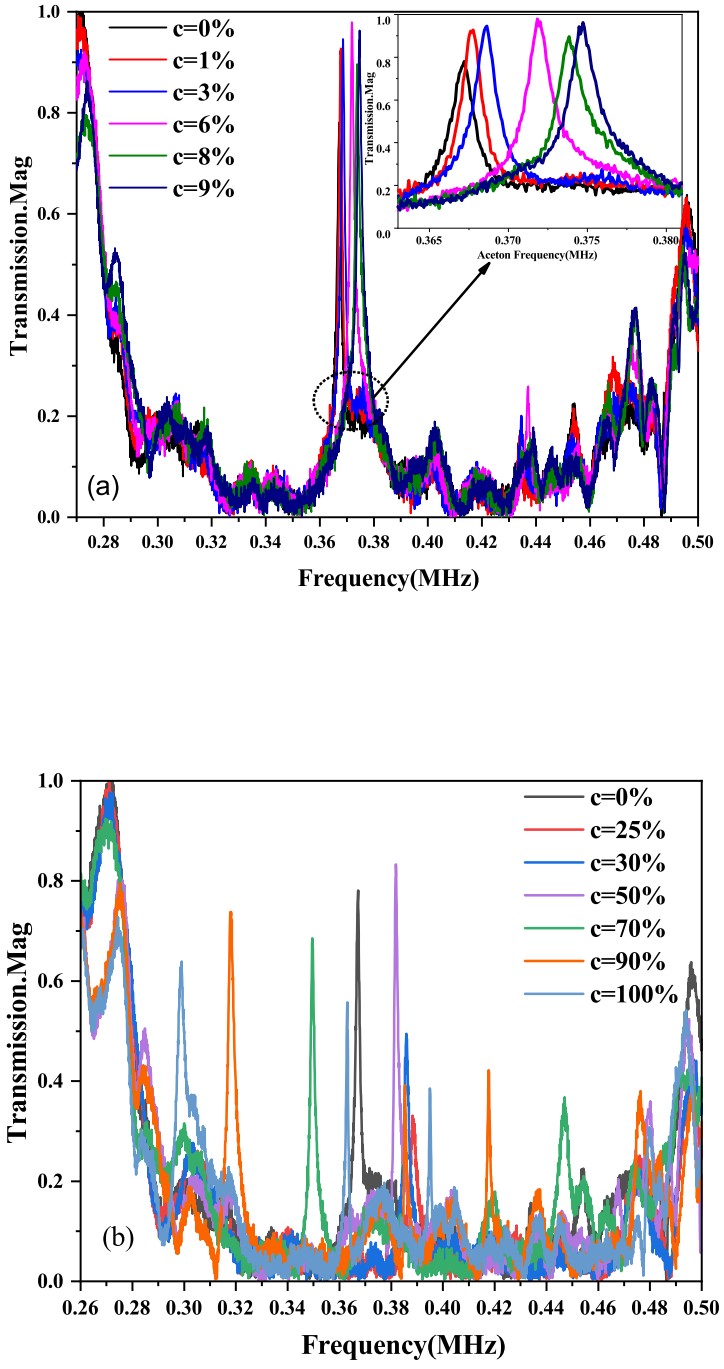

Figure III.11: Measured transmission of the phononic crystal sensor used point defect to detect acetone in water, (a) low concentrations. (b) High concentrations.

III.5.1.2 Acetone concentration measurement and calibration curve

Figure III.12 shows the so-called calibration curve of the fabricated liquid phononic sensor, which represents the variation of the resonance frequency as a function of acetone concentration. From this figure, we can determine any unknown acetone concentration in water. We can observe that the resonance frequency increases as the acetone concentration rises, reaching its maximum at an acetone concentration equal to 25%. Beyond this point, the resonance frequency starts to decrease with further increases in concentration.

Moreover, the figure displays both experimental (Exp) and simulated (Sim) data, showing good qualitative agreement, especially in the trend of the curve. Nevertheless, some discrepancies can be seen between the simulated and experimental results. These deviations could be due to factors such as idealized assumptions in the simulation model, limitations in material parameter inputs, or the influence of fabrication imperfections and measurement noise. This behavior can be justified as follows: at low concentrations, the interaction of acetone with water is very weak, and the water phase remains dominant. As the acetone concentration increases, the desolation becomes stronger, and acetone becomes the dominant phase, leading to a decrease in the resonance frequency.The clear peak around 25% acetone can serve as a reference point in practical sensing applications, enabling the design of automated systems for concentration estimation based on frequency shifts.

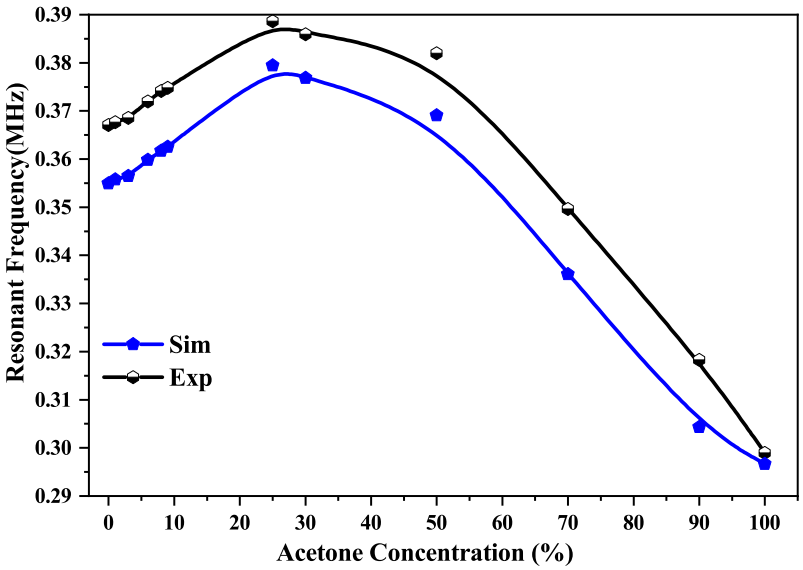

Figure III.12: Calibration curve of the fabricated liquid phononic sensor. (a) Measured resonant frequency as a function of acetone concentration in water.

Additionally, the mass density decreases with acetone concentration, meaning that the longitudinal velocity rises proportionally to the acetone concentration; see Figure III.13.

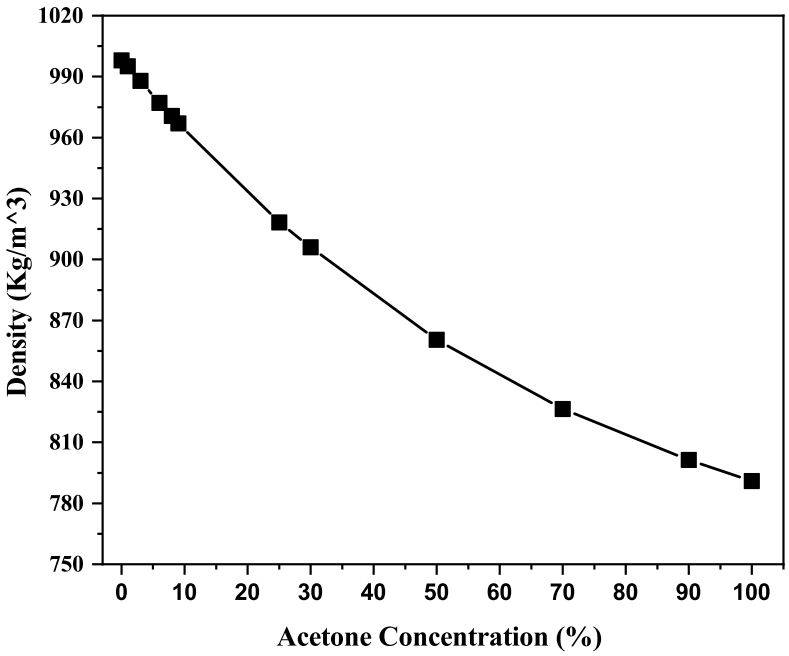

Figure III.13: (b) Mass density as function of acetone concentration in water

It is important to note that we compared our simulation results with the experimental data and observed excellent agreement between them, as clearly demonstrated in the same figure.

III.5.1.3 Measurement of Quality Factor, Sensitivity, and Figure of Merit

Based on the measured transmission in collaboration with the equations mentioned in chapter II, we have determined the quality factor, sensitivity, and figure of merit of the mixture. The results are presented in Table Table III.1. From this table, we can conclude that the acetone concentration has a significant impact on the performance of the phononic sensor, including the quality factor (Q-factor), sensitivity, and figure of merit (FoM).

A high Q-factor (> 1000) indicates low energy loss and produces sharp resonance peaks, which are essential for high-resolution sensing applications. Conversely, a low Q-factor (< 100) suggests strong damping effects, resulting in broad resonance peaks.

At low acetone concentrations (0–9%), the Q-factor shows a relatively high and stable performance, peaking at 287.24 for 1% concentration and staying above 227 until 9%. This suggests that the sensor exhibits low energy loss and sharp resonance peaks in this range, which is desirable

for precise detection. However, beyond 9%, the Q-factor begins to decline significantly, reaching a minimum value of 95.00 at 90%, indicating increasing acoustic losses or damping effects in the medium as acetone concentration increases.

The sensitivity peaks at 9% acetone concentration (0.00769 MHz), indicating the sensor's highest responsiveness to frequency shifts at this point. Beyond 25%, sensitivity drops, reducing the sensor's effectiveness in detecting small concentration changes. Similarly, the Figure of Merit (FOM) is highest at 9% (4.66061), reflecting optimal sensing performance, but it declines at both low and high concentrations due to reduced sensitivity and Q-factor. This typically occurs due to material losses or structural imperfections in the crystal lattice.

Table III.1: Measurement value of quality factor, sensitivity, and figure of merit

Acetone concentration%	Quality Factor	Sensitivity (MHz)	FOM
0	253.17	/	/
1	287.24	5.7E-4	0.44
3	245.70	7.25E-4	0.48
6	267.61	0.00163	1.17
8	273.08	0.00352	2.56
9	227.14	0.00769	4.66
25	130.85	0.00135	0.45
30	160.80	0.00376	1.56
50	220.80	7.45E-4	0.43
70	144.48	8.72E-4	0.36
90	95	0.00244	0.72
100	137.14	6.813E-4	0.31

III.5.2 Nickel Chloride –Water Mixture Characterization

Following the same procedure as before, we conducted an experimental investigation to characterize a new liquid mixture: nickel chloride ($NiCl_2$) dissolved in water.

III.5.2.1 Transmission measurement

Figure III.14 presents the acoustic transmission spectra of the phononic crystal measured for aqueous nickel chloride ($NiCl_2$) solutions across a concentration range of 0-1.046 mol/kg. The data reveal a strong dependence of transmission characteristics on $NiCl_2$ concentration, with each solution exhibiting a well-defined transmission peak within the phononic bandgap.

We also investigated higher concentrations of nickel chloride ($NiCl_2$). However, the transmission peaks for these elevated concentrations were located outside the phononic bandgap, rendering them unsuitable for sensing applications.

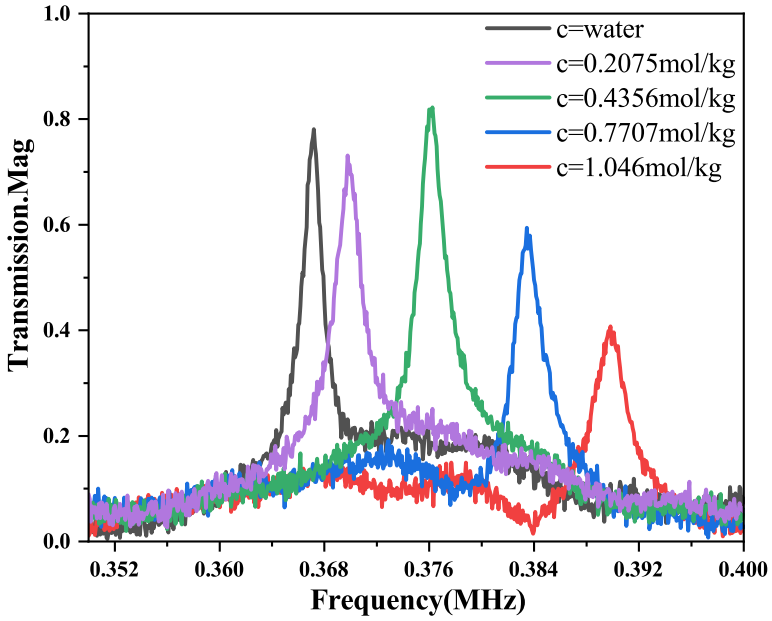

Figure III.14: Measured transmission as function of frequency of the phononic crystal sensor used Nickel Chloride –Water Mixture Characterization with point defect.

III.5.2.2 Nickel Chloride concentration measurement and calibration curve

Figure III.15 shows the variation of the resonant frequency as a function of nickel chloride ($NiCl_2$) concentration. The resonant frequency exhibits an approximately linear increase with $NiCl_2$ concentration. Furthermore, we compared the experimental data with simulation results and observed excellent agreement between them.

The observed linear dependence of the resonant frequency on $NiCl_2$ concentration can be attributed to the following key factors:

1. **Mass Density Effect:** Increasing $NiCl_2$ concentration raises the mass density of the fluid mixture. For a 2D phononic crystal, the resonant frequency is inversely proportional to the square root of the effective density:In the other hand, the stiffness (elastic modulus) of the fluid mixture likely increases with $NiCl_2$ concentration, compensating for the density effect and resulting in a net linear frequency increase.Following this equation :

$$f \propto \frac{1}{\sqrt{\rho}}$$

2. **Dominance of Elastic Properties:** At low-to-moderate $NiCl_2$ concentrations, the elastic modulus of the fluid (governed by ion-water interactions) becomes the dominant factor over density changes. This leads to a proportional linear increase of the frequency with concentration.

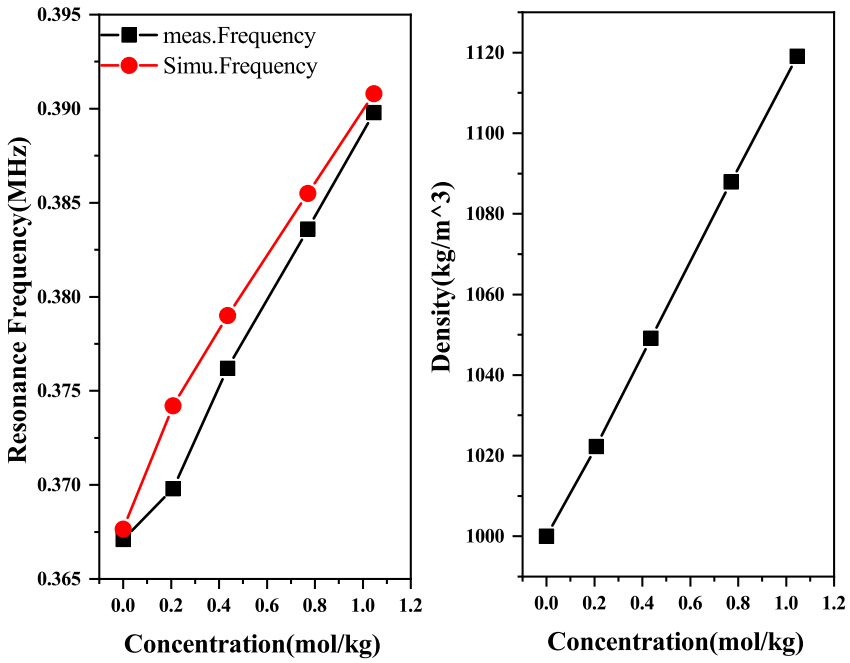

Figure III.15: Calibration curve of the fabricated liquid phononic sensor. Measured resonant frequency as a function of $NiCl_2$ concentration in water. the Mass density of the Mixture as function of $NiCl_2$ concentration in water

III.5.2.3 Measurement of Quality Factors, Sensitivity, and Figure of Merit

Quality factor (Q-factor), sensitivity (kHz), and figure of merit (FOM) for the phononic crystal sensor were determined using equations mentioned in chapter II and the measured transmission. The results are shown in Figure Figure III.16. From this figure, it can be concluded that concentration levels of $NiCl_2$ greatly influence the performances of the sensor. As seen in this figure, the Q-factor shows a clear inverse relationship with $NiCl_2$ concentration, going down from about 223.84 at 0.0 mol/kg to 133.95 at 1.046 mol/kg. The sensitivity and figure of merit take on a positive correlation with the rise in $NiCl_2$ concentration. Sensitivity increases from 13.01 kHz at 0.2075 mol/kg to 82.45 kHz at 1.046 mol/kg, and FOM increases from 6440.59 at 0.2075 mol/kg to 28333.33 at 1.046 mol/kg.

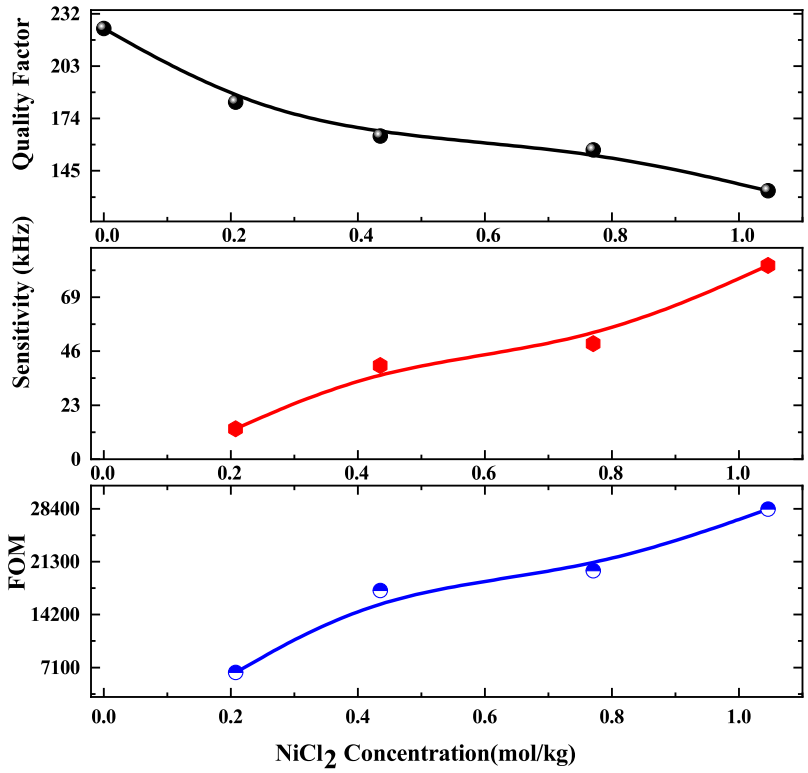

Figure III.16: Measurement of quality factors, sensitivity, and figure of merit of phononic crystal sensor.

III.5.2.4 Comparison with Other Technique: Electrical Conductivity Measurement

To evaluate the performance of our phononic $NiCl_2$ sensor, we compare it with conventional conductivity-based measurement techniques, which are widely used for electrolyte concentration detection.

For measuring electrical conductivities, calibrated MODEL OHAUS equipment was used for all concentrations of $NiCl_2$ after calibrating it with reference "EC Standard 1413 µs/cm@25°C", see Figure Figure III.17. The electrode was immersed in glass beakers containing solutions of $NiCl_2$ at different concentrations.

As seen in Figure Figure III.18, the electrical conductivity increases as a function of the concentration of $NiCl_2$, starting from about 0.0052 mS/cm at 0 mol/kg up to 125.9 mS/cm at 1.046mol/kg. This is explained in terms of the higher ionic Ni^{2+} and Cl^- content released into solution at higher concentrations, which affects the transport capability of charge. At the same time, phononic crystal sensor measurements showed that the peak frequency jumped up to 0.3908 MHz, which was measured in the same concentration range, indicating similar trends between the two techniques.

Figure III.17: Calibrated MODEL OHAUS equipment used for the electrical conductivity measurement

The important advantage of the phononic crystal sensing compared to conventional conductivity measurement is that the phononic crystal measurement is used for a wide variety of liquid mixtures, especially with organic solutions, which is usually difficult for the conventional electrical conductivity instruments.

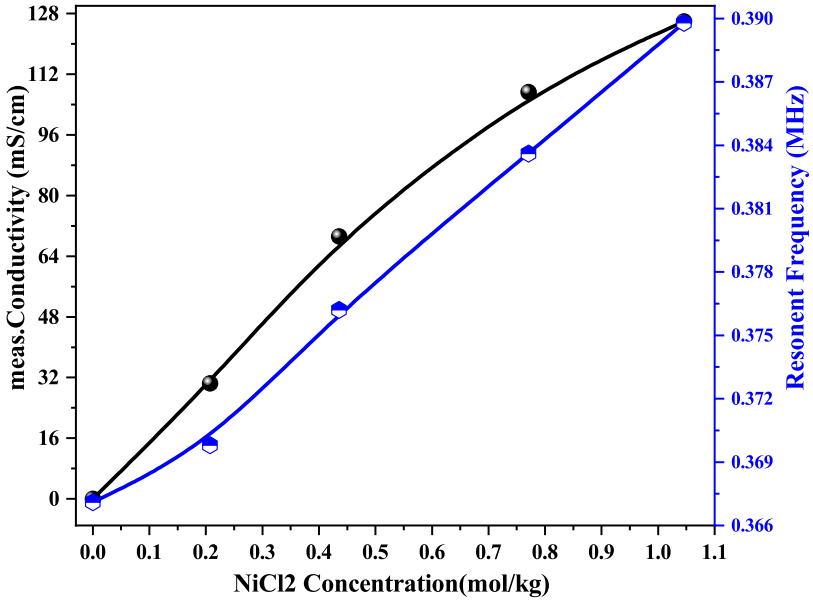

Figure III.18: Conventional conductivity-based measurement technique and phononic crystal sensor measurement

This comparative analysis, visualized in FigureFigure III.18,suggested that the phononic crystal sensor could be an effective alternative for liquid characterization applications.

III.5.3 Sodium Chloride (NaCl) –Water Mixture Characterization

III.5.3.1 Transmission measurement

In this section, we have used the same technique to characterize and to determine the concentration of the Sodium Chloride (NaCl) in distilled water.The Figure III.19 shows the acoustic transmission of the Sodium Chloride (NaCl)–water mixture for different NaCl concentrations ranging from 0 to 22.6%.

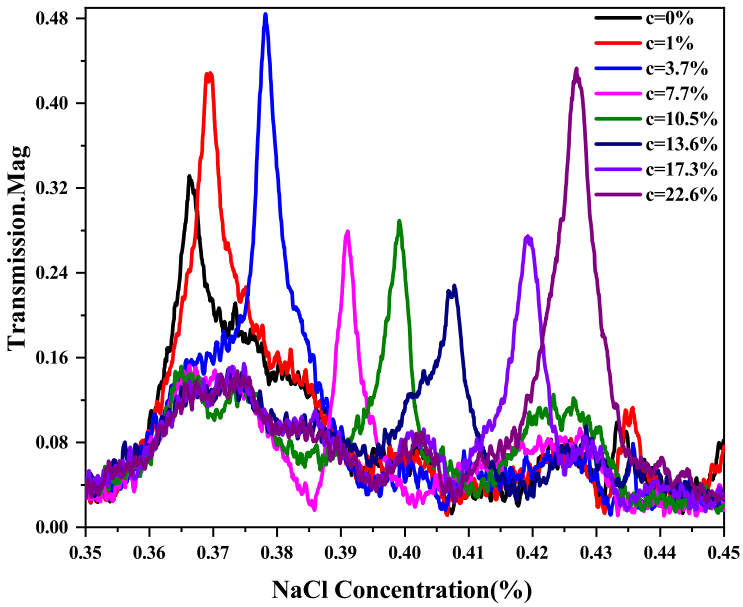

Figure III.19: Measured transmission as function of frequency of the phononic crystal sensor used Sodium Chloride (NaCl) –Water Mixture Characterization with point defect.

We found that each resonance peak corresponds to a specific NaCl concentration, and all peaks are localized in the phononic band gap. This correspondence between resonance features and solution concentration indicates the possibility of our acoustic method as a sensitive quantitative analyzer for saline solutions.

III.5.3.2 Concentration measurement and calibration curve

The Figure III.20a shows the calibration curve for the phononic-based sensor for Sodium Chloride (NaCl)–water mixture characterization. In this figure we have plotted the resonance frequency as function of the NaCl concentration, and we compare it with the obtained simulation results. We can see that the resonance frequency increases as function of concentration, and it is in good agreement with simulation data. The Figure III.20b shows the impact of the NaCl concentration on the density, which increases linearly.

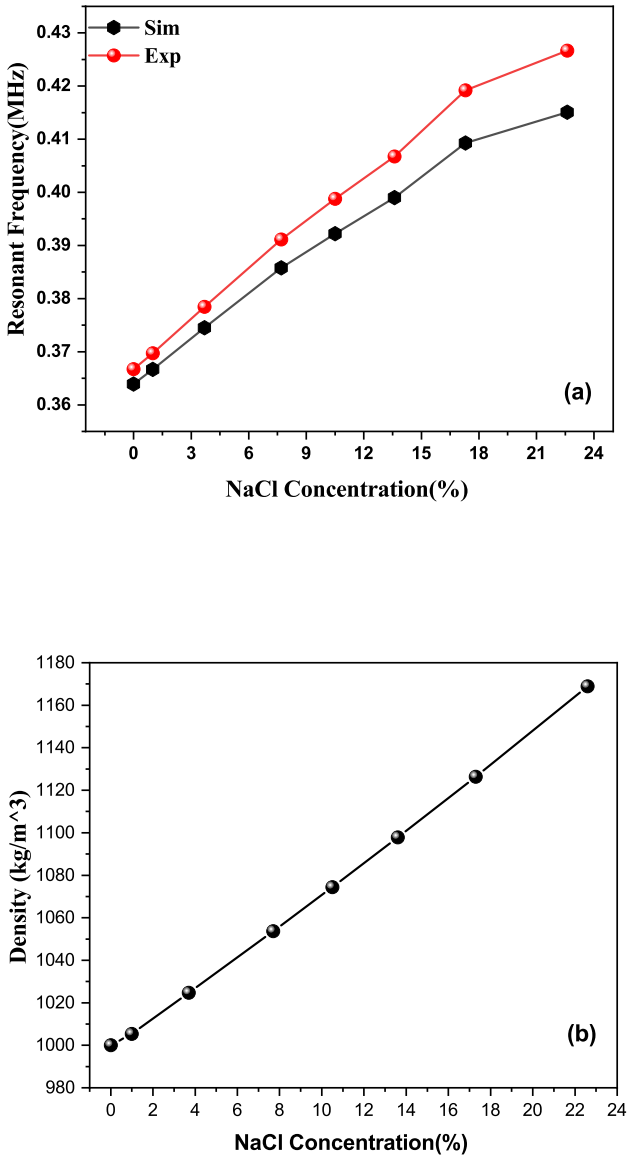

Figure III.20: Calibration curve of the fabricated liquid phononic sensor. (a) Measured resonant frequency as function of NaCl concentration in water. (b) Mass density as function of NaCl concentration in water

III.5.3.3 Measurement of Quality factors, Sensitivity and Figure of Merit

The measured values of the performance (Quality factor, sensitivity and FoM) of the phononic-fluid sensor are presented in the Table Tablle III.2. In this table, we can conclude that the sensitivity increases as function of concentration. In addition, the FoM increases for concentration ranged between 0 and 10.6% and after that started to decrease. The quality factor is direct related to the Full width half maximum of the corresponding peak.

Table III.2: Measurement of Quality factors, Sensitivity and Figure of Merit

Concentration (%)	Quality Factor	Sensitivity (MHz)	FOM
0	115.32	/	/
1	58.22	2.98	0.46
3.7	89.26	4.34	1.02
7.7	107.16	6.1	1.67
10.5	119.39	11.4	3.41
13.6	88.04	12.9	2.79
17.3	101.01	14.18	3.41
22.6	70.17	11.3	1.85

III.6 Conclusion

In this chapter, we focused on the experimental design, fabrication, and testing of 2D phononic crystal sensors, with validation through acoustic transmission measurements and performance evaluation for different liquid mixtures. Three different liquid mixtures were tested: water-acetone, nickel chloride ($NiCl_2$)-water, and Sodium chloride (NaCl)-water. These mixtures were chosen to evaluate the phononic crystal's performance across different types of substances, including alcohols, salts, and chlorides. In addition, we have compared the simulation results with the data obtained experimentally and we found excellent agreement between them.

CHAPTER IV: Development of a Graphical User Interface

GUI for the Phononic-Fluidic Sensor

CHAPTER 4

DEVELOPMENT OF A GRAPHICAL USER INTERFACE GUI FOR THE PHONONIC-FLUIDIC SENSOR

IV.1. INTRODUCTION

The monitoring in real-time of a very small change in acetone concentration using a phononic crystal sensor is highly critical. The defect mode peak in the scattering parameter S21 exhibited characteristic shifts in response to any small change in acetone concentrations. However, accurate detection, interpretation, and processing of these defect modes and peaks in real-time require specialized and highly particular tools.

This chapter presents the design and implementation of a **Graphical User Interface (GUI)** tailored for our phononic crystal sensor to easily monitor in real-time of every small change in acetone concentration. The objective of the proposed Graphical User Interface (GUI) is to be like a bridge between the complex acoustic data of the sensor and the end-users.

IV.2. GRAPHICAL USER INTERFACE (GUI)

Graphical User Interface (GUI) is an interactive user-machine interface that allows interacting with sensor data in a sensitive way. The GUI constructed by a digital interface contains graphical components such as icons, buttons, and menus. These components allowed the users to control and signal processing of the sensors in real-time

IV.3. GRAPHICAL USER INTERFACE FOR PHONONIC CRYSTAL SENSOR

IV.3.1. Physical architecture diagram

The purpose of this section is to interface the phononic-fluidic sensor with the MATLAB Graphical User Interface (GUI). The MATLAB GUI will display the result and the data that it gets from the

phononic sensor. The block diagram of the physical architecture of connecting the phononic sensor and the GUI to the end-users is presented in Figure IV.1.

BLOCK 1. Phononic–fluidic sensor

- Added the liquid in the central defect hole.
- Microfluidic pump to automatically deliver the samples.
- 2-Connected to the VNA via RF cables (SMA or coaxial).

BLOCK 2. Vector network analyzer

- Measured the acoustic transmission S21 for each concentration.
- Communicate with the computer with software called DG8-SAQ.

BLOCK 3. Computer GUI

- Communicate in real time with DG8-SAQ.
- Process S21 data in real-time (peak detection, high of the peak, FWHM).
- Upload the calibration curve.
- Determine in real-time the concentration.

BLOCK 4. Users display and Control interface

- MATLAB coding for user interface.
- icons, buttons, and menus.

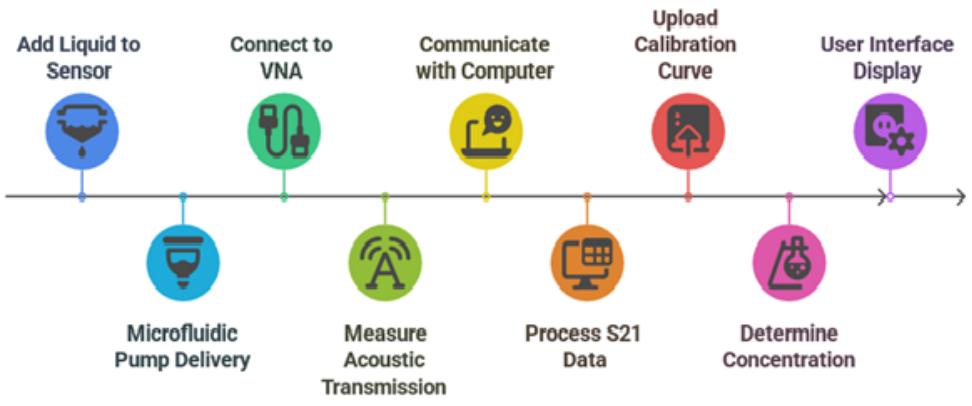

Figure IV.1: Block diagram of the physical architecture of graphical user interface (GUI) used for phononic crystal sensor

IV.3.2. MATLAB PROGRAM

MATLAB software is able to create and design a GUI using programming (coding). The design in GUI must be **user-friendly to make the user understand how to use it**. In this work, we use MATLAB functions to define the layout and behavior of our GUI. In this approach, we create a figure to serve as the container for our user interface and add components to it programmatically. In this section, we present the GUI main interface result from the MATLAB code developed for the phononic sensor;see Figure VI.2 . **The MATLAB code is presented in ANNEXE I.** All main GUI elements are explicitly mapped to their corresponding MATLAB code modules through detailed program comments.

The GUI in Figure IV.2 has been modified to fit the workflow of the phononic liquid sensor, automating the process of concentration calculation. The system retrieves the calibration curve from the VNA data and outputs system concentration using the peak frequency of the transmission spectrum. The program in MATLAB contained in ANNEXE I is designed so that each task: data collection, calibration, and measurement, can be replaced without impacting the rest of the system, allowing easy future modifications. These features build up to greater accuracy and efficiency, which greatly benefits real-time liquid analysis for many applications in both science and industry.

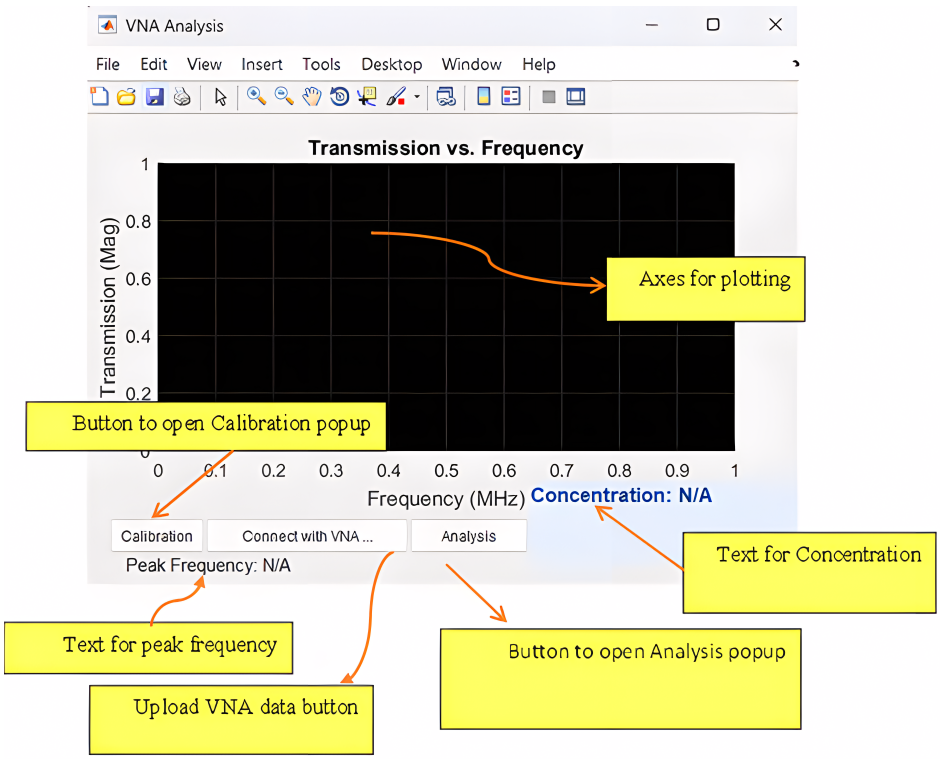

Figure IV.2: Main GUI developed for controlling of our phononic liquid sensor

V.4. A GUI IMPLEMENTATION FOR REAL-TIME ACETONE MONITORING

In order to develop a GUI for real-time monitoring of the acetone concentration in water mixture placed in the phononic crystal sensor, we divide this task into three parts:

IV.4.1. Calibration: Upload the type of the liquid

Implementation begins by loading the calibration curves for all three liquid mixtures (acetone-water, $NiCl_2$ -water, and NaCl-water). The GUI features a dedicated **"**Calibration" button that, when selected, opens a new window within the main interface displaying the complete set of calibration curves for different mixtures, as shown in Figure IV.3 . Moreover, more calibration curves could be uploaded for other mixtures, isopropanol, methanol, and so on.

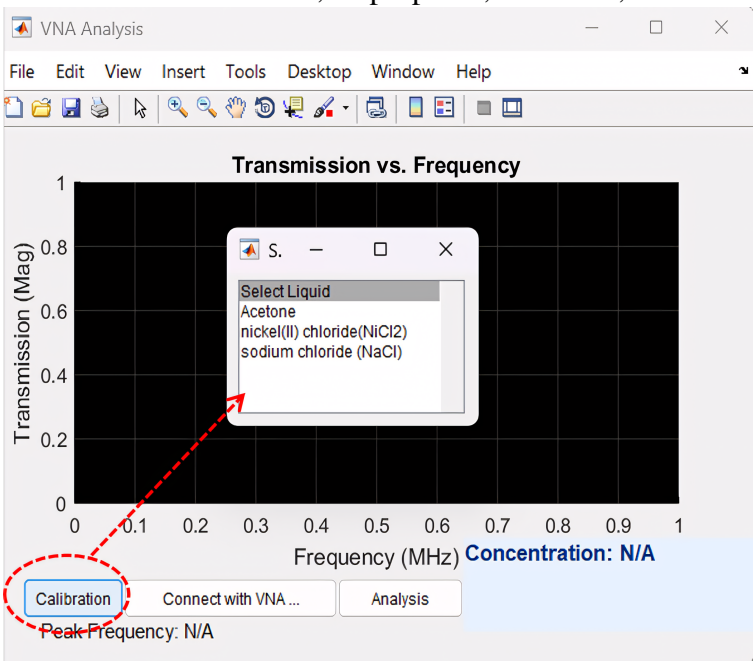

Figure IV.3: The main GUI interface displaying the complete set of calibration curves for different mixtures

IV.4.2. Connecting with VNA

The second step is to communicate with vector network analyzer (VNA) to transmit the acoustic transmission S21 graphic to the main GUI interface. For that, we have added a **"**Connect with VNA" button that, when selected, opens a new window displaying "**Select VNA Data file**", as shown in Figure VI.4 . This window allowed uploading the acoustic transmission of the unknown concentration. The transmission file of each liquid concentration has an extension of **'s1p.'**

It should be noted that the proposed GUI only has the capability to upload the tests that come

from the VNA software, not to control the VNA hardware. Our GUI needs more improvement to directly control the VNA hardware. In order to control in a direct manner the VNA hardware, we need the **IP address or VNA License** to have access to the main code of the VNA. In addition, we have to add more icons such as **'start frequency' , 'End frequency', 'sweep'**, and **'calibration'**. Figure VI.5 shows the uploaded acoustic transmission S21 of unknown acetone concentration in water. The acoustic transmission S21 is normalized by 10^{-3} .

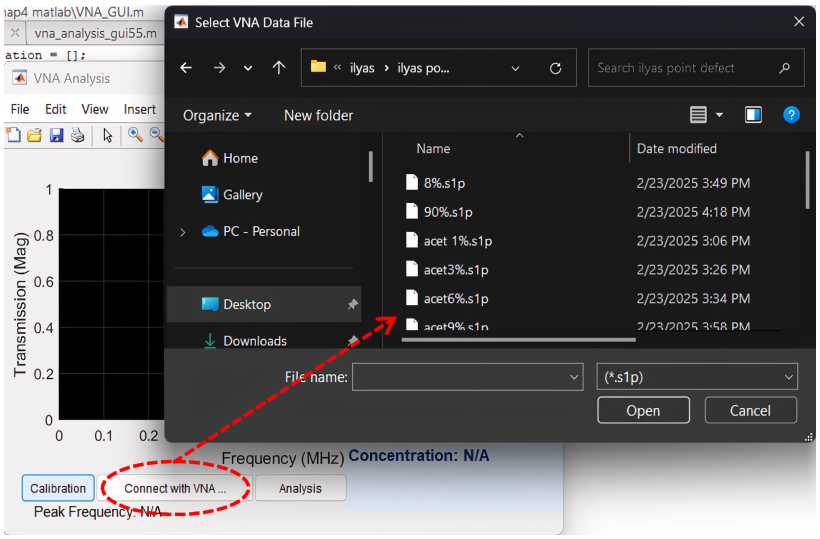

Figure IV.4: The main interface of GUI and window files of the acoustic transmission of the unknown concentration

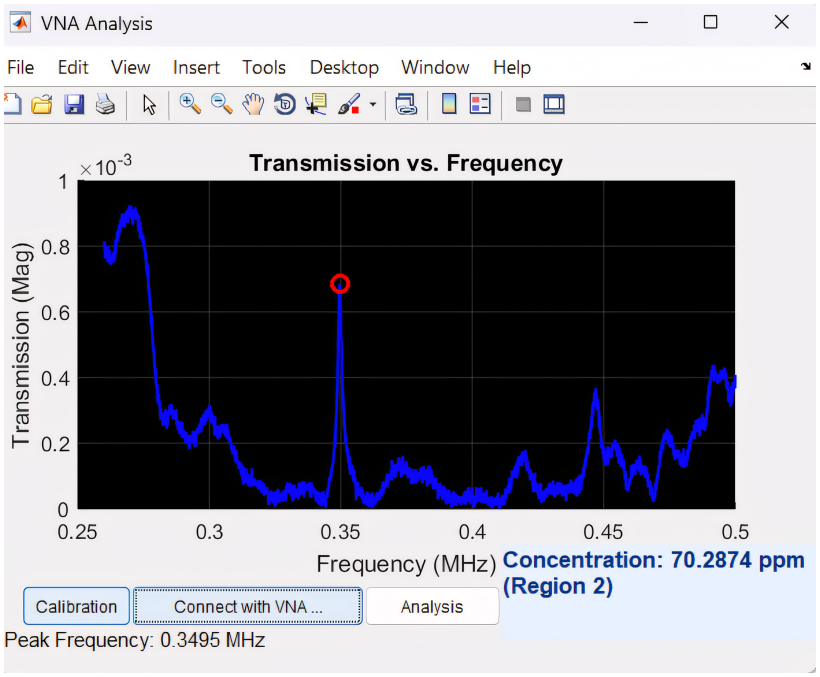

Figure IV.5: Acoustic transmission S21 of unknown acetone concentration in water. The acoustic transmission S21 is normalized by 10^{-3}

IV.4.3. Results analysis

The third step involved processing and analyzing the experimental results, beginning with detection and identification of the resonant peak associated with the unknown's concentration. In our GUI, we have incorporated a new button called **'analysis'**, which when activated, opens a new window displaying **"Analysis Results"**, as shown in Figure VI.6 .

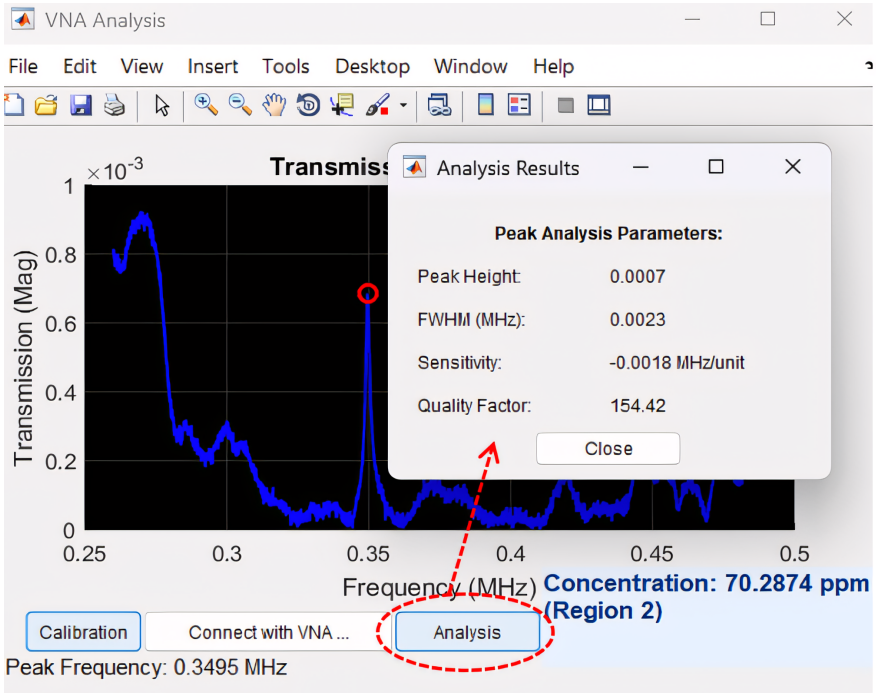

Figure IV.6: The analysis window displays the resonant peak characteristics: peak height, FWHM (full width half maximum), sensitivity, and quality factor.

1. Peak Height The maximum intensity (amplitude) of the resonant peak.

Significance: Indicates the strength of the signal response. A higher peak height typically means a stronger detection.

2. FWHM (Full Width at Half Maximum) The width of the peak at half of its maximum height, measured in MHz.

Significance:

- A smaller FWHM indicates a sharper, more well-defined peak (better resolution)
- Used to assess the precision of the measurement system

3. Sensitivity The change in resonant frequency (MHz) per unit change in the measured quantity (e.g., concentration, temperature).

Negative Sign: Indicates an inverse relationship (e.g., frequency decreases as the measured quantity increases).

Significance: Quantifies how responsive the system is to changes in the target variable.

4. **Quality Factor (Q)** A dimensionless parameter describing the sharpness of the resonant peak, calculated as:

$$Q = \frac{\text{Resonant Frequency (MHz)}}{\text{FWHM (MHz)}}$$

Significance:

- Higher Q = Narrower peak, lower energy loss (better system performance)
- Critical in oscillator and filter applications

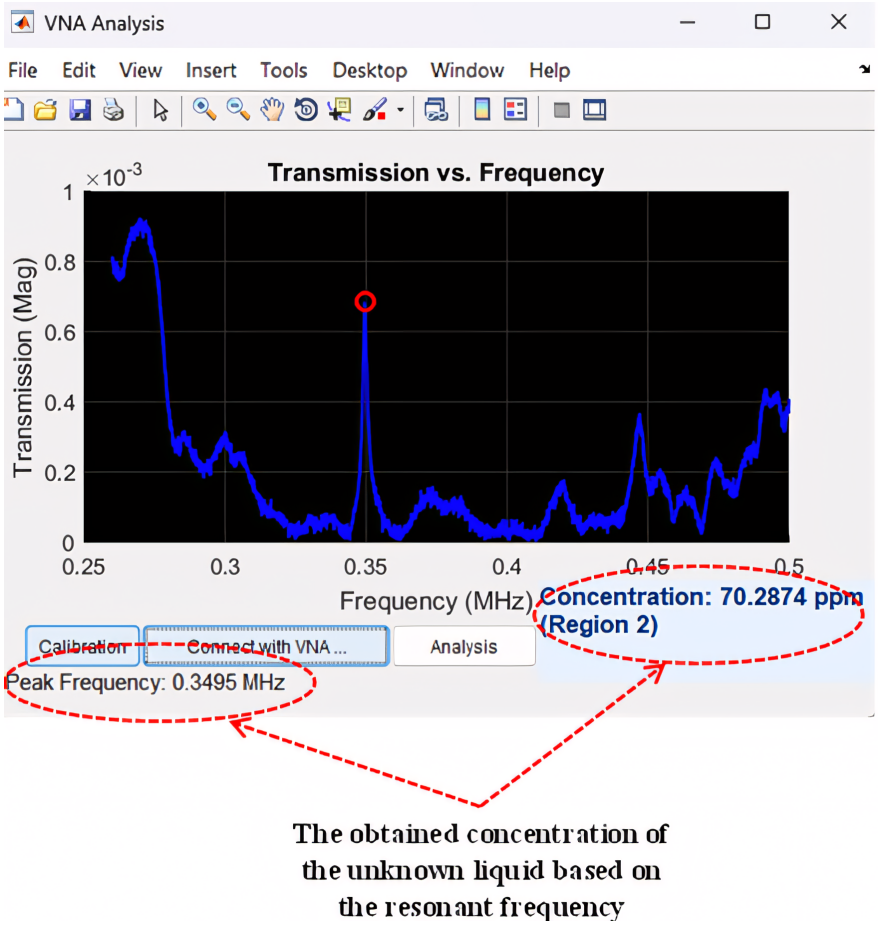

Figure IV.7: Computers' exact acetone concentration and acoustic velocity

The analysis window displays the resonant peak characteristics needed to determine the sensor performances, As the final analytical step, the GUI computes exact acetone concentration based on the uploaded calibration curve;see Figure VI.7 . Moreover, GUI also defines the resonant frequency to find the acoustic velocity of the unknown acetone concentration.

IV.5. CONCLUSION

In this chapter, a dedicated Graphical User Interface (GUI) was successfully designed and implemented in MATLAB to enable **real-time monitoring and concentration estimation** of acetone and other liquids using a **phononic crystal sensor**. The GUI acts as a critical bridge between the complex acoustic data provided by the sensor and the end-user, offering a clear, interactive, and user-friendly interface for data visualization and analysis.

The system architecture integrates several components:

- A **phononic-fluidic sensor** to detect acoustic transmission characteristics,
- A **Vector Network Analyzer (VNA)** to measure transmission (S21 parameter),
- A MATLAB-based GUI for signal processing, peak detection, calibration, and concentration calculation.

Although the GUI currently only supports data upload and analysis, further improvements could include direct **hardware control of the VNA**, requiring additional configuration (e.g., IP or license access). Adding frequency sweep settings and calibration automation would enhance functionality and real-time control.

This work demonstrates the feasibility of integrating MATLAB GUI with phononic crystal sensors for rapid, accurate, and real-time chemical concentration monitoring. The system can be adapted for other liquid mixtures beyond acetone, supporting broader applications in environmental, chemical, and biomedical sensing.

ANNEXE I

MATLAB code of GUI for phononic-fluidic sensors

```
function vna_analysis_gui22


fig = figure('Name', 'VNA Analysis', 'NumberTitle', 'off', 'Position',
    [100 100 600 400]);


ax = axes('Parent', fig, 'Position', [0.1 0.3 0.8 0.6], 'color', 'black');
xlabel(ax, 'Frequency (MHz)');
ylabel(ax, 'Transmission (Mag)');
title(ax, 'Transmission vs. Frequency');
grid(ax, 'on');
hold(ax, 'on');
set(ax, 'GridColor', 'white');


uicontrol('Style', 'pushbutton', 'String', 'Connect with VNA ...', ...
'Position', [100 35 170 30], ...
'Callback', @(~,~) uploadVNA(fig, ax));


uicontrol('Style', 'pushbutton', 'String', 'Calibration', 'Position', [20
    35 80 30], ...
'Callback', @(~,~) openLiquidPopup(fig));


uicontrol('Style', 'pushbutton', 'String', 'Analysis', 'Position', [270 35
     100 30], ...
'Callback', @(~,~) openAnalysisPopup(fig));


peakText = uicontrol('Style', 'text', 'Position', [3 5 200 30], ...
'String', 'Peak Frequency: N/A', 'FontSize', 10);


concText = uicontrol('Style', 'text', ...
'Position', [370 25 240 70], ...
'String', 'Concentration: N/A', ...
'FontSize', 11, ...
'FontWeight', 'bold', ...
'ForegroundColor', [0 0.2 0.5], ...
'BackgroundColor', [0.9 0.95 1], ...
'HorizontalAlignment', 'left');


guidata(fig, struct('vnaData', [], 'peakText', peakText, 'concText',
    concText, ...
'calibrationCurve', [], 'calibRegion1', [], 'calibRegion2', [], 'peakConc'
    , [], ...
```

```
    'peakHeight', [], 'fwhm', [], 'sensitivity', [], 'qualityFactor', []));

    end

    function uploadVNA(fig, ax)
    dataStruct = guidata(fig);
    [file, path] = uigetfile('*.s1p', 'Select VNA Data File');
    if file
    filePath = fullfile(path, file);
    fid = fopen(filePath, 'r');
    rawData = {};
    while ~feof(fid)
    line = fgetl(fid);
    if isempty(line) || line(1) == '!' || line(1) == '#'
    continue;
    end
    rawData{end+1, 1} = str2num(line); %#ok<ST2NM>
    end
    fclose(fid);
    data = cell2mat(rawData);
    if size(data, 2) < 2
    errordlg('Invalid file format.', 'File Error');
    return;
    end
    dataStruct.vnaData = data(:, 1:2);
    cla(ax);
    plot(ax, dataStruct.vnaData(:, 1), dataStruct.vnaData(:, 2), 'b', '
        LineWidth', 1.5);
    validIndices = (dataStruct.vnaData(:, 1) >= 0.315) & (dataStruct.vnaData
        (:, 1) <= 0.46);
    filteredData = dataStruct.vnaData(validIndices, :);
    if ~isempty(filteredData)
    [peakValue, peakIndex] = max(filteredData(:, 2));
    peakFrequency = filteredData(peakIndex, 1);
    plot(ax, peakFrequency, peakValue, 'ro', 'MarkerSize', 8, 'LineWidth', 2);
    set(dataStruct.peakText, 'String', sprintf('Peak Frequency: %.4f MHz',
        peakFrequency));

    dataStruct.peakHeight = peakValue;

    halfMax = peakValue / 2;
    leftIdx = find(filteredData(1:peakIndex, 2) <= halfMax, 1, 'last');
    rightIdx = peakIndex + find(filteredData(peakIndex:end, 2) <= halfMax, 1,
        'first') - 1;
    if ~isempty(leftIdx) && ~isempty(rightIdx)
    xLeft = interp1(filteredData(leftIdx:leftIdx+1, 2), filteredData(leftIdx:
        leftIdx+1, 1), halfMax);
    xRight = interp1(filteredData(rightIdx-1:rightIdx, 2), filteredData(
        rightIdx-1:rightIdx, 1), halfMax);
    dataStruct.fwhm = xRight - xLeft;
    dataStruct.qualityFactor = peakFrequency / dataStruct.fwhm;

    if ~isempty(dataStruct.calibrationCurve)
    [concentration, ~] = findConcentration(dataStruct, peakFrequency);
```

```
    if ~isempty(concentration)

    conc = concentration(1);

    idx = find(abs(dataStruct.calibrationCurve(:,1) - conc) < 0.1, 1);
    if ~isempty(idx) && idx > 1
    df = diff(dataStruct.calibrationCurve(idx-1:idx, 2));
    dc = diff(dataStruct.calibrationCurve(idx-1:idx, 1));
    dataStruct.sensitivity = df / dc;

    end
    end
    end
    end
    if ~isempty(dataStruct.calibrationCurve)
    [concentration, region] = findConcentration(dataStruct, peakFrequency);
    if numel(concentration) == 1
    set(dataStruct.concText, 'String', ...
    sprintf('Concentration: %.4f ppm (Region %d)', concentration, region));
    else
    set(dataStruct.concText, 'String', ...
    sprintf('Concentration: %.4f ppm (Region 1) or %.4f ppm (Region 2)', ...
    concentration(1), concentration(2)));
    end
    else
    set(dataStruct.concText, 'String', 'Concentration: N/A');
    end
    else
    set(dataStruct.peakText, 'String', 'Peak Frequency: N/A');
    set(dataStruct.concText, 'String', 'Concentration: N/A');
    end
    guidata(fig, dataStruct);
    end
    end

    function openLiquidPopup(mainFig)
    popup = figure('Name', 'Select Liquid', 'NumberTitle', 'off', ...
    'Position', [300 300 200 120], 'WindowStyle', 'modal');
    liquids = {'Select Liquid', 'Acetone', 'nickel(II) chloride(NiCl2)', '
        sodium chloride (NaCl)'};
    uicontrol('Style', 'listbox', 'Position', [10 10 180 100], ...
    'String', liquids, ...
    'Callback', @(src,~) onLiquidSelected(mainFig, popup, src));
    end

    function openAnalysisPopup(mainFig)
    dataStruct = guidata(mainFig);

    popup = figure('Name', 'Analysis Results', 'NumberTitle', 'off', ...
    'Position', [350 250 300 200], 'WindowStyle', 'modal', ...
    'MenuBar', 'none', 'ToolBar', 'none');

    uicontrol('Style', 'text', 'Position', [20 160 260 20], ...
    'String', 'Peak Analysis Parameters:', 'FontWeight', 'bold');
```

```
    uicontrol('Style', 'text', 'Position', [20 130 120 20], ...
    'String', 'Peak Height:', 'HorizontalAlignment', 'left');
    peakHeightText = uicontrol('Style', 'text', 'Position', [150 130 120 20],
        ...
    'String', ifelse(isempty(dataStruct.peakHeight), 'N/A', sprintf('%.4f',
        dataStruct.peakHeight)), ...
    'HorizontalAlignment', 'left');
    uicontrol('Style', 'text', 'Position', [20 100 120 20], ...
    'String', 'FWHM (MHz):', 'HorizontalAlignment', 'left');
    fwhmText = uicontrol('Style', 'text', 'Position', [150 100 120 20], ...
    'String', ifelse(isempty(dataStruct.fwhm), 'N/A', sprintf('%.4f',
        dataStruct.fwhm)), ...
    'HorizontalAlignment', 'left');
    uicontrol('Style', 'text', 'Position', [20 70 120 20], ...
    'String', 'Sensitivity:', 'HorizontalAlignment', 'left');
    sensitivityText = uicontrol('Style', 'text', 'Position', [150 70 120 20],
        ...
    'String', ifelse(isempty(dataStruct.sensitivity), 'N/A', sprintf('%.4f MHz
        /unit', dataStruct.sensitivity)), ...
    'HorizontalAlignment', 'left');
    uicontrol('Style', 'text', 'Position', [20 40 120 20], ...
    'String', 'Quality Factor:', 'HorizontalAlignment', 'left');
    qFactorText = uicontrol('Style', 'text', 'Position', [150 40 120 20], ...
    'String', ifelse(isempty(dataStruct.qualityFactor), 'N/A', sprintf('%.2f',
         dataStruct.qualityFactor)), ...
    'HorizontalAlignment', 'left');

    uicontrol('Style', 'pushbutton', 'Position', [100 10 100 25], ...
    'String', 'Close', 'Callback', @(~,~) close(popup));
    end

    function onLiquidSelected(mainFig, popupFig, listbox)
    index = listbox.Value;
    liquids = listbox.String;
    if index == 1
    return;
    end
    liquidName = liquids{index};
    fileName = [lower(liquidName), '.txt'];
    dataStruct = guidata(mainFig);
    if exist(fileName, 'file')
    fid = fopen(fileName, 'r');
    rawData = [];
    while ~feof(fid)
    line = fgetl(fid);
    if isempty(line) || line(1) == '%' || line(1) == '#'
    continue;
    end
    rawData = [rawData; str2num(line)]; %#ok<ST2NM>
    end
    fclose(fid);
    if size(rawData, 2) < 2
    errordlg('Invalid calibration file format.', 'Error');
    return;
```

```
194     end
195     dataStruct.calibrationCurve = rawData;
196     [~, peakIdx] = max(rawData(:, 2));
197     dataStruct.peakConc = rawData(peakIdx, 1);
198     region1 = rawData(rawData(:,1) <= dataStruct.peakConc, :);
199     region2 = rawData(rawData(:,1) >= dataStruct.peakConc, :);
200     dataStruct.calibRegion1 = sortrows(region1, 2);
201     dataStruct.calibRegion2 = sortrows(region2, -2);
202     guidata(mainFig, dataStruct);
203     disp(['Loaded calibration curve for ', liquidName]);
204     close(popupFig);
205     else
206     errordlg(['Calibration file "', fileName, '" not found.'], 'File Missing')
            ;
207     end
208     end
209
210     function [concentration, region] = findConcentration(dataStruct,
            peakFrequency)
211     concentration = [];
212     region = [];
213     allFreqs = dataStruct.calibrationCurve(:, 2);
214     if peakFrequency < min(allFreqs) || peakFrequency > max(allFreqs)
215     return;
216     end
217     freq1 = dataStruct.calibRegion1(:, 2);
218     conc1 = dataStruct.calibRegion1(:, 1);
219     if peakFrequency >= min(freq1) && peakFrequency <= max(freq1)
220     concentration = [concentration, interp1(freq1, conc1, peakFrequency)];
221     region = [region, 1];
222     end
223     freq2 = dataStruct.calibRegion2(:, 2);
224     conc2 = dataStruct.calibRegion2(:, 1);
225     if peakFrequency >= min(freq2) && peakFrequency <= max(freq2)
226     concentration = [concentration, interp1(freq2, conc2, peakFrequency)];
227     region = [region, 2];
228     end
229     end
230
231     function result = ifelse(condition, trueResult, falseResult)
232     if condition
233     result = trueResult;
234     else
235     result = falseResult;
236     end
237     end
```

CONCLUSION

OVERALL CONCLUSION

In this master thesis, a numerical and experimental investigation on the properties of 2D phononic crystal composed of steel/air structure of square symmetry filled defect central hole were conducted. The applications of the proposed phononic crystal as liquid sensor for complex liquid characterization are also discussed. This goal of this project is that the uses of the phononic crystal as sensor to determine the bulk properties of complex mixture such as acetone–water, nickel chloride–water and sodium chloride–water. The main points discussed in this work are:

- COMSOL multiphysics optimization helps to define the edge of the phononic band gap that can receive different liquids.
- Volumetric properties such as the density and the acoustic velocity of the liquids can be determined by the proposed phononic crystal sensor.
- The acoustic transmission of the resonant peak localized in the phononic band gap is linked directly to the defined concentrations.
- The shift of the resonant frequencies as function of concentrations helps to determine the calibration curve for the sensor.
- The proposed sensor based phononic crystal gives a high quality factor, which is dependent on the bulk physical properties of the liquids.
- The development of a graphical user interface (GUI) to facilitate real-time control, data acquisition, and analysis of the phononic-fluidic sensor.

In future work, we aim to employ artificial intelligence tools, particularly machine learning models, to predict the acoustic resonant peak corresponding to unknown concentrations, using a limited set of input parameters such as transmission.

Technical Skills Acquired from this work:

- **Chemical Handling and Laboratory Practices**
  - Proficient in handling chemical compounds and preparing complex mixtures under laboratory safety protocols.
  - Skilled in operating and maintaining standard laboratory equipment, including balances, mixers, dryers, and cleaning systems.
- **Instrumentation and Analytical Techniques**
  - Experienced in using and calibrating pH meters and conductivity meters for precise chemical analysis.
  - Proficient in sensor characterization using the SDR-KIT, including signal processing and experimental setup optimization.
  - Skilled in the operation of Vector Network Analyzers (VNA) for scattering parameter extraction and RF/microwave characterization.
  - Skilled in UV-visible spectrometer for liquid optical characterization.
- **Numerical Modeling and Simulation**
  - Competent in developing and modeling MATLAB scripts and algorithms for scientific computing and data analysis.
  - Advanced proficiency in COMSOL Multiphysics, particularly in Solid Mechanics and Acoustic Pressure modules, for simulation and multiphysics modeling.
  - Skilled in using LaTeX for writing.
  - Extensive use of the ORIGIN software for results visualization, computation, handling.
- **Ultrasonic Testing and Measurement Systems**
  - Designed and developed advanced ultrasonic measurement systems, including 3D alignment procedures and emitter-receiver signal configuration, for nondestructive material testing.

Group Worker Skills Acquired:

- Successfully integrated into a multidisciplinary research team, contributing effectively to collaborative scientific projects.
- Developed strong communication skills through regular interactions with laboratory staff, engineers, technicians, and researchers from various backgrounds.
- Experienced in drafting formal requests for the procurement of chemical products and authorization to operate specialized laboratory equipment.
- Competent in preparing and submitting scientific communications, including abstracts, posters, and presentations, for conferences and professional events.

REFERENCES

References

[1] S. Valiya Valappil, A. M. Aragón, and H. Goosen, "Phononic crystals' band gap manipulation via displacement modes," *Solid State Commun.*, vol. 361, p. 115061, Feb. 2023, doi: 10.1016/j.ssc.2022.115061.

[2] T. Gorishnyy, "Hypersonic Phononic Crystals," 2007.

[3] T. Vasileiadis, J. Varghese, V. Babacic, J. Gomis-Bresco, D. Navarro Urrios, and B. Graczykowski, "Progress and perspectives on phononic crystals," *J. Appl. Phys.*, vol. 129, no. 16, p. 160901, Apr. 2021, doi: 10.1063/5.0042337.

[4] A.-C. Hladky-Hennion, C. Granger, J. Vasseur, and M. De Billy, "Propagation of elastic waves in one-dimensional periodic stubbed waveguides," *Phys. Rev. B*, vol. 82, no. 10, p. 104307, Sep. 2010, doi: 10.1103/PhysRevB.82.104307.

[5] V. Laude, "Principles and properties of phononic crystal waveguides," *APL Mater.*, vol. 9, no. 8, p. 080701, Aug. 2021, doi: 10.1063/5.0059035.

[6] J. Sánchez-Dehesa and A. Krokhin, "Introduction to Acoustics of Phononic Crystals. Homogenization at Low Frequencies," in *Phononic Crystals*, A. Khelif and A. Adibi, Eds., New York, NY: Springer New York, 2016, pp. 1–21, doi: 10.1007/978-1-4614-9393-8-1.

[7] M. S. Kushwaha, P. Halevi, L. Dobrzynski, and B. Djafari-Rouhani, "Acoustic band structure of periodic elastic composites," *Phys. Rev. Lett.*, vol. 71, no. 13, 1993.

[8] P. A. Deymier, Ed., *Acoustic Metamaterials and Phononic Crystals*, in *Springer Series in Solid-State Sciences*, vol. 173. Berlin, Heidelberg: Springer Berlin Heidelberg, 2013, doi: 10.1007/978-3-642-31232-8.

[9] L. Li, X. Gang, Z. Sun, X. Zhang, and F. Zhang, "Design of phononic crystals plate and application in vehicle sound insulation," *Adv. Eng. Softw.*, vol. 125, pp. 19–26, Nov. 2018, doi: 10.1016/j.advengsoft.2018.08.002.

[10] A. Khelif and A. Adibi, Eds., *Phononic Crystals: Fundamentals and Applications*. New York, NY: Springer New York, 2016, doi: 10.1007/978-1-4614-9393-8.

[11] Y. Pennec, J. O. Vasseur, B. Djafari-Rouhani, L. Dobrzyński, and P. A. Deymier, "Two-dimensional phononic crystals: Examples and applications," *Surf. Sci. Rep.*, vol. 65, no. 8, pp. 229–291, Aug. 2010, doi: 10.1016/j.surfrep.2010.08.002.

[12] R. Lucklum and J. Li, "Phononic crystals for liquid sensor applications," *Meas. Sci. Technol.*, vol. 20, no. 12, p. 124014, Dec. 2009, doi: 10.1088/0957-0233/20/12/124014.

[13] P. A. Deymier, Ed., *Acoustic Metamaterials and Phononic Crystals*, in *Springer Series in Solid-State Sciences*, vol. 173. Berlin, Heidelberg: Springer Berlin Heidelberg, 2013, doi: 10.1007/978-3-642-31232-8.

[14] F. Lucklum and M. J. Vellekoop, "Bandgap engineering of three-dimensional phononic crystals in a simple cubic lattice," *Appl. Phys. Lett.*, vol. 113, no. 20, p. 201902, Nov. 2018, doi: 10.1063/1.5049663.

[15] F. Lucklum and M. Vellekoop, "Design and Fabrication Challenges for Millimeter-Scale Three-Dimensional Phononic Crystals," *Crystals*, vol. 7, no. 11, p. 348, Nov. 2017, doi: 10.3390/cryst7110348.

[16] R. Lucklum, M. Ke, and M. Zubtsov, "Two-dimensional phononic crystal sensor based on a cavity mode," *Sens. Actuators B Chem.*, vol. 171–172, pp. 271–277, Aug. 2012, doi: 10.1016/j.snb.2012.03.063.

[17] M. Gorakifard, I. Cuesta, C. Salueña, and E. Kian Far, "Acoustic wave propagation and its application to fluid structure interaction using the Cumulant Lattice Boltzmann Method," *Comput. Math. Appl.*, vol. 87, pp. 91–106, Apr. 2021, doi: 10.1016/j.camwa.2021.02.011.

[18] M. M. Sigalas, "Elastic and Acoustic Wave Band Structure."

[19] L. D. Landau and E. M. Lifshitz, *Theory of Elasticity*.

[20] L. E. Kinsler, Ed., *Fundamentals of Acoustics*, 4th ed. New York: Wiley, 2000.

[21] M. A. Sahin, M. Ali, J. Park, and G. Destgeer, "Fundamentals of Acoustic Wave Generation and Propagation," in *Acoustic Technologies in Biology and Medicine*, 1st ed., A. Ozcelik, R. Becker, and T. J. Huang, Eds., Wiley, 2023, pp. 1–36, doi: 10.1002/9783527841325.ch1.

[22] M. I. Hussein, M. J. Leamy, and M. Ruzzene, "Dynamics of Phononic Materials and Structures: Historical Origins, Recent Progress, and Future Outlook," *Appl. Mech. Rev.*, vol. 66, no. 4, p. 040802, Jul. 2014, doi: 10.1115/1.4026911.

[23] H. Lv, "Analysis of Rayleigh wave dynamic response and propagation characteristics in layered site," *Sci. Rep.*, vol. 14, no. 1, p. 22524, Sep. 2024, doi: 10.1038/s41598-024-73600-8.

[24] A. Palermo and A. Marzani, "Control of Love waves by resonant metasurfaces," *Sci. Rep.*, vol. 8, no. 1, p. 72320, May 2018, doi: 10.1038/s41598-018-25503-8.

[25] B. Xu, J. Huang, and Y. Jie, "Application of the Lamb Wave Mode of Acoustic Emission for Monitoring Impact Damage in Plate Structures," *Sensors*, vol. 23, no. 20, p. 8611, Oct. 2023, doi: 10.3390/s23208611.

[26] F. Hadj-Larbi and R. Serhane, "Sezawa SAW devices: Review of numerical-experimental studies and recent applications," *Sens. Actuators Phys.*, vol. 292, pp. 169–197, Jun. 2019, doi: 10.1016/j.sna.2019.03.037.

[27] P. Kiełczyński, M. Szalewski, A. Balcerzak, A. J. Rostocki, and D. B. Tefelski, "Application of SH surface acoustic waves for measuring the viscosity of liquids in function of pressure and temperature," *Ultrasonics*, vol. 51, no. 8, pp. 921–924, Dec. 2011, doi: 10.1016/j.ultras.2011.05.006.

[28] C. Zhang, J. J. Caron, and J. F. Vetelino, "The Bleustein–Gulyaev wave for liquid sensing applications," *Sens. Actuators B Chem.*, vol. 76, no. 1–3, pp. 64–68, Jun. 2001, doi: 10.1016/S0925-4005(01)00569-X.

[29] Y. Belahurau, J. S. Jensen, and F. Lucklum, "Numerical and Experimental Study of a Phononic-Fluidic Sensor Using a Cubic Unit Cell with Spherical Void," in *2021 IEEE Sensors*, Sydney, Australia: IEEE, Oct. 2021, pp. 1–4, doi: 10.1109/SENSORS47087.2021.9639587.

[30] A. Rostami, H. Kaatuzian, and B. RostamiDogolsara, "Phononic Crystals: Physical Principles and Novel Structures," *AUT J. Mech. Eng.*, no. Online First, Oct. 2024, doi: 10.22060/ajme.2024.23250.6118.

[31] Y. Jin *et al.*, "The 2024 phononic crystals roadmap," *J. Phys. Appl. Phys.*, vol. 58, no. 11, p. 113001, Mar. 2025, doi: 10.1088/1361-6463/ad9ab2.

[32] N. Mukhin, M. Kutia, A. Aman, U. Steinmann, and R. Lucklum, "Two-Dimensional Phononic Crystal Based Sensor for Characterization of Mixtures and Heterogeneous Liquids," *Sensors*, vol. 22, no. 7, p. 2816, Apr. 2022, doi: 10.3390/s22072816.

[33] Z. Liu *et al.*, "Locally Resonant Sonic Materials," *Science*, vol. 289, no. 5485, pp. 1734–1736, Sep. 2000, doi: 10.1126/science.289.5485.1734.

[34] K. Singh, G. Wilson, and J. A. H. Stotz, "Optimizing Phononic Crystal Waveguides for Acoustically Induced Spin Transport," 2024, arXiv, doi: 10.48550/ARXIV.2411.08125.

[35] S. Yang, H. Chang, Y. Wang, M. Yang, and T. Sun, "A phononic crystal suspension for vibration isolation of acoustic loads in underwater gliders," *Appl. Acoust.*, vol. 216, p. 109731, Jan. 2024, doi: 10.1016/j.apacoust.2023.109731.

[36] F. Ma, Z. Huang, C. Liu, and J. H. Wu, "Acoustic focusing and imaging via phononic crystal and acoustic metamaterials," *J. Appl. Phys.*, vol. 131, no. 1, p. 011103, Jan. 2022, doi: 10.1063/5.0074503.

[37] Y. Yang, J. Lu, M. Yan, X. Huang, W. Deng, and Z. Liu, "Hybrid-Order Topological Insulators in a Phononic Crystal," *Phys. Rev. Lett.*, vol. 126, no. 15, p. 156801, Apr. 2021, doi: 10.1103/PhysRevLett.126.156801.

[38] T. Li, G. Liu, H. Kong, G. Yang, G. Wei, and X. Zhou, "Recent advances in photonic crystal-based sensors," *Coord. Chem. Rev.*, vol. 475, p. 214909, Jan. 2023, doi: 10.1016/j.ccr.2022.214909.

[39] Y. Achaoui, A. Khelif, S. Benchabane, and V. Laude, "Polarization state and level repulsion in two-dimensional phononic crystals and waveguides in the presence of material anisotropy," *J. Phys. Appl. Phys.*, vol. 43, no. 18, p. 185401, May 2010, doi: 10.1088/0022-3727/43/18/185401.

[40] H. Li and P. Sun, "Vibration Isolation and Noise Reduction Method Based on Phononic Crystal," *Comput. Intell. Neurosci.*, vol. 2022, pp. 1–7, Oct. 2022, doi: 10.1155/2022/9903645.

[41] S.-H. Jo, "Temperature-Controlled Defective Phononic Crystals with Shape Memory Alloys for Tunable Ultrasonic Sensors," *Crystals*, vol. 15, no. 5, p. 412, Apr. 2025, doi: 10.3390/cryst15050412.

[42] M. Haras *et al.*, "Fabrication of Thin-Film Silicon Membranes With Phononic Crystals for Thermal Conductivity Measurements," *IEEE Electron Device Lett.*, vol. 37, no. 10, pp. 1358–1361, Oct. 2016, doi: 10.1109/LED.2016.2600590.

[43] H. Imanian, M. Noori, and A. Abbasiyan, "Highly efficient gas sensor based on quasi-periodic phononic crystals," *Sens. Actuators B Chem.*, vol. 345, p. 130418, Oct. 2021, doi: 10.1016/j.snb.2021.130418.

[44] R. Lucklum, M. Zubtsov, R. Grundmann, and S. Villa Arango, "Phononic cystal sensor for medical applications," in *IEEE SENSORS 2014 Proceedings*, Valencia, Spain: IEEE, Nov. 2014, pp. 903–906, doi: 10.1109/ICSENS.2014.6985147.

[45] R. Lucklum, N optimised. Mukhin, B. Djafari Rouhani, and Y. Pennec, "Phononic Crystal Sensors: A New Class of Resonant Sensors—Chances and Challenges for the Determination of Liquid Properties," *Front. Mech. Eng.*, vol. 7, p. 705194, Jul. 2021, doi: 10.3389/fmech.2021.705194.

[46] R. Lucklum, J. Li, and M. Zubtsov, "1D and 2D phononic crystal sensors," *Procedia Eng.*, vol. 5, pp. 436–439, 2010, doi: 10.1016/j.proeng.2010.09.140.

[47] F. Lucklum and M. Vellekoop, "Design and Fabrication Challenges for Millimeter-Scale Three-Dimensional Phononic Crystals," *Crystals*, vol. 7, no. 11, p. 348, Nov. 2017, doi: 10.3390/cryst7110348.

[48] Y. Belahurau, N. Aage, R. E. Christiansen, and F. Lucklum, "Design of a 3D phononic-fluidic sensor using shape optimization."

[49] Y. Belahurau and F. Lucklum, "Design of a Phononic-Fluidic Cavity Sensor: Influence of Finite Size Lattice on Sensor Performance," 2023.

[50] S. E. Zaki, A. Mehaney, and A. H. Aly, "Novel highly-sensitive heavy metals sensor-based 1D phononic crystal for NiCl2 detection," *Opt. Quantum Electron.*, vol. 54, no. 12, p. 811, Dec. 2022, doi: 10.1007/s11082-022-04212-7.

[51] S. E. Zaki, A. Mehaney, H. M. Hassanein, and A. H. Aly, "High-performance liquid sensor based one-dimensional phononic crystal with demultiplexing capability," *Mater. Today Commun.*, vol. 26, p. 102045, Mar. 2021, doi: 10.1016/j.mtcomm.2021.102045.

[52] F. Ma, Z. Huang, C. Liu, and J. H. Wu, "Acoustic focusing and imaging via phononic crystal and acoustic metamaterials," *J. Appl. Phys.*, vol. 131, no. 1, p. 011103, Jan. 2022, doi: 10.1063/5.0074503.

[53] P. Narang and A. Arora, "Topological phononics is cataloged," *Science*, vol. 384, no. 6696, pp. 626–626, May 2024, doi: 10.1126/science.adp3736.

[54] A. H. Aly and A. Mehaney, "Phononic crystals with one-dimensional defect as sensor materials," *Indian J. Phys.*, vol. 91, no. 9, pp. 1021–1028, Sep. 2017, doi: 10.1007/s12648-017-0989-z.

[55] S. Villa-Arango, R. Torres, P. A. Kyriacou, and R. Lucklum, "Fully-disposable multilayered phononic crystal liquid sensor with symmetry reduction and a resonant cavity," *Measurement*, vol. 102, pp. 20–25, May 2017, doi: 10.1016/j.measurement.2017.01.051.

[56] G. Sharma, S. Kumar, and V. Singh, "Design of Si–SiO2 phoxonic crystal having defect layer for simultaneous sensing of biodiesel in a binary mixture of diesel through optical and acoustic waves," *Acoust. Phys.*, vol. 63, no. 2, pp. 159–167, Mar. 2017, doi: 10.1134/S1063771017020117.

[57] H. Heo *et al.*, "Multifunctional Acoustic Device Based on a Phononic Crystal with Independently Controlled Asymmetric Rotating Rods," *Phys. Rev. Appl.*, vol. 19, no. 5, p. 054008, May 2023, doi: 10.1103/PhysRevApplied.19.054008.

[58] A. Oseev, M. Zubtsov, and R. Lucklum, "Gasoline properties determination with phononic crystal cavity sensor," *Sens. Actuators B Chem.*, vol. 189, pp. 208–212, Dec. 2013, doi: 10.1016/j.snb.2013.03.072.

[59] N. Mukhin, M. Kutia, A. Oseev, U. Steinmann, S. Palis, and R. Lucklum, "Narrow Band Solid-Liquid Composite Arrangements: Alternative Solutions for Phononic Crystal-Based Liquid Sensors," *Sensors*, vol. 19, no. 17, p. 3743, Aug. 2019, doi: 10.3390/s19173743.

[60] M. Zubtsov *et al.*, "2D phononic crystal sensor with normal incidence of sound," *Sens. Actuators Phys.*, vol. 186, pp. 118–124, Oct. 2012, doi: 10.1016/j.sna.2012.03.017.

[61] E. Walker, D. Reyes, M. M. Rojas, A. Krokhin, Z. Wang, and A. Neogi, "Tunable ultrasonic phononic crystal controlled by infrared radiation," *Appl. Phys. Lett.*, vol. 105, no. 14, p. 143503, Oct. 2014, doi: 10.1063/1.4894489.

[62] F. Lucklum and M. J. Vellekoop, "Ultra-Sensitive and Broad Range Phononic-Fluidic Cavity Sensor for Determination of Mass Fractions in Aqueous Solutions," in *2019 20th International Conference on Solid-State Sensors, Actuators and Microsystems & Eurosensors XXXIII (TRANSDUCERS & EUROSENSORS XXXIII)*, Berlin, Germany: IEEE, Jun. 2019, pp. 885–888, doi: 10.1109/TRANSDUCERS.2019.8808509.

[63] F. Lucklum, F. Bunge, and M. J. Vellekoop, "Experimental and numerical analysis of complete acoustic band gaps in three-dimensional phononic crystals," in *2017 19th International Conference on Solid-State Sensors, Actuators and Microsystems (TRANSDUCERS)*, Kaohsiung: IEEE, Jun. 2017, pp. 958–961, doi: 10.1109/TRANSDUCERS.2017.7994209.

[64] Y. Belahurau and F. LuckF. Lucklum, "Numerical and Experimental Systematic Design Study of 3d Ultrasonic Phononic-Fluidic Sensor Using a Cubic Cell with Spherical Void," 2023, SSRN, doi: 10.2139/ssrn.4493605.

[65] L. D. Landau, E. M. Lifšic, J. B. Sykes, and W. H. Reid, *Fluid Mechanics*, 2nd ed., in *Course of Theoretical Physics*, no. 6. Oxford: Pergamon Press, 1987.

[66] M. J. Holmes, N. G. Parker, and M. J. W. Povey, "Temperature dependence of bulk viscosity in water using acoustic spectroscopy," *J. Phys. Conf. Ser.*, vol. 269, p. 012011, Jan. 2011, doi: 10.1088/1742-6596/269/1/012011.

[67] A. Mehaney and I. I. Ahmed, "Acetone sensor based 1D defective phononic crystal as a highly sensitive biosensor application," *Opt. Quantum Electron.*, vol. 53, no. 2, p. 97, Feb. 2021, doi: 10.1007/s11082-021-02737-x.

[68] A. Mehaney, M. S. Hassan, and H. A. Elsayed, "Fuel Phononic Crystal Sensor for the Determination and Discrimination of Gasoline Components," May 04, 2021, In Review, doi: 10.21203/rs.3.rs-420715/v1.

[69] Z. A. Zaky, S. Alamri, E. I. Zohny, and A. H. Aly, "Simulation study of gas sensor using periodic phononic crystal tubes to detect hazardous greenhouse gases," *Sci. Rep.*, vol. 12, no. 1, p. 21553, Dec. 2022, doi: 10.1038/s41598-022-26079-0.